

## **Distribution Agreement**

In presenting this thesis or dissertation as a partial fulfillment of the requirements for an advanced degree from Emory University, I hereby grant to Emory University and its agents the non-exclusive license to archive, make accessible, and display my thesis or dissertation in whole or in part in all forms of media, now or hereafter known, including display on the world wide web. I understand that I may select some access restrictions as part of the online submission of this thesis or dissertation. I retain all ownership rights to the copyright of the thesis or dissertation. I also retain the right to use in future works (such as articles or books) all or part of this thesis or dissertation.

Signature:

---

Christopher P. Vellano

---

Date

**Regulator of G Protein Signaling 14 (RGS14) at the Interface of Conventional and Unconventional G Protein Signaling**

By  
Christopher P. Vellano  
Doctor of Philosophy

Graduate Division of Biological and Biomedical Sciences  
Molecular Systems Pharmacology

---

John R. Hepler, PhD  
Advisor

---

Randy A. Hall, PhD  
Committee Member

---

Zixu Mao, MD/PhD  
Committee Member

---

Eric A. Ortlund, PhD  
Committee Member

Accepted:

---

Lisa A. Tedesco, PhD  
Dean of the Graduate School

---

Date

**Regulator of G Protein Signaling 14 (RGS14) at the Interface of Conventional and Unconventional G Protein Signaling**

By

Christopher P. Vellano  
B.S., Wake Forest University, 2006

Advisor: John R. Hepler, PhD

An abstract of a dissertation submitted to the Faculty of the James T. Laney School of Graduate Studies of Emory University in partial fulfillment of the requirements for the degree of Doctor of Philosophy

Graduate Division of Biological and Biomedical Sciences  
Molecular Systems Pharmacology  
2012

## Abstract

The Regulators of G protein Signaling (RGS) proteins were discovered as key modulators of G protein-coupled receptor (GPCR) signaling. Acting as GTPase accelerating proteins (GAPs), RGS proteins catalyze GTP hydrolysis of activated  $G\alpha$ -GTP subunits through binding of their conserved RGS domain to activated  $G\alpha$  subunits. One of the most complex RGS proteins, RGS14, has a unique sequence structure that suggests it serves additional physiological roles aside from acting as a GAP for activated  $G\alpha$  subunits. In addition to the canonical RGS domain that binds activated  $G\alpha_i$  and  $G\alpha_o$  subunits, RGS14 possesses two tandem Ras/Rap-binding domains (RBDs) and a G protein regulatory (GPR) motif. This GPR motif binds directly and selectively to *inactive*  $G\alpha_{i1}$  and  $G\alpha_{i3}$  subunits. When bound to inactive  $G\alpha_{i1/3}$ , RGS14 acts as a guanine nucleotide dissociation inhibitor (GDI), preventing these  $G\alpha$  subunits from binding GTP and becoming activated. The capacity of RGS14 to bind both activated and inactivated  $G\alpha_i$  subunits indicates that RGS14 may play roles in unconventional G protein signaling pathways, which do not require GPCR-mediated activation of the  $G\alpha$  subunit. In this case, RGS14 would act similarly to other GPR-domain containing proteins that function with  $G\alpha_i$  in the absence of GPCRs. The data presented here show the first evidence of an RGS protein participating in unconventional G protein signaling, and support the idea that RGS14 sits at the interface of both conventional GPCR-dependent and unconventional GPCR-independent G protein signaling. Our data show that an RGS14: $G\alpha_{i1}$ -GDP complex can be acted on by the non-receptor guanine nucleotide exchange factor (GEF) Ric-8A, a protein found to be highly involved in specific unconventional G protein signaling pathways. RGS14 also forms  $G\alpha_{i/o}$ -dependent complexes with GPCRs, which are subsequently regulated by Ric-8A depending on the activation state of the receptor. Our results showing that RGS14 can interact with activated H-Ras in a  $G\alpha_i$ -regulated manner suggest that RGS14 may serve as a molecular switch between binding H-Ras/Raf and regulating MAP kinase signaling to binding  $G\alpha_i$  and regulating G protein signaling. Together, these data illustrate that RGS14 is a very unique RGS/GPR protein that may lie at the nexus of divergent G protein signaling pathways.

**Regulator of G Protein Signaling 14 (RGS14) at the Interface of Conventional and Unconventional G Protein Signaling**

By

Christopher P. Vellano  
B.S., Wake Forest University, 2006

Advisor: John R. Hepler, PhD

A dissertation submitted to the Faculty of the James T. Laney School of Graduate Studies of Emory University in partial fulfillment of the requirements for the degree of Doctor of Philosophy

Graduate Division of Biological and Biomedical Sciences  
Molecular Systems Pharmacology  
2012

## TABLE OF CONTENTS

	<u>Page</u>
<b><u>Chapter 1: Introduction</u></b>	1
<b>1.1 G Protein-Coupled Receptors</b>	2-3
<b>1.11 GPCRs as Drug Targets</b>	3-4
<b>1.2 Conventional G Protein Signaling</b>	4-7
<b>1.3 Unconventional G Protein Signaling</b>	7-11
<b>1.4 Regulators of G Protein Signaling Proteins</b>	11-12
<b>1.41 RGS Proteins in Physiology and Disease</b>	12-16
<b>1.42 RGS Proteins as Drug Targets</b>	16-18
<b>1.5 Regulator of G Protein Signaling 14 (RGS14)</b>	18-21
<b>1.51 RGS14 Modulates Ras/Raf-mediated MAP Kinase Signaling</b>	21-22
<b>1.52 RGS14 Participates in Unconventional G Protein Signaling Pathways</b>	22-24
<b>1.6 Overall Hypothesis and Objective of this Research</b>	24-25
<b><u>Chapter 2: Activation of the Regulator of G protein Signaling 14 (RGS14):G<i>α</i>1-GDP signaling complex is regulated by Resistance to Inhibitors of Cholinesterase-8A (Ric-8A)</u></b>	26
<b>2.1 Introduction</b>	27-28
<b>2.2 Experimental Procedures</b>	28-33
<b>2.3 Results</b>	33-48
<b>2.4 Discussion</b>	48-55
<b><u>Chapter 3: G protein-coupled receptors and Resistance to Inhibitors of Cholinesterase-8A (Ric-8A) both regulate the Regulator of G protein Signaling 14(RGS14):G<i>α</i>1 complex in live cells</u></b>	56

3.1 Introduction	57-59
3.2 Experimental Procedures	59-62
3.3 Results	62-77
3.4 Discussion	77-84
<b><u>Chapter 4: G<i>α</i>1 and G protein-coupled receptors regulate Regulator of G protein Signaling 14(RGS14) interactions with H-Ras in live cells</u></b>	85
4.1 Introduction	86-87
4.2 Experimental Procedures	88-90
4.3 Results	90-99
4.4 Discussion	99-104
<b><u>Chapter 5: Discussion</u></b>	105
5.1 RGS14 Participates in Unconventional G Protein Signaling: Experimental Limitations and Future Directions	106-108
5.2 RGS14 Links Both Conventional GPCR-dependent and Unconventional GPCR-independent G Protein Signaling Pathways	108-112
5.3 Working Model for RGS14 Integration of Both G Protein and MAP Kinase Signaling	112-115
5.4 RGS14 Exhibits Similarities and Differences with its Closest Relative, RGS12	115-117
5.5 Concluding Remarks	117-118
<b><u>References</u></b>	119-129

## INDEX OF FIGURES

	<u>Page</u>
<b>Figure 1.1</b> - Conventional vs. unconventional G protein signaling	8
<b>Figure 1.2</b> - RGS14 domain structure and its identified binding partners	19
<b>Figure 2.1</b> - RGS14 and Ric-8A are recruited to the plasma membrane by wild-type G $\alpha$ i1	35
<b>Figure 2.2</b> - Ric-8A induces dissociation of the RGS14:G $\alpha$ i1-GDP complex in cells	36
<b>Figure 2.3</b> - Ric-8A induces dissociation of the RGS14:G $\alpha$ i1-GDP complex <i>in vitro</i>	38
<b>Figure 2.4</b> - Ric-8A-induced dissociation of the RGS14:G $\alpha$ i1-GDP complex allows G $\alpha$ i1 to bind GTP	40
<b>Figure 2.5</b> - Ric-8A reverses RGS14 inhibition of GTP $\gamma$ S binding to G $\alpha$ i1	42
<b>Figure 2.6</b> - Ric-8A reverses RGS14 inhibition of G $\alpha$ i1 steady-state GTPase activity	44
<b>Figure 2.7</b> - RGS14 and Ric-8A bind to distinct and overlapping regions of G $\alpha$ i1	46
<b>Figure 2.8</b> - RGS14 and Ric-8A co-exist and co-localize within the same hippocampal neurons	47
<b>Figure 2.9</b> - Working model depicting Ric-8A regulation of the RGS14:G $\alpha$ i1-GDP complex	54
<b>Figure 3.1</b> - RGS14 selectively interacts with G $\alpha$ i1 and G $\alpha$ i3 in the basal state of live cells as observed by BRET	63
<b>Figure 3.2</b> - RGS14 BRET signals with G $\alpha$ i1 in live cells are dependent on the GPR motif	66
<b>Figure 3.3</b> - RGS14 co-localization with G $\alpha$ i1 and the $\alpha$ <sub>2A</sub> -AR in live cells is regulated by receptor agonist	69
<b>Figure 3.4</b> - RGS14 forms a G $\alpha$ i/o-dependent complex with the $\alpha$ <sub>2A</sub> -AR in live cells	70
<b>Figure 3.5</b> - RGS14 remains bound to G $\alpha$ i1 following $\alpha$ <sub>2A</sub> -AR activation in live cells	73
<b>Figure 3.6</b> - Ric-8A facilitates dissociation of RGS14 from G $\alpha$ i1 in live cells	75
<b>Figure 3.7</b> - Ric-8A induces dissociation of both G $\alpha$ i1 and the $\alpha$ <sub>2A</sub> -AR from RGS14 following receptor stimulation	76
<b>Figure 3.8</b> - Working model for regulation of RGS14 complexes with G $\alpha$ i1 and $\alpha$ <sub>2A</sub> -AR	79



<b>Figure 3.9</b> - Working model depicting Ric-8A regulation of the $\alpha_{2A}$ -AR:G $\alpha$ i1:RGS14 complex	80
<b>Figure 4.1</b> - RGS14 selectively interacts with activated H-Ras in live cells as observed by BRET	91
<b>Figure 4.2</b> - RGS14 interactions with activated H-Ras in live cells are facilitated by G $\alpha$ i1	92
<b>Figure 4.3</b> - RGS14/H-Ras(G/V) interactions depend on the G $\alpha$ i1 activation state	94
<b>Figure 4.4</b> - RGS14 interactions with activated H-Ras are only partially inhibited by the R333L mutation	95
<b>Figure 4.5</b> - RGS14/H-Ras(G/V) interactions depend on H-Ras(G/V) membrane localization	97
<b>Figure 4.6</b> - H-Ras(G/V) and the $\alpha_{2A}$ -AR regulate one another's interactions with RGS14	98
<b>Figure 4.7</b> - Working model for regulation of RGS14 complexes with activated H-Ras, G $\alpha$ i1, and $\alpha_{2A}$ -AR	101
<b>Figure 5.1</b> - Possible role for RGS14 in suppressing LTP in CA2 hippocampal neurons	111
<b>Figure 5.2</b> - Proposed working model of how the RGS, RBD, and GPR domains of RGS14 may function coordinately to regulate G $\alpha$ i signaling	113

## LIST OF ABBREVIATIONS

<b>ADP</b>	adenosine diphosphate
<b>AIDS</b>	Acquired immune deficiency syndrome
<b>CA</b>	<i>Cornu Ammonis</i>
<b>cAMP</b>	cyclic adenosine monophosphate
<b>CCR</b>	C-C chemokine receptor
<b>CFP</b>	cyan fluorescent protein
<b>CXCR</b>	C-X-C chemokine receptor
<b>DEP</b>	Dishevelled, Egl-10, and Pleckstrin
<b>DG</b>	dentate gyrus
<b>EDG1</b>	endothelial differentiation gene 1
<b>EDTA</b>	ethylenediaminetetraacetic acid
<b>EGF</b>	epidermal growth factor
<b>EGL-2</b>	egg-laying defective-2
<b>EGTA</b>	ethylene glycol tetraacetic acid
<b>ERK</b>	extracellular signal-regulated kinase
<b>GABA</b>	gamma-aminobutyric acid
<b>GAIP</b>	G $\alpha$ -interacting protein
<b>GDP</b>	guanosine diphosphate
<b>GFP</b>	green fluorescent protein
<b>GTP</b>	guanosine triphosphate
<b>HEK</b>	human embryonic kidney
<b>HEPES</b>	4-(2-hydroxyethyl)-1-piperazineethanesulfonic acid
<b>HRP</b>	horseradish peroxidase
<b>IgG</b>	immunoglobulin

<b>I<math>\kappa</math>B<math>\alpha</math></b>	inhibitor of $\kappa$ B- $\alpha$
<b>IL</b>	interleukin
<b>kDa</b>	kilodalton
<b>LPA</b>	lysophosphatidic acid
<b>MAGUK</b>	Membrane-associated guanylate kinase
<b>MDM2</b>	murine double minute 2
<b>MEK</b>	mitogen extracellular kinase
<b>NF-<math>\kappa</math>B</b>	nuclear factor- $\kappa$ B
<b>PBS</b>	phosphate-buffered saline
<b>PDZ</b>	PSD-95/Dlg/ZO-1
<b>PIPES</b>	piperazine-N,N'-bis(2-ethanesulfonic acid)
<b>PSD</b>	postsynaptic density
<b>S1P1</b>	sphingosine-1-phosphate receptor 1
<b>SDS-PAGE</b>	sodium dodecyl sulfate polyacrylamide gel electrophoresis
<b>SEM</b>	standard error of the mean
<b>TBS</b>	tris-buffered saline
<b>Tx</b>	thioredoxin
<b>YFP</b>	yellow fluorescent protein

**CHAPTER 1:****Introduction<sup>1</sup>**

<sup>1</sup>A portion of this chapter has been published. Vellano CP, Lee SE, Dudek SM, and Hepler JR. (2011) RGS14 at the interface of hippocampal signaling and synaptic plasticity. *Trends Pharmacol. Sci.* 32: 666-74.

## 1.1 G Protein-Coupled Receptors

Many signaling events within the cells of eukaryotes are transduced through G protein-coupled receptors (GPCRs), which comprise over 1000 genes of the human genome and are the most widely targeted proteins with regard to therapeutics and drug discovery. A majority of GPCRs are “orphan” receptors, meaning that they have no known endogenous ligand (1-4). Although variability exists between each GPCR, the basic structure of all GPCRs consists of an extracellular N-terminus, seven transmembrane domains (7TMDs), and an intracellular C-terminus. In addition to having hydrophobic alpha-helical 7TMDs, all GPCRs are able to bind and couple to specific G proteins based on the sequence of their specific intracellular loops and C-termini (2,5).

G protein-coupled receptors are classified based on how their ligands bind, which may be a reflection of the structure of the N-terminus and respective binding pocket. The most common classification of GPCRs utilizes a letter system, with receptors lying in one of six classes, A-F. The largest family is Class A, modeled after the rhodopsin receptor. The members of this class are divided into four main subclasses:  $\alpha$ ,  $\beta$ ,  $\gamma$ , and  $\delta$ . The  $\alpha$  group consists of amine, prostaglandin, and adenosine receptors, among others. Members of the  $\alpha$  class also bind a variety of ligands, including peptides, lipids, and small molecules. This is in contrast to the  $\beta$  group of receptors, which are referred to as peptide hormone receptors because they mostly bind peptides. The  $\gamma$  group consists of opioid, chemokine, and somatostatin receptors, while the  $\delta$  receptor group includes olfactory receptors, which comprise the largest GPCR gene superfamily. The ligands of most Class A receptors bind within a region between the TMDs. Class B, known as the adhesion or secretin receptor family, includes receptors that have N-termini rich in cysteine-bridge structures that influence ligand binding. These receptors also contain a proteolysis domain near the first TMD that results in a cleaved N-terminus, which may also dictate ligand binding. A common characteristic of many Class B receptors is the presence of an EGF domain, which can

bind calcium and regulate protein-protein interactions. The metabotropic glutamate receptor family, Class C, includes GPCRs that have an extremely large N-terminus where the ligand binds. The size of the N-terminus allows the protein to engulf the ligand upon binding. In addition to metabotropic glutamate receptors, this family includes specific GABA and taste receptors. The other, less common classes, include fungal pheromone receptors (Class D), cAMP receptors (Class E), and Frizzled/Taste2 receptors (Class F) (2,6).

### **1.11 GPCRs as Drug Targets**

GPCRs compose almost 3% of the human genome and play significant roles in cell and organ physiology, making them highly attractive targets in drug development (7). Although approximately 30% of prescribed drugs target GPCRs, only a select few receptors are acted on by these drugs. Most antipsychotic drugs target D<sub>2</sub>-dopamine receptors by serving as antagonists. Both  $\alpha$ - and  $\beta$ -adrenergic receptor therapies have been instrumental in treating high blood pressure, heart failure, and asthma. Specifically,  $\beta$ <sub>1</sub>-adrenergic receptor agonists are given to increase cardiac contractility in the treatment of congestive heart failure ((8) and references therein). GPCRs are also important targets for many anti-inflammatory drugs. Allegra® and Clarinex® are common over-the-counter drugs used as anti-histamines, acting as antagonists of the Histamine H<sub>1</sub> receptor. Asthmatic reactions can be treated with Singulair®, an antagonist of the cysteinyl leukotriene 1 (CysLT-1) receptor, which helps reduce bronchial constriction (9).

Targeting GPCRs is also important because mutations in certain GPCRs have been associated with physiological ailments and disease. Some of the most common include mutations in the visual receptor rhodopsin that result in certain types of blindness. Other mutations account for specific endocrine, cardiac, and nervous system disorders. Mutations in GPCRs, such as single nucleotide polymorphisms (SNPs), may result in constitutive receptor activity, receptor deactivation, or altered capacity to respond to agonist binding (8,10). Individuals with specific SNPs in the  $\beta$ <sub>2</sub>-adrenergic receptor display altered responses to agonists that may lead to

asthmatic symptoms. Progress in AIDS research has also been dependent on identifying SNPs in GPCRs, as multiple SNPs in the CC chemokine receptor 5 (CCR5) have been implicated in the progression of AIDS (reviewed in (8)).

One of the main advantages in developing drugs that target GPCRs is tissue specificity. Some GPCRs are expressed in multiple tissues, thus it is essential to identify ways to target GPCRs in the organ or tissue of interest. One breakthrough in solving this issue was the discovery of dimerized GPCRs. Studies have shown that GPCRs can both homo and heterodimerize (11,12), creating a new arena for drug discovery. An agonist thought to be specific to the  $\kappa$ -opioid receptor (KOR), 6'-guanidinonaltrindole (6'GNTI), was discovered to bind and act preferentially on  $\kappa$ -opioid/ $\delta$ -opioid (DOR) receptor heterodimers (13). This suggests that receptor dimers can differ substantially from GPCR monomers pharmacologically, creating greater specificity of drug targeting. Specific receptor dimers, such as the KOR/DOR heterodimer, are differentially expressed within tissues (13). Such expression patterns not only allow specific GPCR heterodimers to be targeted, but they also provide a means of targeting certain receptors within specific tissues.

## **1.2 Conventional G Protein Signaling**

Established models propose that GPCRs are coupled to heterotrimeric G proteins ( $G\alpha\beta\gamma$ ) by direct binding of the GPCR to the  $G\alpha$  subunit via the receptor's intracellular domains or loops. Upon ligand binding, GPCRs serve as guanine nucleotide exchange factors (GEFs) to trigger GTP binding on the  $G\alpha$  subunit followed by  $G\beta\gamma$  dissociation and/or rearrangement (14-17). Activated  $G\alpha$ -GTP and  $G\beta\gamma$  interact with downstream effectors and signaling pathways to regulate cell and organ physiology. Signaling is terminated by hydrolysis of GTP to GDP through the intrinsic GTPase activity of the  $G\alpha$  subunit, whereby  $G\alpha$  and  $G\beta\gamma$  reassociate (14).

Although there are 21  $G\alpha$ , 6  $G\beta$ , and 12  $G\gamma$  subunits, G proteins are grouped into four major families based on the sequence homology between the  $G\alpha$  subunits: the  $G\alpha_i$ ,  $G\alpha_s$ ,  $G\alpha_q$ , and

$G\alpha_{12}$  families (4,18,19). The  $G\alpha_i$  family of G proteins includes  $G\alpha_o$ ,  $G\alpha_z$ , and  $G\alpha_t$  in addition to  $G\alpha_i$  members  $G\alpha_{i1}$ ,  $G\alpha_{i2}$ , and  $G\alpha_{i3}$ , with expression patterns differing slightly between family members. While  $G\alpha_i$  members are expressed fairly ubiquitously,  $G\alpha_o$  proteins are expressed almost exclusively within the heart and brain. Upon activation,  $G\alpha_{i1-3}$  proteins couple to and inhibit the downstream effector adenylyl cyclase, resulting in a decrease in intracellular cAMP and a subsequent decrease in Protein Kinase A (PKA) activity.  $G\alpha_s$  proteins also couple to adenylyl cyclase; however, they activate the effector, resulting in increased cAMP levels and increased activity of PKA.  $G\alpha_s$  proteins are ubiquitously expressed, with significant implications in cardiac physiology through inhibition of  $Na^+$  channels in the heart muscle. Members of the  $G\alpha_q$  family of G proteins ( $G\alpha_q$ ,  $G\alpha_{11}$ ,  $G\alpha_{14}$ ,  $G\alpha_{15}$ , and  $G\alpha_{16}$ ) couple to phospholipase C $\beta$  (PLC $\beta$ ), which hydrolyzes phosphatidylinositol 4,5-bisphosphate (PIP $_2$ ) into inositol 1,4,5-trisphosphate (IP $_3$ ) and diacylglycerol. Accumulation of IP $_3$  results in intracellular calcium release, which signals through a variety of cascades depending on the cell type. Aside from PLC $\beta$ ,  $G\alpha_{q/11}$  can signal through p63RhoGEF to induce Rho GTPase activation (20,21) and regulate actin/myosin dynamics.  $G\alpha_{q/11}$  proteins are also expressed in all tissues, serving critical roles in both heart and skeletal muscle through promotion of excitation-contraction coupling via calcium release and Rho activation. The  $G\alpha_{12}$  family consists of  $G\alpha_{12}$  and  $G\alpha_{13}$ , ubiquitously expressed proteins that activate Rho via initial activation of RhoGEF. Rho-GTP then activates downstream effector kinases to regulate actin polymerization and cytoskeleton remodeling. Through these actions,  $G\alpha_{12/13}$  is responsible for regulating cell migration and proliferation, highlighting its significance in certain metastatic cancers ((19,22) and references therein).

GPCRs are also classified based on the specific G proteins they couple to; however, many GPCRs signal through multiple types of G proteins (4), resulting in activation of a variety of signaling pathways through both the  $G\alpha$  subunit and the  $\beta\gamma$  subunit. Examining the G protein specificity of GPCRs has been a hotbed of scientific study, and unique properties of certain G proteins have been instrumental in aiding the field. Specifically,  $G\alpha_s$  and  $G\alpha_{i/o}$  have residues that



are covalently modified by certain bacterial toxins. Pertussis toxin (PTX) ADP-ribosylates a specific cysteine residue at the extreme C-terminus of  $G_{\alpha i/o}$  proteins, which blocks the capacity of the G protein to couple to activated GPCRs. Cholera toxin catalyzes the attachment of an ADP-ribose group to  $G_{\alpha s}$  and certain  $G_{\alpha i}$  family members, resulting in constitutively active G proteins (22). Identifying the specific G proteins that known GPCRs couple to will continue to be of great therapeutic interest, and will ultimately lead to the discovery of drugs with greater target specificity.

Aside from the conventional GPCR, G protein, and effector protein cascade, there are other hallmarks of GPCR-dependent G protein signaling that increase its complexity. Not only does the  $G_{\alpha}$  subunit become activated following receptor stimulation, but  $G\beta\gamma$  also becomes activated depending on the signal.  $G\beta\gamma$  released from  $G_{\alpha i}$  has been shown to activate ERK through phosphatidylinositol 3-kinase (PI3K) following  $G_{\alpha i}$ -coupled GPCR activation (23,24), indicating that  $G_{\alpha i}$ -linked GPCRs transduce signals through multiple cellular pathways.  $\beta\gamma$  subunits also bind and regulate the activation of both G protein-coupled inward rectifying potassium (GIRK) channels and N and P/Q calcium channels. In addition,  $\beta\gamma$  dimers have also been shown to bind G protein-coupled receptor kinases (GRKs) to regulate receptor desensitization, activate PLC $\beta$ , and also indirectly regulate Rac GTPase ((25) and references therein). Studies are showing that  $\beta\gamma$  dimers can signal through a variety of mechanisms on their own, creating another branch to conventional G protein signaling.

A trademark of most GPCRs is their capacity to internalize following stimulation. GPCRs may undergo desensitization following activation, which is characterized by the decreased responsiveness to agonist binding. Desensitization occurs due to uncoupling of the GPCR from the G protein following phosphorylation of the receptor by second messenger kinases PKA/PKC or GRKs.  $\beta$ -arrestin proteins recognize the GRK-mediated phosphorylated receptor and promote receptor internalization through clathrin-coated vesicles. It is here that receptors are either downregulated through degradation or decreases in receptor transcription, or recycled to

the plasma membrane as resensitized receptors ((26) and references therein). These other components of GPCR signaling are also ideal drug targets for modulating G protein signals, as evidenced by the effects of GRKs and arrestins on morphine efficacy and addiction (27).

Recent work with  $\beta$ -arrestins has suggested that they perform signaling roles similar to, but distinct from, G proteins.  $\beta$ -arrestins can form scaffolding complexes with ERK, resulting in attenuation of ERK functions in the nucleus and promotion of ERK activity within the cytosol.  $\beta$ -arrestins also play roles in apoptosis, as they can bind the oncoprotein MDM2 and suppress its ubiquitination of the tumor suppressor p53 following opioid or bradykinin receptor activation. Related to its role in regulating gene transcription,  $\beta$ -arrestin can also complex with I $\kappa$ B $\alpha$  to attenuate NF- $\kappa$ B nuclear translocation and gene targeting ((28,29) and references therein). Taken together, these findings indicate that  $\beta$ -arrestins may signal on their own following GPCR activation, creating scaffolding complexes with a variety of different proteins to regulate downstream gene transcription.

### **1.3 Unconventional G Protein Signaling**

Growing evidence suggests that G proteins can signal through mechanisms independent of GPCRs, participating in newly appreciated “unconventional” G protein signaling cascades (30,31). Unlike the well-established “conventional” G protein systems that involve a GPCR, a heterotrimeric G $\alpha\beta\gamma$  complex, and an effector protein, these unconventional pathways involve a G $\alpha$  protein and other proteins that substitute for the receptor, effector, and G $\beta\gamma$  in a functional signaling complex (Figure 1.1). Though little is known about the physiological roles of unconventional G protein signaling complexes, evidence suggests that these proteins and their linked signaling pathways regulate key aspects of cell division in lower and higher eukaryotes and synaptic signaling in mammalian brain (30-36). At the center of these unconventional complexes is a family of proteins that share one or more G protein regulatory (GPR) motifs (also

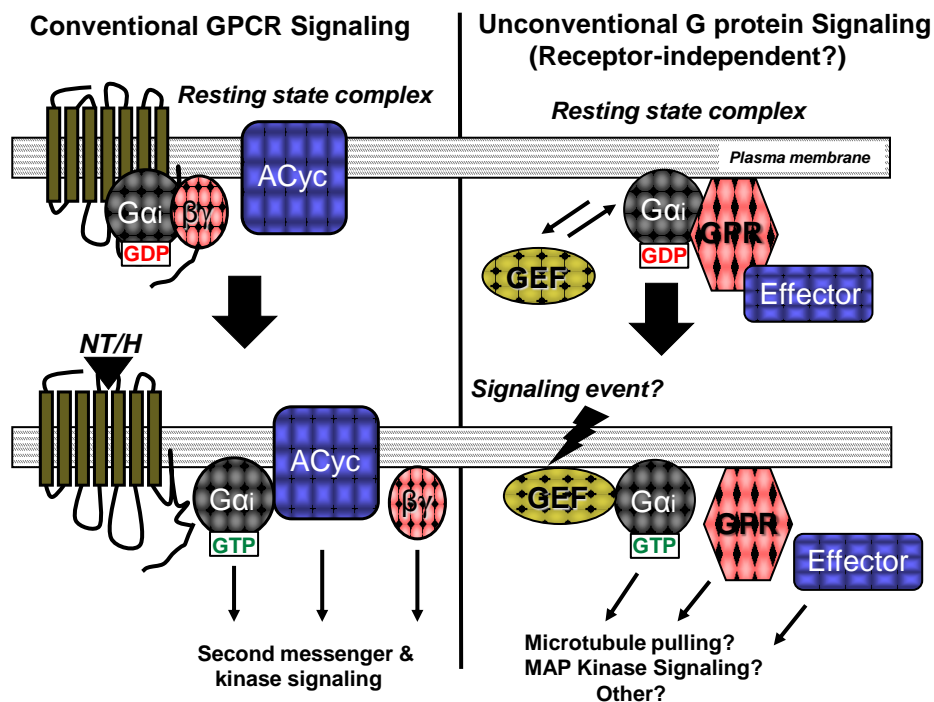


**Figure 1.1. Conventional vs. unconventional G protein signaling.** *Top:* Before stimulation, conventional GPCR/G protein signaling (left) consists of a GPCR, Gαi-GDP bound to Gβγ, and a downstream effector protein (i.e. Adenylyl cyclase; ACyc). In unconventional signaling (right), a cytosolic GEF substitutes for and serves a role similar to that of the GPCR, while the GPR protein, perhaps in complex with an effector, substitutes for Gβγ. *Bottom:* In the presence of a stimulating neurotransmitter or hormone (NT/H), the GPCR exhibits GEF activity toward Gαi, resulting in GTP binding, heterotrimer dissociation, and subsequent Gαi-GTP and Gβγ coupling to the effector protein to regulate signaling pathways. In unconventional signaling, the cytosolic GEF catalyzes GTP exchange on the Gαi subunit, resulting in free Gαi-GTP, GPR protein, and effector that are able to regulate downstream signaling.

known as a GoLoco domain) (30,31,37), which are 19-22 amino acid long motifs that bind selectively to inactive  $G\alpha_i/o$  subunits in the absence of  $G\beta\gamma$  (37,38).

Early evidence for a function of GPR motifs came from studies with the Activator of G protein Signaling 3 (AGS3) protein. AGS3 was reported to activate a pheromone response pathway in *Saccharomyces cerevisiae* independent of a GPCR, and to selectively interact with  $G\alpha$ -GDP instead of  $G\alpha$ -GTP (38). Overexpression of AGS3 in cells was also shown to alter the expression of receptors and ion channels involved in synaptic plasticity, inducing an increase in  $GABA_B$ ,  $M_1$ -muscarinic cholinergic receptor, and the GIRK channel Kir2.1 expression levels (33). These findings suggested a novel mechanism of G protein activation that involved GPR domain-containing proteins functioning in the absence of GPCRs.

In addition to AGS3, the GPR domain-containing protein *mammalian partner of inscutable* (mPins, aka LGN) has been implicated in GPCR-independent signaling. Specifically, the GPR motifs of LGN regulate its capacity to traffick PSD-95 and *N*-methyl *D*-aspartate (NMDA) glutamate receptors within dendritic spines (36). In dividing cells, LGN binds to the Nuclear mitotic apparatus (NuMA) protein to regulate spindle pole formation and microtubule organization during mitosis. Binding of LGN to NuMA prevents NuMA from binding microtubules, suggesting a regulatory mechanism underlying microtubule assembly and orientation (39). This effect is mediated by the GPR motifs of LGN, as  $G\alpha_{i1}$  induces translocation of LGN and NuMA to the apical cortex and facilitates LGN binding to NuMA. A ternary  $G\alpha_{i1}$ :LGN:NuMA complex disregulates spindle pole formation, resulting in chromosome oscillation and rocking during mitosis (40).

Subsequent studies have shown that, in some cases, the GPR motif is capable of forcing dissociation of  $G\alpha\beta\gamma$  heterotrimers to free  $G\alpha$  from  $G\beta\gamma$  (41). When in complex with  $G\alpha$ -GDP, GPR motifs inhibit GDP release from  $G\alpha$  to prevent GTP binding (42-45), thereby exhibiting guanine nucleotide dissociation inhibitor (GDI) activity. Binding and subsequent GDI effects of the GPR motif on  $G\alpha$  are dependent on a conserved acidic glutamine-arginine triad at the end of

the motif, as mutating these residues inhibits AGS3 and RGS14 GPR motif function (reviewed in (31)). In many ways, the resulting effects of GPR association with  $G\alpha$ -GDP functionally resemble those of  $G\beta\gamma$  when in complex with  $G\alpha$ -GDP, implying that  $G\alpha$  can exist in two distinct pools within host cells: one bound to  $G\beta\gamma$  and one bound to GPR proteins. In this scenario,  $G\alpha$  either binds  $G\beta\gamma$  at the plasma membrane or anchors GPR proteins to the plasma membrane. The source(s) of  $G\alpha$  that bind to GPR proteins and how  $G\alpha$  comes to associate with GPR proteins is unclear, but several possibilities exist. Following activation of a GPCR and dissociation of  $G\alpha\beta\gamma$ , free  $G\alpha$  could be captured by a nearby GPR protein immediately after GTP hydrolysis, thereby swapping binding partners (GPR in place of  $G\beta\gamma$ ). Alternatively, a pool of  $G\alpha$ -GDP distinct from that associated with  $G\beta\gamma$  may be sorted/targeted independently for association with GPR proteins for functions unrelated to GPCR signaling. It remains unclear what factor(s) regulates the activation states of GPR: $G\alpha$ -GDP complexes, though recent studies suggest a role for novel non-receptor, cytosolic GEFs (46-48).

Some underlying mechanisms of GPR: $G\alpha$ i signaling were elucidated following the discovery of Resistance to Inhibitors of Cholinesterase (RIC-8; also known as Synembryn) in *Caenorhabditis elegans*, and its mammalian counterparts Ric-8A and Ric-8B (49,50). Unlike GPCRs, Ric-8 proteins exist as soluble cytosolic proteins in the absence of binding partners. However, much like GPCRs, Ric-8A acts as a GEF toward  $G\alpha$ i1,  $G\alpha$ q, and  $G\alpha$ o subunits and only binds the inactive form of these subunits in the absence of  $G\beta\gamma$  to induce GDP release and GTP binding to the subunit (50). In contrast to Ric-8A, Ric-8B exhibits GEF activity toward  $G\alpha$ s (50,51). Because Ric-8A only acts on inactive  $G\alpha$  subunits, it was thought that Ric-8A may act on GPR: $G\alpha$ -GDP protein complexes. Studies designed to test this idea found that purified Ric-8A protein binds and acts on both the purified GPR protein complexes LGN: $G\alpha$ i1-GDP and AGS3: $G\alpha$ i1-GDP, catalyzing nucleotide binding to  $G\alpha$ i1 and subsequently inducing dissociation of these complexes (46,47).  $G\alpha$ i1 simultaneously binds both Ric-8A and the GPR motif of AGS3 to form a transient ternary complex (47). Roles for Ric-8A in regulating microtubule dynamics

are implied by studies showing that Ric-8A is able to displace  $G\alpha_i1$  from LGN:NuMA complexes, causing NuMA to dissociate from LGN and presumably allowing it to bind microtubules (46). Also, both knockdown of Ric-8A expression and disruption of Ric-8A/ $G\alpha_i$  interactions in cells disregulated LGN/NuMA localization and altered normal spindle pole positioning and movements in mitotic cells (52).

Other non-receptor cytosolic proteins besides Ric-8A and Ric-8B have been identified (53,54) that may also serve as GEFs for GPR: $G\alpha_i$  complexes. The newly-discovered protein GIV ( $G\alpha$ -interacting vesicle-associated protein), also known as Girdin, binds inactive  $G\alpha_i3$  to regulate GPCR-independent signaling (54). GIV acts as a non-receptor GEF toward  $G\alpha_i3$ , resulting in an increase in PI3K-induced phosphorylation of Akt and subsequent cancer cell migration (53). Like Ric-8A, GIV also acts on AGS3: $G\alpha_i$ -GDP complexes. Here, GIV induces dissociation of  $G\alpha_i3$  from AGS3, catalyzing GTP exchange on the resulting free  $G\alpha_i3$ . This GEF function on  $G\alpha_i3$  enhances Akt phosphorylation and ultimately triggers anti-autophagic signals within cells (55).

The presence of non-receptor GEF regulation of certain GPR: $G\alpha_i$ -GDP complexes opens a new door into the realm of G protein signaling, illustrating an extensive (though poorly understood) network of unconventional G protein signaling pathways.

#### **1.4 Regulators of G Protein Signaling Proteins**

In canonical G protein signaling, the lifetime of the G protein signal depends on how long  $G\alpha$  remains bound to GTP. The intrinsic rate of  $G\alpha$  GTP hydrolysis measured using purified proteins is much lower than hydrolysis rates examined from  $G\alpha$  proteins in cellular model systems, suggesting the presence of an intracellular G protein regulator that stimulates the rate of  $G\alpha$  GTP hydrolysis (reviewed in (56)). Research into this phenomenon uncovered the first evidence of a new protein class that regulates the intrinsic rate of  $G\alpha$  GTP hydrolysis, specifically the characterization of the *S. cerevisiae* protein Sst2p (57) and the discoveries of the  $G\alpha$ -

interacting proteins GOS8, GAIP, and the *C. elegans* protein EGL-2 (58-60). These proteins were found to share a conserved domain of approximately 130 amino acids, which led to the discovery of the first fifteen members of mammalian Regulators of G protein Signaling (RGS) proteins (59,61).

Presently, there are approximately 40 mammalian RGS protein family members that share a conserved ~130 amino acid RGS domain (62,63). The RGS proteins are classified into eight distinct subfamilies (ten total subfamilies) based on the conserved homology of their RGS domain, from the simple, single domain-containing proteins, to the more complex, multi-domain-containing proteins. These subfamilies include the RZ, R4, R7, R12, RA, guanine nucleotide exchange factor (GEF), GRK, and sorting nexin (SNX), with the R4, R7, and R12 families being the most well-known (62,63). Regardless of subfamily classification, most RGS proteins are GTPase accelerating proteins (GAPs) toward  $G\alpha$  subunits, catalyzing the intrinsic rate of  $G\alpha$  GTP hydrolysis to terminate the G protein signal. The RGS proteins exhibit GAP activity by binding directly to  $G\alpha$  in its GTP hydrolysis transition state (64), locking the  $G\alpha$  switch regions into their transition state to enhance the rate of GTP hydrolysis (reviewed in (62)). The amino acid responsible for RGS-induced GAP activity toward  $G\alpha$  subunits is a conserved glycine residue within the switch I region of  $G\alpha$ , which can be mutated to a serine to block RGS GAP effects (65). The fact that RGS proteins selectively regulate G protein signaling through GPCRs makes them ideal therapeutic targets for diseases caused by abnormalities in G protein signaling pathways.

#### **1.41 RGS Proteins in Physiology and Disease**

Recent studies of RGS proteins have focused mainly on their physiological effects in specific tissues rather than their mechanistic functions as GAPs. For example, RGS proteins have been implicated in immune signaling within B-cell and T-cell lymphocytes. RGS1 has been shown to decrease B-cell migration and intracellular  $Ca^{2+}$  release, ultimately affecting the

capacity of the cell to respond to chemokines (66). Specifically, the chemokine receptors CXCR4 and CXCR5 fail to desensitize in RGS1 knockout (KO) B-cells (67), causing an overall decrease in response to chemokines. Work with RGS2 has shown that loss of RGS2 in mice leads to a decrease in T-cell proliferation and IL-2 production, suggesting impaired T-cell activation (68). T-cells in *Rgs16* transgenic mice display reduced migration capacities following chemokine stimulation through CXCR4 and CCR3 receptors, further supporting the role of RGS proteins in cellular immunology (reviewed in (69)).

In addition to regulating immune responses, RGS proteins are also implicated in cardiovascular physiology and disease. The primary risk factors for heart disease include hypertension, which can be caused by increased cardiac contractility and vasoconstriction. Hypertension leads to cardiac remodeling and ventricular hypertrophy, ultimately reducing the efficiency of the heart to pump blood (70,71). G protein-coupled receptors, specifically angiotensin II, adrenergic, cholinergic, and vasopressin receptors, are highly expressed within cardiac muscle and blood vessels (62,70). Stimulation of  $G\alpha_q$  through cholinergic or angiotensin II receptors activates  $PLC\beta$  and subsequently induces intracellular  $Ca^{2+}$  release. Rises in intracellular calcium stimulate myosin light chain kinase (MLCK) and excitation-contraction coupling (62). Roles for  $PLC\epsilon$  in cardiac signaling have also been established, as  $PLC\epsilon$  is necessary for thrombin-induced ERK activation (72) and can bind muscle-specific A kinase anchoring protein to regulate cardiac hypertrophy (73). RGS2 effects on relieving hypertension (reviewed in (62)) may be due to its strong selectivity toward  $G\alpha_q$ -coupled GPCRs (74) in vascular smooth muscle cells. It is postulated that RGS2-induced  $G\alpha_q$  GTP hydrolysis may limit the lifetime of the  $G\alpha_q$  signal following angiotensin II stimulation (75,76), resulting in a decrease in intracellular calcium release and subsequent vascular smooth muscle relaxation. This is supported by findings showing that RGS2-KO mice have a hypertensive phenotype (77). Human SNPs within the *Rgs2* gene inhibit RGS2 membrane localization, decreasing its capacity to bind and regulate activated  $G\alpha_q$  following vasoconstriction stimuli (78,79).



*Rgs4* gene expression is upregulated in myocardium from patients suffering from heart failure. Endothelin-1 (ET-1) receptor stimulation of PLC $\beta$  through G $\alpha_q$  is disrupted by RGS4, blocking the positive inotropic effects of ET-1 (80). RGS5 is also expressed within vascular smooth muscle and has been implicated in angiogenesis (81) and vasoconstriction through its GAP effects on G $\alpha_q$  stimulated by angiotensin II receptors (82,83). In contrast to RGS2, RGS5 inhibits vasodilation and helps promote tumor angiogenesis (84,85), making RGS5 an ideal target for cancer therapy. Finally, cardiac myocytes of RGS6-KO mice exhibit prolonged activation of GIRK channels following stimulation of the G $\alpha_i$ -linked M<sub>2</sub>-muscarinic cholinergic receptor, resulting in abnormal heart rate (86,87). Together, these findings illustrate the therapeutic potential of targeting RGS proteins in cardiovascular disease.

Nervous system signaling pathways are also regulated by RGS proteins. RGS4 mRNA levels are significantly decreased within the brain motor and prefrontal cortices of schizophrenic patients (88). Transcription of another R4 family member, RGS2, is also altered within brain, particularly during development in response to stimuli that promote synaptic and neuronal plasticity (89). In addition, *Rgs2* gene expression is upregulated in response to antipsychotic drugs that block D<sub>2</sub>-dopamine receptors. Work with RGS2-KO mice show RGS2 is involved in promoting aggression and maintaining normal anxiety levels (68), which may be due to its GAP activity toward both G $\alpha_q$  and G $\alpha_i$ .

Work done with the R7 family member, RGS9, also implicates RGS proteins in nervous system function. RGS9 is transcribed as two isoforms: a short RGS9-1 form that is expressed within the retina, and a longer RGS9-2 form that is almost exclusively expressed within brain striatum (90,91). RGS9-2-KO mice exhibit elevated locomotor activity compared to wild-type mice in response to cocaine treatment, indicating a role for RGS9-2 in attenuating D<sub>2</sub>-dopamine receptor signaling by exhibiting GAP activity toward G $\alpha_i$  (91). In humans, patients with Parkinson's Disease (PD) have elevated levels of RGS9-2 protein in striatum. These levels are inversely regulated by the presence of the dopamine metabolite, L-Dopa (92). In addition, RGS

proteins regulate opioid receptor signaling to alter pain responses. Expression of RGS19 facilitates DOR internalization through GAP effects on G $\alpha$ i, while blocking RGS19 induces morphine tolerance due to opioid receptor desensitization. GIRK channels are deactivated indirectly by RGS4 following DOR and MOR stimulation. This effect is due to RGS4 GAP effects on G $\alpha$ i that promote reassociation of the G protein heterotrimer. Finally, knocking out *Rgs9-2* enhances the analgesic effects of morphine in mice and greatly suppresses their susceptibility to developing morphine tolerance (reviewed in (93)). Collectively, these data implicate RGS9-2 in multiple Central Nervous System (CNS) disease states through its actions as a GAP and also potentially through its role in mediating D<sub>2</sub>-Dopamine receptor desensitization (94).

Cancer signaling pathways are some of the most widely studied due to the high mortality rates of the disease and the resistance of cancer cells to common chemotherapeutic agents. Roles for RGS proteins in cancer were examined and identified following studies looking into the involvement of other proteins participating in cancer signaling, such as receptor tyrosine kinases (RTKs) and GPCRs. Stimulation of the RTK epidermal growth factor receptor (EGFR) promotes proliferation, migration, and differentiation through stimulation of Src kinase, Ras, and Raf kinase. Mutations of proteins within this pathway, particularly overactivated EGFR and Ras, are implicated in an abundance of cancers (95). Some of the most common cancer drugs target RTKs, such as Imatinib and Trastuzumab for treatment of leukemia and breast cancer, respectively (reviewed in (96)). Activation and subsequent signaling of RTKs are thus critical areas of study in the treatment of cancer.

Many GPCRs are implicated in cancers as well, including overexpression of CXCR4, LPA, and endothelin receptors in lung, breast, and skin cancers, respectively (reviewed in (96)). Activation of certain GPCRs have also been shown to transactivate RTK growth factor receptors (97), defining newly-appreciated mechanisms of GPCR-induced tumor growth and metastasis. Stimulation of GPCRs can lead to transactivation of EGFR through activation of Src, Protein

Kinase C (PKC), and rises in intracellular  $\text{Ca}^{2+}$  following  $\text{G}\alpha_q$  activation (reviewed in (98)). Other mechanisms of GPCR-induced EGFR transactivation involve GPCR-mediated activation of metalloproteases that process the EGF-like ligand HB-EGF (99).

Since GPCRs are involved in promoting cancer, it is no surprise that RGS proteins have been implicated in certain cancers. Most R4 family members are upregulated in specific cancers, such as RGS1 in skin and ovarian cancers, RGS4 in ovarian and thyroid cancers, RGS5 in myeloma, melanoma, and hepatocellular cancers, and RGS16 in pediatric leukemia. Other RGS proteins are downregulated, such as RGS2 in ovarian and prostate cancers and RGS13 in mantle cell lymphoma. The R7 family member RGS6 is upregulated in ovarian cancer, while the RA family members Axin1 and Axin2 are downregulated in certain breast, endometrial, and lung cancers (reviewed in (96)). In addition to expression patterns, certain SNPs have been identified in RGS proteins that are associated with cancer. A series of SNPs causing a Ser146Gly mutation in the GEF family member PDZ-RhoGEF reduces the risk of lung cancer in Mexican American smokers, a result that varies according to the nucleic acid base change (100). A SNP in RGS6 is responsible for reducing the risk of bladder cancer by approximately 34%, an effect that is enhanced in smokers (101).

From the immune system to the CNS to cancer, RGS proteins have been implicated in a wide range of diseases and conditions. The molecular mechanisms behind RGS protein effects in disease are not completely known; however, evidence suggests that RGS effects revolve around their GAP activity on  $\text{G}\alpha$  subunits. These findings make RGS proteins attractive drug targets due to their tissue, G protein, GPCR, and disease-state specificity.

#### **1.42 RGS Proteins as Drug Targets**

As discussed above, RGS proteins are proving more and more to be excellent candidates for drug targets in a variety of disease states, including inflammation, heart disease, hypertension, chronic pain, and cancer. Although the interacting residues between the RGS domain and  $\text{G}\alpha$

responsible for RGS GAP function are potential sites for small molecule intervention, other regions and domains of complex RGS proteins are also significant targets due to their interactions with other binding partners that may regulate G proteins and/or other signaling pathways.

The most logical site of intervention for developing drugs that modulate RGS function is the site on either the RGS protein or  $G\alpha$  that is responsible for RGS/ $G\alpha$  interactions. Specific amino acids include the conserved Gly residue in the switch I region of  $G\alpha$  (65), as well as the adjacent Thr residue (in the case of  $G\alpha_i1$ ) that binds the RGS domain at multiple sites (64). Other RGS regions have been postulated as targets following studies showing that  $PIP_2$  inhibits RGS4 GAP activity, while intracellular  $Ca^{2+}$  release facilitates RGS4 activity and subsequent effects on GIRK channels (102,103). Recently, novel small molecule modulators of RGS protein function have been identified using novel high-throughput screening technology (104). The first small molecule regulating RGS function, 1, methyl *N*-[(4-chlorophenyl)sulfonyl]-4-nitrobenzenesulfonimidoate (CCG-4986), was found to inhibit RGS4 GAP activity toward  $G\alpha_o$  and to inhibit RGS4 regulation of cAMP production following MOR stimulation (105). The most potent small molecule inhibitor of an RGS protein, CCG-50014, is 20-times more selective for RGS4 over any other RGS protein. Mechanistically, CCG-50014 covalently modifies RGS4 at two Cys residues in an allosteric site (106). Pharmaceutical research has also uncovered small molecules that maintain RGS/ $G\alpha_q$  complexes in an inactive state following muscarinic receptor activation (107).

The complex structures of various RGS proteins provide means to target these proteins at other regions besides the  $G\alpha$ -interacting site. The DEP domain of RGS7 selectively binds to the  $M_3$ -muscarinic receptor and inhibits  $G\alpha_q$  coupling in a GAP-independent manner (108,109). This effect is inhibited by  $G\beta_5$  binding to the DEP domain (108), suggesting that the DEP domain of RGS7 (and perhaps other R7 family members) may be a novel therapeutic target for modulating  $G\alpha_q$  signaling. Other secondary sites on RGS proteins can be targeted that modulate their degradation since certain RGS proteins are either upregulated or downregulated in disease states.

Some R4 RGS family members can undergo a mechanism of degradation termed the N-end rule pathway (110), which is an extension of the typical ubiquitin pathway. In some instances, the start methionine codon of RGS4, RGS5, and RGS16 is proteolytically cleaved, leaving the second protein residue exposed. These residues (usually charged or aromatic) can then be direct substrates for E3 ubiquitin ligases, resulting in protein proteosomal degradation (reviewed in (111)). Targeting these second residues, such as Cys2 in RGS4 (112), can be crucial in either enhancing or inhibiting degradation of these RGS proteins.

Equally important to identifying small molecule regulators of both RGS GAP activity and the RGS/G $\alpha$  interaction is discovering small molecules that can: modulate RGS protein function through regions outside the RGS domain, disrupt or enhance RGS protein binding partners, and stabilize/destabilize RGS protein expression in cells. The latter two cases create an opportunity to develop drugs with greater RGS protein specificity, which may ultimately lead to targeted RGS protein regulation in the desired tissue(s) of interest.

### **1.5 Regulator of G Protein Signaling 14 (RGS14)**

Regulator of G protein Signaling 14 (RGS14) is a 61 kDa protein classified within the D/R12 subfamily of RGS proteins. The closest relatives of RGS14 are RGS12 and RGS10, although RGS10 is much smaller and shares only a single RGS domain in common with RGS14 (62,113). Besides the conserved RGS domain that confers GAP activity, RGS14 possesses a second G $\alpha$  binding domain (GPR/GoLoco domain) and two Ras/Rap-binding domains (RBDs) (114,115) (Figure 1.2; top). RGS14 acts as a GAP toward activated G $\alpha$ <sub>i/o</sub> subunits; however, it exhibits selective GDI activity toward inactive G $\alpha$ <sub>i1</sub> and G $\alpha$ <sub>i3</sub> subunits through binding of the GPR motif (42,43,115-118). Phosphorylation of RGS14 by PKA at Thr494, which sits adjacent to the GPR motif, enhances the GDI activity of RGS14 approximately 3-fold, while having no effect on its GAP activity (119). The GPR motif interaction with inactive G $\alpha$ <sub>i1/3</sub> is responsible

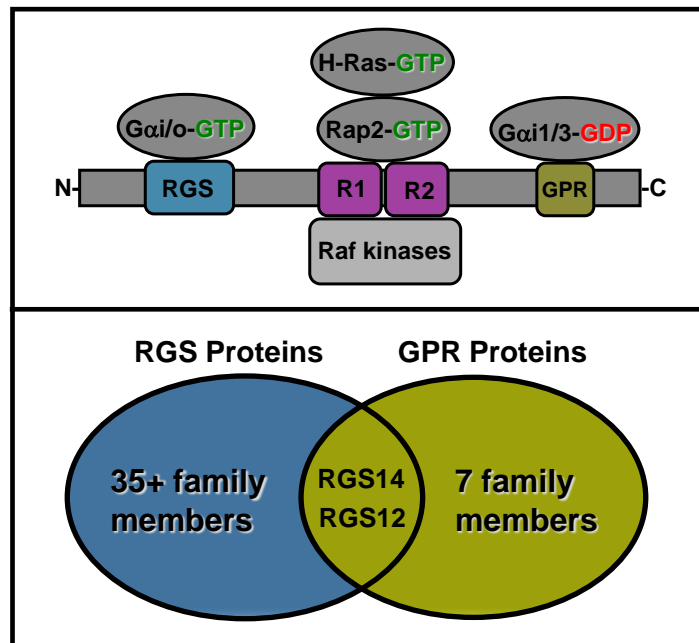


**Figure 1.2. RGS14 domain structure and its identified binding partners.** *Top:* RGS14 directly binds activated G $\alpha$ i family members and G $\alpha$ o through its RGS domain, and it also specifically binds inactive G $\alpha$ i1 and G $\alpha$ i3 via its GPR motif. Activated H-Ras, Rap2, and Raf kinases directly interact with the Ras/Rap-binding domains (R1 and R2). *Bottom:* RGS14 is structurally and functionally unique in that it shares both an RGS domain and a GPR motif that places it and its closest relative RGS12 into both the RGS protein and the Group II AGS protein (GPR motif-containing) subfamilies.

for RGS14 localization at the plasma membrane in cells, as evidenced by the fact that constitutively-activated  $G\alpha$  subunits recruit RGS14 to the plasma membrane weakly compared to inactive subunits (117). The presence of distinct binding sites on both RGS14 and RGS12 for  $G\alpha$  in either its active GTP-bound or inactive GDP-bound form indicates that RGS14 and RGS12 are unique among RGS proteins (Figure 1.2; bottom). Adding to the complexity of RGS14 is its tandem RBDs that bind activated H-Ras, Rap2, and Raf kinases. Since RGS14 was initially discovered as a novel Rap binding partner (114), recent studies have focused on the capacity of RGS14 to bind Ras and Raf through its RBDs. RGS14 preferentially interacts with activated H-Ras (120,121), which binds directly to the first RBD via residue Arg333 (121,122). Through this interaction, RGS14 is able to regulate Ras/Raf-mediated mitogen-activated protein (MAP) kinase signaling in a  $G\alpha_i$ -dependent manner (121). Similarly, RGS12 also binds activated H-Ras and B-Raf via its RBDs and regulates platelet-derived growth factor receptor (PDGF $\beta$ -R) and TrkA receptor signaling (123).

Physiologically, RGS14 is selectively expressed within only a few tissues: thymus, spleen, lymphocytes, and brain (115,116,118,124). Within brain, RGS14 is expressed almost exclusively within neurons of the hippocampal CA2 subregion (118,124). Past attempts to study the biological consequences of knocking out RGS14 proved unsuccessful due to the embryonic lethality of knocking out the gene (125), which was proposed to arise from RGS14's potential role in mitosis (126,127). However, recent work from our lab has shown that RGS14-KO mice are not embryonic lethal, and are in fact perfectly viable (124). Morris water maze and novel object recognition tests showed that loss of RGS14 in mice actually enhances hippocampal-based learning, memory, and cognition, having no effect on other non-hippocampal behaviors. The strong presence of RGS14 within dendritic spines led our lab to examine the effects of RGS14 on long-term potentiation (LTP) and synaptic plasticity (124). We found that even with very active calcium handling in CA2 neurons, loss of RGS14 permits Schaffer collateral synapses in CA2 to now exhibit robust LTP (124). This effect is surprising given that the CA2 subregion typically

displays no LTP (128,129), which strongly suggests that RGS14 is a natural suppressor of LTP in most CA2 synapses. The induction of LTP in RGS14-KO mice is ablated by MEK inhibitors (124), indicating that RGS14 regulation of H-Ras/Raf-mediated MAP kinase signaling may be involved in RGS14's capacity to suppress synaptic plasticity. These findings strongly suggest that the CA2's role in learning and memory is likely dependent on RGS14-containing dendritic spines of CA2 synapses, which does not necessarily include the trisynaptic DG-CA3-CA1 circuit (130-132). Dendritic spines act to limit the synaptic microenvironments with distinct protein expression profiles and calcium handling properties. Of note, we find that a subset of RGS14 protein appears to localize to the PSD of dendritic spines (118,124), indicating that RGS14 is well positioned to modulate signaling events important for synaptic plasticity.

The unique structure and binding partners of RGS14 described above highlight the idea that RGS14 serves as a multifunctional scaffolding protein that integrates G protein and MAP kinase signaling pathways, which may underlie the effects of RGS14 in suppressing learning, memory, and synaptic plasticity within the hippocampus.

### **1.51 RGS14 Modulates Ras/Raf-mediated MAP Kinase Signaling**

RGS14 interacts directly with and regulates the function of signaling proteins that are critically important for synaptic plasticity, learning, and memory. RGS14 was first discovered as a Rap1/2 binding partner (115), and each of the identified RGS14 binding partners  $G\alpha i/o$ , H-Ras, Rap2, and Raf kinases has been shown to control various aspects of synaptic plasticity within hippocampal neurons (133-138). Following an initial report that one of the isolated purified RBDs of RGS14 can interact with H-Ras *in vitro* (122), we and others discovered that RGS14 binds both activated H-Ras and Raf-1 in cells (120,121) to inhibit ERK-mediated MAP kinase signaling by PDGF (121). Activated H-Ras recruits RGS14 to the plasma membrane in the absence of exogenous  $G\alpha i$ , allowing RGS14 to bind Raf-1 and regulate PDGF-induced signaling (121). Co-expressed wild-type  $G\alpha i$  reverses the capacity of RGS14 to inhibit PDGF-induced



ERK phosphorylation because, while bound to G $\alpha$ i1, RGS14 can no longer bind Raf-1 (121). This indicates that RGS14 may act as a molecular switch between binding/regulating G $\alpha$ i1 and binding/regulating Raf-1 and subsequent Raf-1-induced ERK phosphorylation.

Although RGS14 regulates PDGF-induced ERK phosphorylation in an H-Ras- and G $\alpha$ i1-dependent manner (121), how this occurs remains unknown. Various groups have reported unconventional roles for G proteins and interactions of G proteins with receptors that are not GPCRs (for a recent review, see (139)). Relevant to RGS14, recent studies have examined the role of G $\alpha$ i in directly regulating PDGF receptor/ERK-mediated MAP kinase signaling. Pertussis toxin treatment of cells prevents G $\alpha$ i/o-coupling to receptors, which subsequently blocks c-Src activation and ERK phosphorylation by PDGF, indicating a possible role for G $\alpha$ i in PDGF receptor regulation of c-Src signaling (140). Though speculative, it is also possible that pertussis toxin may inhibit the function of non-receptor GEFs (*e.g.* Ric-8A) on G $\alpha$ i (52) to reverse the effects of G $\alpha$ i on c-Src activation, although there is no evidence yet to support this idea. The PDGF $\beta$  receptor is also shown to induce phosphorylation of G $\alpha$ i upon stimulation, which enhances ERK phosphorylation (141). A key element to the involvement of G $\alpha$ i in this process is the potential role of a GPCR. Germane to this point was the discovery that the PDGF $\beta$  receptor interacts with the EDG1 receptor (also known as S1P1), a G $\alpha$ i-linked GPCR (141). Co-expression of both the PDGF $\beta$  receptor and EDG1 stimulates an increase in both G $\alpha$ i phosphorylation and subsequent ERK activation following PDGF treatment (141). How or even if RGS14 participates in PDGF $\beta$ /EDG1 receptor signaling is not known, but these studies highlight potential mechanisms for how RGS14 may switch from binding G $\alpha$ i to binding activated H-Ras and regulating MAP kinase signaling.

### **1.52 RGS14 Participates in Unconventional G Protein Signaling Pathways**

Little evidence suggests RGS14 is involved with conventional GPCR-dependent G protein signaling; however, several examples exist. Overexpression of RGS14 attenuates IL-8-

induced ERK phosphorylation via  $G\alpha_i$  activation, and also impairs serum-response element (SRE) activation via  $M_1$ -muscarinic receptor stimulation (116). RGS14 has also been implicated in MOR signaling, as silencing of RGS14 in mouse periaqueductal gray (PAG) neurons induces GRK-mediated MOR phosphorylation and subsequent internalization in response to morphine (142). Also, very recent findings with RGS14 suggest that other  $G\alpha_i$ -binding regions aside from the RGS domain and GPR motif may be responsible for regulating G protein signaling. Following  $M_2$ -muscarinic receptor activation, RGS14 potentiates RGS4 interactions with both  $G\alpha_i$  and  $G\alpha_o$  and ultimately enhances RGS4-induced GAP activity toward both  $G\alpha$  subunits. These RGS14 effects are independent of the RGS domain, suggesting that another region spanning the RBDs and GPR motif of RGS14 is responsible in facilitating RGS4 GAP effects on  $G\alpha_i/o$  subunits (143). Aside from these few findings, most studies have focused on the unconventional signaling roles of RGS14 that involve GPR motif/ $G\alpha_i$  interactions.

The  $G\alpha_i$ -GDP-interacting GPR motif that is present in RGS14 is a shared and defining feature of the Group II AGS proteins (30). Of note, RGS14 and its closest relative RGS12 are the only RGS proteins (excluding splice variants) among the nearly 40 family members that contain a GPR motif. This attests to the unique multifunctional nature of these two proteins, and also highlights the fact that RGS14 and RGS12 alone sit at the interface of the very distinct mammalian RGS family and the Group II AGS family of signaling proteins (Figure 1.2). RGS14 shares many properties with other GPR proteins in that it: 1) binds  $G\alpha_{i1}$ -GDP and/or  $G\alpha_{i3}$ -GDP independent of  $G\beta\gamma$ , 2) is recruited from the cytosol to the plasma membrane by inactive  $G\alpha_{i1/3}$ -GDP, and 3) can act as a GDI to inhibit nucleotide exchange (30,37,42,43,115-118). In this respect, RGS14 complexes with  $G\alpha_{i1}$ -GDP may serve as signaling complexes in GPCR-independent signaling similar to LGN: $G\alpha_{i1}$ -GDP and AGS3: $G\alpha_{i1}$ -GDP complexes (46,47).

Collectively, these findings support a role of RGS14 in unconventional GPCR-independent signaling. RGS14 forms a stable complex at the plasma membrane with inactive  $G\alpha_{i1}$  and  $G\alpha_{i3}$  via its GPR motif (117), a complex that may be regulated by non-receptor GEFs

similar to LGN:G $\alpha$ i1-GDP and AGS3:G $\alpha$ i1-GDP complexes (46,47). A non-receptor GEF may be the catalyst for inducing RGS14 to switch from binding H-Ras/Raf-1 and regulating MAP kinase signaling (121) to binding G $\alpha$ i and regulating G protein signaling.

## **1.6 Overall Hypothesis and Objective of this Research**

Although much work has examined RGS14 roles in cell division (125-127), our lab has focused on studying the roles of RGS14 with respect to binding inactive G $\alpha$ i1 through its GPR motif and activated H-Ras via its first RBD. Recent work in our lab has shown that RGS14 acts as a scaffold to regulate PDGF and H-Ras/Raf/ERK signaling (121). We demonstrate that RGS14 preferentially binds both activated H-Ras and Raf-1 kinase in cell lysates; however, binding of G $\alpha$ i1 to RGS14 inhibits Raf-1 binding to RGS14. Correlating with this idea is the fact that co-expression of RGS14 with G $\alpha$ i1 in cells inhibits the capacity of RGS14 to block PDGF stimulation, suggesting that RGS14 regulation of PDGF signaling is dependent on Raf-1 binding. Taken together, this data illustrates that RGS14 serves as a molecular switch between binding Ras/Raf-1 and regulating MAP kinase signaling, and binding G $\alpha$ i and regulating G protein signaling. Since we already know some mechanisms underlying how RGS14 can modulate MAP kinase signaling through binding Ras and Raf-1 (121), my thesis project focused on characterizing the RGS14/G $\alpha$ i-GDP interaction via the GPR motif and determining mechanisms by which it may be regulated in cells.

The first aim of this work was to identify whether a non-receptor GEF may regulate the RGS14:G $\alpha$ i-GDP complex, and also how it may do so mechanistically. Studies with other GPR motif-containing proteins have suggested that they can act as substrates for the non-receptor GEF, Ric-8A, when in complex with inactive G $\alpha$ i1 (46,47). Knowing this, I wanted to determine whether Ric-8A could regulate the RGS14:G $\alpha$ i1-GDP complex both in cells and *in vitro* using purified proteins. These findings are discussed in Chapter 2.

The second aim of this project was to study the potential role of a GPCR in regulating the RGS14:G $\alpha$ i complex using live cell bioluminescence resonance energy transfer (BRET). Our interest in GPCR-mediated regulation of this complex was piqued by results showing evidence that GPR proteins can form complexes with GPCRs (144). Ideally, I also wanted to examine the impact of the non-receptor GEF found in Aim 1 on any GPCR-mediated regulation of the RGS14:G $\alpha$ i1 complex. These findings are discussed in Chapter 3.

The final aim of this research was to elucidate the regulatory mechanisms of RGS14 interactions with activated H-Ras in live cells. Specifically, I wanted to explore how both inactive and active G $\alpha$ i and GPCRs could regulate RGS14/H-Ras interactions, and how H-Ras could regulate RGS14 interactions with G $\alpha$ i1 and receptors. Finally, I wanted to determine how these interactions translated to regulating GPCR signaling. These findings are discussed in Chapter 4.

Collectively, the goal of this research project was to characterize RGS14 interactions with G $\alpha$ i through its GPR motif, and to identify ways in which this interaction can be regulated. Elucidating these mechanisms will help us understand exactly how RGS14 may act as a molecular switch from binding Ras/Raf-1 and regulating MAP kinase signaling to binding G $\alpha$ i and regulating G protein signaling. Finally, these studies will clarify potential mechanisms underlying the physiological effects of RGS14 regulation of both G protein and MAP kinase signaling in the hippocampus, especially how it serves as a brake in promoting synaptic plasticity (124).

**CHAPTER 2:**

**Activation of the Regulator of G protein Signaling 14 (RGS14):G*α*i1-GDP signaling complex is regulated by Resistance to Inhibitors of Cholinesterase-8A (Ric-8A)<sup>2</sup>**

<sup>2</sup>This chapter has been slightly modified from the published manuscript. Vellano CP, Shu FJ, Ramineni S, Yates CK, Tall GG, and Hepler JR. (2011) Activation of the Regulator of G protein Signaling 14 (RGS14):G*α*i1-GDP signaling complex is regulated by Resistance to Inhibitors of Cholinesterase-8A (Ric-8A). *Biochemistry*. 50: 752-62.

## 2.1 Introduction

Conventional models of G protein signaling (14,145) indicate that activated G protein-coupled receptors (GPCRs) serve as guanine nucleotide exchange factors (GEFs) toward coupled heterotrimeric ( $G\alpha\beta\gamma$ ) G proteins. GPCR activation facilitates GDP release and subsequent GTP binding to the  $G\alpha$  subunit, which is followed by  $G\beta\gamma$  dissociation from  $G\alpha$ -GTP. This allows free  $G\beta\gamma$  and  $G\alpha$ -GTP to engage downstream effectors and linked signaling pathways. The lifetime of this signaling event is terminated by the regulators of G protein signaling (RGS) proteins, a large family of multifunctional signaling proteins that regulate the intrinsic GTPase activity of the  $G\alpha$  subunit and promote heterotrimer reassociation (113,146,147).

RGS14 is a highly unusual RGS protein that is enriched in brain (115,118) and binds to  $G\alpha_{i/o}$  and H-Ras/Raf to integrate G protein and MAP kinase signaling pathways (121). RGS14 contains a conserved RGS domain, two adjacent Ras/Rap-binding domains (RBDs), and a G protein regulatory (GPR; also known as a GoLoco [GL]) motif (114,115). Like all RGS proteins, the RGS domain of RGS14 binds directly to active  $G\alpha$  (specifically  $G\alpha_i$  and  $G\alpha_o$ ) to serve as a non-selective GTPase Activating Protein (GAP) toward both of these  $G\alpha$  subunits (115,116,118). Unlike other RGS proteins, the GPR motif of RGS14 binds directly to inactive  $G\alpha_{i1}$ -GDP and  $G\alpha_{i3}$ -GDP to inhibit guanine nucleotide binding and exchange (42,43,117). Furthermore, the GPR motif of RGS14 forms a tight complex at the plasma membrane with inactive  $G\alpha_{i1}$  and  $G\alpha_{i3}$  independent of  $G\beta\gamma$  (117), suggesting RGS14 serves a different role in G protein signaling compared to other RGS proteins.

Independent of conventional GPCR/G protein signaling, several unconventional G protein signaling pathways have been described recently that are involved in cell division and synaptic signaling (30-34,36,148). Ric-8A (Synembryn) is a cytosolic protein reported to bind to and act as a non-receptor GEF for  $G\alpha_{i1}$ ,  $G\alpha_q$ , and  $G\alpha_o$  proteins (50). Ric-8A recognizes inactive  $G\alpha$ -GDP proteins when they are in complex with several GPR-motif containing proteins, including LGN/mPins and Activator of G protein Signaling 3 (AGS3). Like RGS14, LGN/mPins

and AGS3 bind directly to inactive G $\alpha$ i (46,47), with LGN also being recruited to the plasma membrane by G $\alpha$ i1 (40). However, unlike RGS14, these proteins lack an RGS domain.

Given these similarities between RGS14, LGN/mPins, and AGS3, we sought to investigate if RGS14 functionally interacts with Ric-8A to regulate unconventional G protein signaling. Here we report that RGS14 is the first example of an RGS protein that also serves as a GPR protein, forming a complex with G $\alpha$ i1-GDP that is regulated by Ric-8A. We show that Ric-8A interacts with RGS14 in cells and acts on the RGS14:G $\alpha$ i1-GDP protein complex *in vitro*, thereby promoting complex dissociation to affect the activation state of G $\alpha$ i1. Moreover, we demonstrate that native RGS14 and Ric-8A co-exist within the same hippocampal neurons, further supporting a functional link between these two proteins. Taken together, these findings demonstrate that RGS14 serves as a multifunctional GPR protein in addition to an RGS protein. We therefore propose a working molecular model to describe how Ric-8A could regulate RGS14:G $\alpha$ i1 signaling functions in cells.

## **2.2 Experimental Procedures**

*Plasmids and antibodies:* The rat RGS14 cDNA used in this study (Genbank accession number U92279) was acquired as described (118). Glu-Glu (EE) tagged recombinant G $\alpha$ i1 plasmid was purchased from UMR cDNA Resource Center (Rolla, Missouri). The plasmids encoding full-length RGS14 and RGS14 deletion mutants coding for amino acids 213-544 and 444-544 cloned in-frame into pcDNA3.1 (Invitrogen) were prepared as described previously (117). Oligonucleotides encoding the 8 amino acid Flag tag (Asp-Tyr-Lys-Asp-Asp-Asp-Asp-Lys) were used to generate N-terminally Flag-tagged RGS14. His<sub>6</sub>-G $\alpha$ i1 (N149I) derived from *Escherichia coli* was generated by changing bases AAC of the rat G $\alpha$ i1 cDNA to ATA using the QuickChange site-directed mutagenesis kit (Stratagene), resulting in an amino acid change of N to I. Truncated His<sub>6</sub>-G $\alpha$ i1 (termed G $\alpha$ i1- $\Delta$ CT throughout the text) derived from *E. coli* was made

by deleting the last 11 amino acids (IKNNLKDCGLF) of the rat G $\alpha$ i1 and cloning the resulting cDNA in-frame into pET20b vector.

Anti-Flag M2 agarose beads, anti-Flag antibody, and anti-Flag HRP antibody were purchased from Sigma. Other antisera include anti-GFP antibody (Clontech), anti-His antibody (Covance), anti-Ric-8A antiserum (a gift from Dr. Greg Tall), anti-G $\alpha$ i1 antibody (Santa Cruz), anti-EE antibody (BD Biosciences), anti-RGS14 antibody (Antibodies, Inc.), a rhodamine-conjugated mouse secondary IgG (Jackson), Alexa 553 goat anti-rabbit secondary IgG (Invitrogen), Alexa 546 goat anti-mouse secondary IgG (Invitrogen), Alexa 488 goat anti-rabbit secondary IgG (Invitrogen), Alexa 633 goat anti-mouse secondary IgG (Invitrogen), peroxidase-conjugated goat anti-mouse IgG antisera (Rockland Immunochemicals, Inc.), and peroxidase-conjugated goat anti-rabbit IgG antisera (Bio-Rad).

*Cell Culture:* HeLa cells were maintained in Dulbecco's modified Eagle's medium (DMEM) with sodium pyruvate and glutamate supplemented with 10% fetal bovine serum (FBS) and a mixture of 100 U/mL penicillin plus 100  $\mu$ g/mL streptomycin (Sigma). Cells were incubated at 37°C with 5% CO<sub>2</sub>.

*Cell transfection and anti-Flag immunoprecipitation:* HeLa cells were obtained from the American Type Culture Collection (ATCC). Transfections were performed using previously described protocols with Lipofectamine 2000 (Invitrogen) (117). Cells were transiently transfected with CFP-Ric-8A and pcDNA3.1, wild-type G $\alpha$ i1-EE, Flag-RGS14 (full-length), and Flag-RGS14 truncation mutants 213-544 and 444-544 either alone or in combination. Eighteen hours post-transfection, cells were lysed in buffer containing 50 mM Tris-HCl, pH 8.0, 150 mM NaCl, 1 mM EGTA, 1 mM EDTA, 2 mM dithiothreitol, 10 mM MgCl<sub>2</sub>, protease inhibitor cocktail (Roche), and 1% TritonX-100. Lysates were incubated on a 4°C rotator for 1 hour, and then cleared by centrifugation at 100,000 x g for 30 mins at 4°C. Lysates were incubated with 50  $\mu$ g anti-Flag M2 resin for 1.5 hours on a 4°C rotator. Resin was washed with ice-cold TBS four times and proteins were eluted by addition of Laemmli sample buffer and subsequent boiling for



5 mins. Samples were resolved by SDS-PAGE, transferred to nitrocellulose membranes, and blotted with anti-Flag HRP, anti-GFP, and anti-EE antibodies followed by appropriate secondary antibodies. Proteins were detected by enhanced chemiluminescence.

*Immunoprecipitation of pure proteins:* 10  $\mu$ g of wild-type His<sub>6</sub>-G $\alpha$ i1 (WT), His<sub>6</sub>-G $\alpha$ i1 (N149I), or His<sub>6</sub>-G $\alpha$ i1- $\Delta$ CT protein derived from *E. coli* lysates was mixed alone or with 5  $\mu$ g of either purified full-length TxHis<sub>6</sub>-RGS14 or His<sub>6</sub>-YFP-Ric-8A (referred to as YFP-Ric-8A). YFP-Ric-8A was made as described (47). Proteins were diluted in buffer containing 20 mM HEPES, 150 mM NaCl, 2 mM dithiothreitol, 1 mM EDTA, and protease inhibitor cocktail. Proteins were incubated with 50  $\mu$ g Protein G sepharose resin (GE Healthcare) and immunoprecipitated with either anti-RGS14 antibody or anti-Ric-8A antibody at 4°C for 3 hours. Resin was washed with ice-cold TBS four times and proteins were eluted by addition of Laemmli sample buffer and subsequent boiling for 5 mins. Samples were resolved by SDS-PAGE, transferred to nitrocellulose membranes, and blotted with anti-His, anti-Ric-8A, and anti-G $\alpha$ i1 antibodies followed by appropriate secondary antibodies. Proteins were detected by enhanced chemiluminescence.

*Immunofluorescence and confocal imaging:* Transfected HeLa cells were fixed at room temperature for 10 mins with buffer containing 20 mM PIPES, pH 7.0, 0.5 mM EGTA, 1 mM MgCl<sub>2</sub>, 1 mM glutaraldehyde, 1 g/mL aprotinin, 0.1% TritonX-100, 2 mM taxol, and 2% paraformaldehyde. Cells were then blocked for 1 hour at room temperature in PBS containing 10% goat serum and 3% bovine serum albumin. Next, cells were incubated in this same buffer with a 1:1000 dilution of rabbit anti-Flag and/or mouse anti-EE antibodies overnight at 4°C. Cells were washed with PBS (3X) and incubated with 1:200 dilutions of Alexa 553 goat anti-rabbit and Alexa 633 goat anti-mouse secondary antibodies at room temperature for 1 hour. Cells were washed with PBS again (3X) and mounted with Vectashield mounting medium (Vector Laboratories). Confocal images were taken using a 63x oil immersion objective from a LSM510

laser scanning microscope (Zeiss). Images were processed using the Zeiss LSM image browser (version 2.801123) and Adobe Photoshop 7.0 (Adobe Systems).

*Immunohistochemistry (IHC) and confocal imaging of mouse brain thin sections:* To obtain brain thin sections, C57BL6 wild-type mice were perfused with saline and then with 4% paraformaldehyde. Brains were isolated, post-fixed in 4% paraformaldehyde, and then embedded in paraffin. After embedding, thin sections were cut. For IHC analysis, brain thin sections were de-paraffinized and pre-treated by microwaving in 1X citrate buffer (0.001 M citrate monohydrate in distilled water, pH 6.0). Sections were treated with 3% H<sub>2</sub>O<sub>2</sub> and blocked with 2% goat serum in Tris-Brij buffer (0.1 M Tris-Cl, 0.1 M NaCl, 0.025 M MgCl<sub>2</sub>, and .075% Brij 35) for 15 mins. Sections were incubated with anti-Ric-8A and anti-RGS14 antibodies overnight at 4°C, and then incubated with either Alexa 546 anti-mouse and Alexa 488 anti-rabbit fluorescent secondary antibodies or anti-mouse and anti-rabbit biotinylated secondary antibodies (Vector Laboratories). Following biotinylated secondary antibody incubation, sections were incubated with avidin-biotin-peroxidase complex, and color was developed with 3, 3'-diaminobenzidine. Control sections were stained with antibody that was pre-blocked with either Ric-8A or RGS14 pure protein (10:1 ratio of protein to antibody). Confocal images were taken and processed as described above. IHC images were taken using a Nikon double-headed microscope.

*Pure protein dissociation assays:* Purified TxHis<sub>6</sub>-ΔRGS14 (encoding amino acids 299-544, including the RBD domains and GPR motif) was created as described (118). Pre-formed ΔRGS14:Gαi1-GDP protein complex was created by mixing 85 μg pure His<sub>6</sub>-Gαi1-GDP with 25 μg pure TxHis<sub>6</sub>-ΔRGS14 at 4°C for 90 minutes. Sample was then separated over a tandem Superdex S75+S200 size-exclusion gel filtration apparatus in buffer containing 50 mM HEPES, pH 8.0, 1 mM EDTA, 150 mM NaCl, and 2 mM dithiothreitol. Elution volume containing the protein complex (500 μL of fraction corresponding to total elution volume 18000 μL – 18500 μL) was taken and mixed with 50 μM GTPγS and 10 mM MgCl<sub>2</sub> either alone or with a 5-fold excess

of YFP-Ric-8A pure protein over  $\Delta$ RGS14 for 15 mins at 30°C. In other dissociation assays, pre-formed  $\Delta$ RGS14:G $\alpha$ i1-GDP complex was collected and mixed with a 30-fold excess of YFP-Ric-8A only, without GTP $\gamma$ S. After treatment, the sample was then reapplied to the gel filtration column, and resulting fractions were collected and subjected to SDS-PAGE and immunoblot analysis. Blots were probed with anti-His and anti-Ric-8A antibodies. For YFP-Ric-8A:G $\alpha$ i1 complex formation, 9  $\mu$ g YFP-Ric-8A was incubated with 30  $\mu$ g His<sub>6</sub>-G $\alpha$ i1-GDP at 4°C for 90 minutes in the buffer described above and then applied over tandem S75+S200 gel filtration columns as described above.

*GTP $\gamma$ S binding assays:* GTP $\gamma$ S binding studies were performed as previously described (149). Briefly, 2  $\mu$ M His<sub>6</sub>-G $\alpha$ i1-GDP (diluted in 20 mM HEPES and 50 mM NaCl) was incubated with 2  $\mu$ M (final concentration) [<sup>35</sup>S]GTP $\gamma$ S (10,000 cpm/pmol) with or without amounts of TxHis<sub>6</sub>- $\Delta$ RGS14 (25  $\mu$ M) and YFP-Ric-8A (either 5  $\mu$ M or 125  $\mu$ M) at 30°C in reaction buffer (20 mM HEPES, 100 mM NaCl, 1 mM dithiothreitol, 2 mM MgSO<sub>4</sub>, and 1 mM EDTA). Reactions were done in triplicate and stopped at the indicated time points in ice cold stop buffer (20 mM Tris, 200 mM NaCl, 2 mM MgSO<sub>4</sub>, and 1 mM GTP), quickly filtered over nitrocellulose membranes, and washed twice with wash buffer (50 mM Tris, 200 mM NaCl, and 2 mM MgSO<sub>4</sub>). Scintillation fluid (MP Biomedicals) was added to filters, and then filters were subjected to scintillation counting. The amount of [<sup>35</sup>S]GTP $\gamma$ S bound to the filters was quantified, and the measurements at the 0 min time point were subtracted out as background. Data are presented as mean  $\pm$  S.E.M. When testing the activity of the G $\alpha$ i1 mutants, the exact same protocol was performed using 2  $\mu$ M G $\alpha$ i1-WT, G $\alpha$ i1 (N149I), and G $\alpha$ i1- $\Delta$ CT alone for 0 min, 5 min, and 10 min time points.

*Steady-state GTPase assays:* Steady-state GTPase assays were performed as described (149,150) at 30°C in buffer A that contained 20 mM HEPES, 100 mM NaCl, 1 mM EDTA, 2 mM MgCl<sub>2</sub>, and 0.05% Lubrol. His<sub>6</sub>-G $\alpha$ i1-GDP (0.5  $\mu$ M) and either full-length TxHis<sub>6</sub>-RGS14 or truncated TxHis<sub>6</sub>- $\Delta$ RGS14 (0.3  $\mu$ M) were incubated for 15 min at 4°C and YFP-Ric-8A (1.5  $\mu$ M)

was added just before initiation of the reaction. To initiate the steady-state reaction, 0.4  $\mu\text{M}$  [ $\gamma$ - $^{32}\text{P}$ ]GTP (specific activity 200 cpm/pmol) in 100  $\mu\text{L}$  buffer A was added. At 5 minute intervals, from 0 to 20 minutes, triplicate aliquots were removed and added to 1 mL of ice cold 5% (w/v) activated charcoal to stop the reactions. The charcoal was pelleted at 4000 x g and the clear supernatant was removed and added to scintillation vials. The resulting [ $^{32}\text{P}$ ]i released in the supernatant was measured by scintillation counting. Data are presented as mean  $\pm$  S.E.M.

For steady-state GTPase experiments measuring the effects of protein concentration on response, various concentrations of full-length TxHis<sub>6</sub>-RGS14 ranging from 0 to 8.0  $\mu\text{M}$  (0 nM, 10 nM, 30 nM, 100 nM, 300 nM, 1000 nM, 3000 nM, and 8000 nM) were incubated with 0.5  $\mu\text{M}$  His<sub>6</sub>-G $\alpha$ i1-GDP for 15 min at 4°C. YFP-Ric-8A (1.5  $\mu\text{M}$ ) was added just before initiation of the reaction. To initiate the steady-state reaction, 0.4  $\mu\text{M}$  [ $\gamma$ - $^{32}\text{P}$ ]GTP (specific activity 200 cpm/pmol) in 100  $\mu\text{L}$  buffer A (see above) was added. After 10 minutes, triplicate aliquots were removed and added to 1 mL of ice cold 5% (w/v) activated charcoal to stop the reactions. The charcoal was pelleted at 4000 x g and the clear supernatant was removed and added to scintillation vials. The resulting [ $^{32}\text{P}$ ]i released in the supernatant was measured by scintillation counting. Data are presented as mean  $\pm$  S.E.M.

### **2.3 Results**

*RGS14 and Ric-8A localize at the plasma membrane with Gai1.* RGS14 is unusual among RGS proteins in that it contains not only an RGS domain that binds active G $\alpha$ i1-GTP, but also a GPR motif that binds *inactive* G $\alpha$ i1-GDP. Therefore, we sought to determine whether RGS14 is the first example of an RGS protein that functionally interacts with Ric-8A, a reported cytosolic GEF that regulates certain GPR proteins. A strong indicator of functional interaction between proteins is their capacity to co-localize together in a cellular environment. Therefore, we

examined the localization of both Ric-8A and RGS14 in cells in the presence and absence of co-expressed G $\alpha$ i1-GDP (Fig. 2.1). Flag-RGS14, YFP-Ric-8A, and wild-type G $\alpha$ i1-EE were transfected alone and in combination into HeLa cells. Cells were fixed, stained with anti-Flag and anti-EE antibodies, and analyzed for immunofluorescence by confocal microscopy (Fig. 2.1). When expressed alone in HeLa cells, wild-type G $\alpha$ i1 localizes at the plasma membrane whereas Ric-8A and RGS14 each predominately localize within the cytosol (Fig. 2.1A); a small amount of RGS14 is visible at the plasma membrane. When both RGS14 and Ric-8A are co-expressed, they remain mostly cytosolic (Fig. 2.1B; top). When either RGS14 or Ric-8A is co-expressed with wild-type G $\alpha$ i1, there is a noticeable translocation of both RGS14 and Ric-8A to the plasma membrane, respectively (Fig. 2.1B; middle). A small portion of Ric-8A remains localized within the cytosol. Since expression of G $\alpha$ i1 induces translocation of RGS14, the small amount of RGS14 visible at the plasma membrane in Fig. 2.1A may be due to the presence of native G $\alpha$ i1 recruiting RGS14 to the membrane. When RGS14 and Ric-8A are expressed together with wild-type G $\alpha$ i1 (Fig. 2.1B; bottom), both RGS14 and Ric-8A translocate from the cytosol to co-localize with G $\alpha$ i1 at the plasma membrane. The Ric-8A that had remained cytosolic following co-expression with wild-type G $\alpha$ i1 was now localized at the plasma membrane, suggesting that these three proteins may functionally interact at the plasma membrane. Taken together, it appears that the major driving force behind RGS14 and Ric-8A membrane localization is the presence of G $\alpha$ i1, which is consistent with the possibility that RGS14 and Ric-8A may be acting on a common G $\alpha$ i1 subunit in a functional signaling complex.

*Ric-8A stimulates dissociation of the RGS14:Gai1-GDP complex in cells.* These findings prompted us to examine if RGS14, Ric-8A, and G $\alpha$ i1 physically interact in cells. We previously demonstrated that RGS14 can form a stable complex with G $\alpha$ i1 that can be recovered from cells by co-immunoprecipitation (117). Here we tested whether RGS14 can interact with Ric-8A in cells (Fig. 2.2A). HeLa cells were transfected with CFP-Ric-8A together with either full-length Flag-RGS14 or truncated forms of RGS14 that were missing either the RGS domain (construct

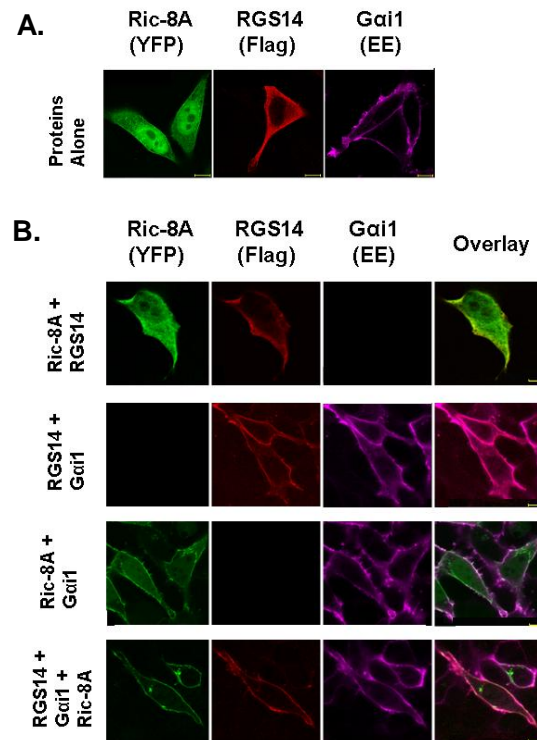


**Figure 2.1. RGS14 and Ric-8A are recruited to the plasma membrane by wild-type Gai1.** Ric-8A and RGS14 translocate from the cytosol to the plasma membrane in the presence of wild-type Gai1. Flag-RGS14, YFP-Ric-8A, and wild-type Gai1-EE were transfected either alone (A) or in combination (B) into HeLa cells. Cells were fixed, subjected to immunofluorescence, and analyzed using confocal microscopy as described in Experimental Procedures. Scale bars represent 10  $\mu$ m. Images are representative of cells observed in three separate experiments.

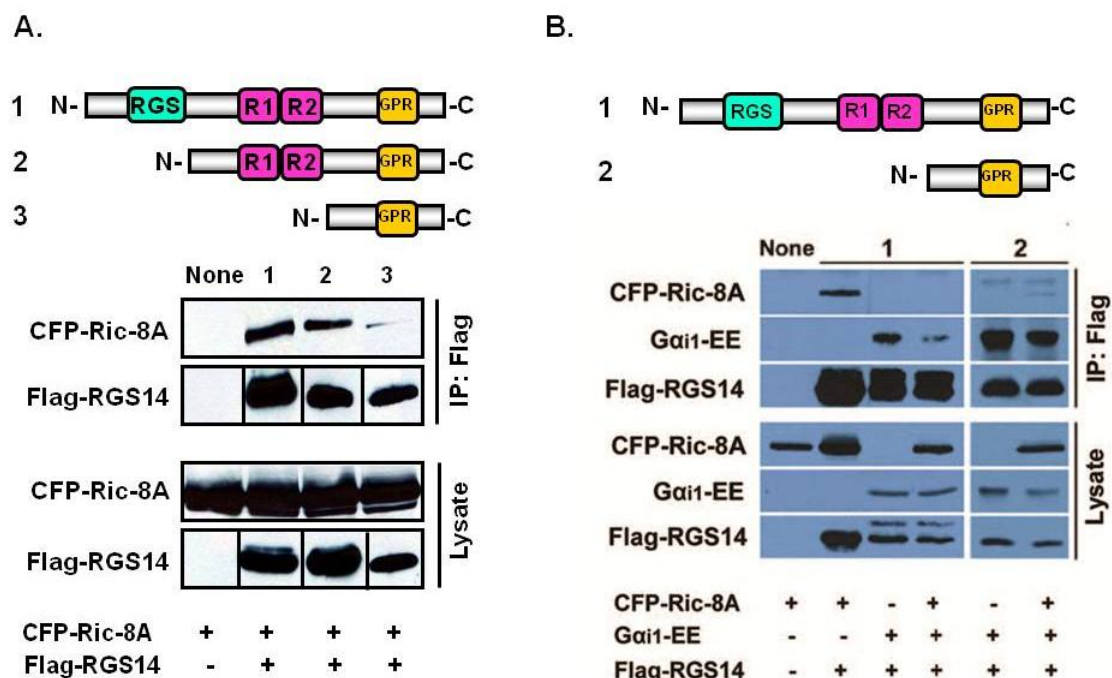


**Figure 2.2. Ric-8A induces dissociation of the RGS14:Gai1-GDP complex in cells.** Ric-8A induces a decrease in Gai1 binding to RGS14 in HeLa cells. (A), CFP-Ric-8A was transfected into HeLa cells with either pcDNA3.1 (None), full-length Flag-RGS14 expressing amino acids 1-544 (1), truncated Flag-RGS14 expressing amino acids 213-544 (2), or Flag-RGS14 expressing amino acids 444-544 (3). Cells were lysed and subjected to anti-Flag immunoprecipitation, SDS-PAGE, and immunoblot. To simplify the figure, Flag-RGS14 truncation bands were cropped from their lower molecular weight positions and inserted to form one horizontal line of bands. Results are indicative of three replicate experiments. (B), Combinations of pcDNA3.1, CFP-Ric-8A, Flag-RGS14, and wild-type Gai1-EE were transfected into HeLa cells (left-most gel). Cells were lysed and subjected to anti-Flag immunoprecipitation. Recovered proteins were subjected to SDS-PAGE and immunoblot. The right-most gel shows results from lysates transfected with combinations of pcDNA3.1, CFP-Ric-8A, wild-type Gai1-EE, and truncated Flag-RGS14 expressing amino acids 444-544 (which does not bind Ric-8A). pcDNA3.1 was transfected in all double-transfections to bring the DNA concentration up to that of a triple-transfection (CFP-Ric-8A+Flag-RGS14+Gai1-EE). This figure is representative of three separate experiments.

expressing amino acids 213-544) or both the RGS domain and the tandem RBDs (construct expressing amino acids 444-544). Ric-8A was recovered together with both full-length RGS14 and RGS14 missing the RGS domain, but not with RGS14 missing the RGS domain and the tandem RBDs (Fig. 2.2A).

We next examined whether Ric-8A stimulates the dissociation of an RGS14:G*ai*1-GDP complex in cells (Fig. 2.2B). CFP-Ric-8A, wild-type G*ai*1-EE, full-length Flag-RGS14, or the truncated Flag-RGS14 expressing residues 444-544 were transfected alone and in combination into HeLa cells. Cell lysates were subjected to a Flag-immunoprecipitation (IP). In the absence of expressed wild-type G*ai*1, Ric-8A interacts with full-length RGS14 (and does not interact non-specifically with the anti-Flag beads). In the absence of expressed Ric-8A, both full-length and truncated RGS14 strongly interact with wild-type G*ai*1. However, when Ric-8A and wild-type G*ai*1 are co-expressed with full-length RGS14, binding of Ric-8A to RGS14 is eliminated and binding of G*ai*1 to RGS14 decreases significantly (Fig. 2.2B). By contrast, the truncated form of RGS14 missing the apparent Ric-8A binding region (see Fig. 2.2A) remains bound to G*ai*1 in the presence of Ric-8A (Fig. 2.2B).

*Purified Ric-8A stimulates dissociation of the purified RGS14:Gai1-GDP complex in vitro.* Our findings thus far (Figs. 2.1 and 2.2) are consistent with the idea that Ric-8A recognizes the RGS14:G*ai*1-GDP complex and stimulates dissociation of the complex in cells, thereby causing release of G*ai*1 (and possible binding of Ric-8A to free G*ai*1). To test this idea directly, we examined Ric-8A interactions with RGS14 and G*ai*1 using purified proteins (Fig. 2.3). Purified YFP-Ric-8A (47), RGS14, and G*ai*1-GDP were mixed in various combinations and then subjected to size-exclusion gel chromatography to examine complex formation. Because expression of full-length recombinant RGS14 yields limiting amounts of functional full-length RGS14, we utilized a more stable truncated form of RGS14 for these studies that lacks the RGS domain ( $\Delta$ RGS14) (118). Ric-8A forms a stable complex with G*ai*1-GDP as shown by a shift toward a higher molecular weight when compared to the Ric-8A monomer (Fig. 2.3, A-B). With



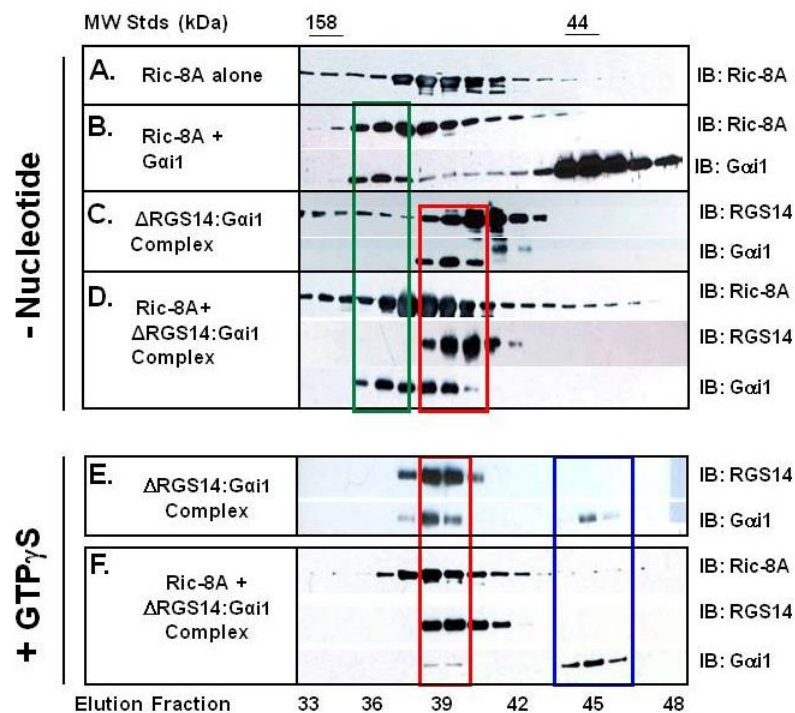


**Figure 2.3. Ric-8A induces dissociation of the RGS14:Gai1-GDP complex *in vitro*.** Ric-8A induces dissociation of the  $\Delta$ RGS14:Gai1-GDP complex, resulting in the formation of a Ric-8A:Gai1 complex and subsequent Gai1-GTP. Either YFP-Ric-8A (A), YFP-Ric-8A and Gai1-GDP (B), pre-formed  $\Delta$ RGS14:Gai1-GDP complex (C), or YFP-Ric-8A and pre-formed  $\Delta$ RGS14:Gai1-GDP complex (D) was incubated for 15 mins at 30°C without any exogenous GTP or GDP added. The reaction samples were then loaded onto tandem S75+S200 gel filtration columns and resulting products were resolved by SDS-PAGE and immunoblot. Pre-formed  $\Delta$ RGS14:Gai1-GDP complex was incubated alone (E) or with YFP-Ric-8A (F) in the presence of 50  $\mu$ M GTP $\gamma$ S and 10 mM MgCl<sub>2</sub> for 15 mins at 30°C. The reaction samples were then loaded onto tandem S75+S200 gel filtration columns and resulting products were resolved by SDS-PAGE and immunoblot. This figure is representative of three separate experiments for each condition.

this information, we next tested whether purified Ric-8A stimulated dissociation of the  $\Delta$ RGS14:Gai1-GDP complex. For this, we prepared a pre-formed  $\Delta$ RGS14:Gai1-GDP complex. After this, we incubated pure YFP-Ric-8A with this pre-formed  $\Delta$ RGS14:Gai1-GDP complex in the absence of added nucleotide or in the presence of GTP $\gamma$ S and MgCl<sub>2</sub>. In the absence of activating nucleotide, Ric-8A induces partial dissociation of the  $\Delta$ RGS14:Gai1-GDP complex along with the formation of a new Ric-8A:Gai1 complex (presumably nucleotide-free, (50)) (see red and green boxes in Fig. 2.3, B-D). However, in the presence of GTP $\gamma$ S/Mg<sup>2+</sup>, Ric-8A induces near-complete dissociation of the  $\Delta$ RGS14:Gai1-GDP complex, resulting in free  $\Delta$ RGS14, free Gai1-GTP $\gamma$ S, and free Ric-8A (Fig. 2.3, E-F). Gai1 can be seen dissociating from  $\Delta$ RGS14 (see red box of Fig. 2.3, E-F) and remaining in its monomeric form (see blue box of Fig. 2.3, E-F). These results clearly show that Ric-8A recognizes, binds, and induces dissociation of the  $\Delta$ RGS14:Gai1-GDP complex. We found that the purified full-length RGS14 behaved similarly to  $\Delta$ RGS14 in these experiments, though our data sets were incomplete due to limiting amounts of available full-length RGS14 (data not shown).

*Ric-8A-induced dissociation of RGS14:Gai1-GDP frees Gai1 to bind GTP.* Our findings above (Figs. 2.2 and 2.3) indicate that Ric-8A binds Gai1 and disrupts the RGS14:Gai1 signaling complex, thus freeing Gai1 from the GPR motif and allowing it to exchange nucleotide and bind GTP. To examine this directly, we measured the capacity of Gai1 released from the  $\Delta$ RGS14:Gai1-GDP complex by Ric-8A to bind [<sup>35</sup>S]GTP $\gamma$ S (Fig. 2.4). In the absence of Ric-8A, Gai1 in complex with RGS14 binds GTP $\gamma$ S very poorly, as expected (42,43,118). When Ric-8A is added in 5-fold excess of the  $\Delta$ RGS14:Gai1-GDP complex, Gai1 readily binds GTP $\gamma$ S. Nucleotide binding is apparent immediately upon addition of Ric-8A, and GTP $\gamma$ S binding continues in a linear fashion for up to 10 min. We observe an approximate 4-fold increase in the rate of GTP $\gamma$ S binding to Gai1 with addition of Ric-8A to the complex (1.04 pmol/min) compared to GTP $\gamma$ S binding to Gai1 when in complex with  $\Delta$ RGS14 alone (0.25 pmol/min).

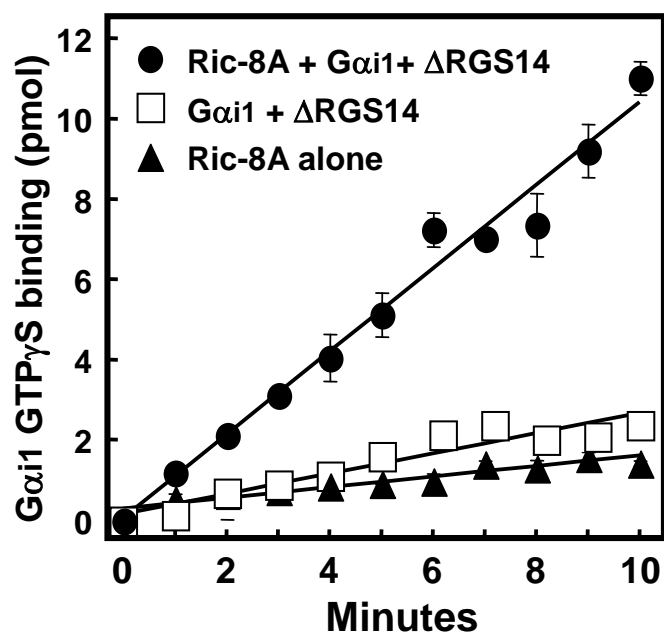


**Figure 2.4. Ric-8A-induced dissociation of the RGS14:Gαi1-GDP complex allows Gαi1 to bind GTP.** Ric-8A-stimulated dissociation of the ΔRGS14:Gαi1-GDP complex permits free Gαi1 to bind GTPγS. GTPγS binding to Gαi1 was analyzed using YFP-Ric-8A alone, pre-formed ΔRGS14:Gαi1-GDP complex, and YFP-Ric-8A plus ΔRGS14:Gαi1-GDP complex. [<sup>35</sup>S]GTPγS (2 μM; 10,000 cpm/pmol) was incubated with these protein mixtures in triplicate at 30°C. The amount of [<sup>35</sup>S]GTPγS bound to protein was quantified using scintillation counting and converted to pmol bound, with background values subtracted out. This figure is representative of three separate experiments for each condition, with data presented as mean ± S.E.M.

Pure Ric-8A protein does not bind GTP $\gamma$ S on its own (Fig. 2.4), thus the increase in nucleotide binding with Ric-8A+G $\alpha$ i1-GDP is due to Ric-8A-catalyzed GTP $\gamma$ S binding to G $\alpha$ i1. These findings show that Ric-8A stimulates dissociation of G $\alpha$ i1 from RGS14, allowing G $\alpha$ i1 to bind nucleotide and become activated.

*Ric-8A GEF activity toward G $\alpha$ i1 is dependent on the molar ratio of Ric-8A to RGS14.*

Ric-8A acts as a GEF toward G $\alpha$ i1 (50). Since Ric-8A is able to displace G $\alpha$ i1-GDP from  $\Delta$ RGS14, it appears that Ric-8A and  $\Delta$ RGS14 compete for G $\alpha$ i1 binding. RGS14 may affect, directly or indirectly, Ric-8A GEF activity toward G $\alpha$ i1. To examine this, we measured the effects of varying the molar ratios of Ric-8A and RGS14 on the rate of nucleotide binding to G $\alpha$ i1. When Ric-8A is in 5-fold molar excess of  $\Delta$ RGS14, Ric-8A is able to induce dissociation of the  $\Delta$ RGS14:G $\alpha$ i1-GDP complex and catalyze nucleotide exchange on G $\alpha$ i1 (4.10 pmol/min) in 2.3-fold excess of that observed for G $\alpha$ i1 alone (1.77 pmol/min) (Fig. 2.5A). At these molar ratios,  $\Delta$ RGS14 only partially inhibits Ric-8A GEF activity toward G $\alpha$ i1 (4.10 pmol/min compared to 6.80 pmol/min with Ric-8A+G $\alpha$ i1-GDP alone). By contrast, when the Ric-8A concentration is decreased so that  $\Delta$ RGS14 is in 5-fold molar excess, Ric-8A no longer has any effect on G $\alpha$ i1 nucleotide binding (0.74 pmol/min compared to 0.88 pmol/min for G $\alpha$ i1 alone) (Fig. 2.5B). Pure Ric-8A protein does not bind GTP $\gamma$ S on its own (Fig. 2.5), indicating that the observed nucleotide binding is due to Ric-8A effects on G $\alpha$ i1. These findings suggest that Ric-8A is neither able to force  $\Delta$ RGS14:G $\alpha$ i1 complex dissociation nor able to act as a GEF toward G $\alpha$ i1 under these experimental conditions (Fig. 2.5B). Of note, the failure of Ric-8A to overcome these effects of RGS14 on G $\alpha$ i1 may be due to the absence of properly modified G $\alpha$ i1, since myristoylated G $\alpha$ i1 has been shown to enhance the capacity of Ric-8A to act on GPR:G $\alpha$ i1-GDP complexes (46). We also tested whether purified full-length RGS14 containing the RGS domain behaved any differently in these assays than did  $\Delta$ RGS14 missing the RGS domain. We found that the presence of the RGS domain in full-length RGS14 had no effect on Ric-8A-directed GEF activity toward G $\alpha$ i1 (data not shown).

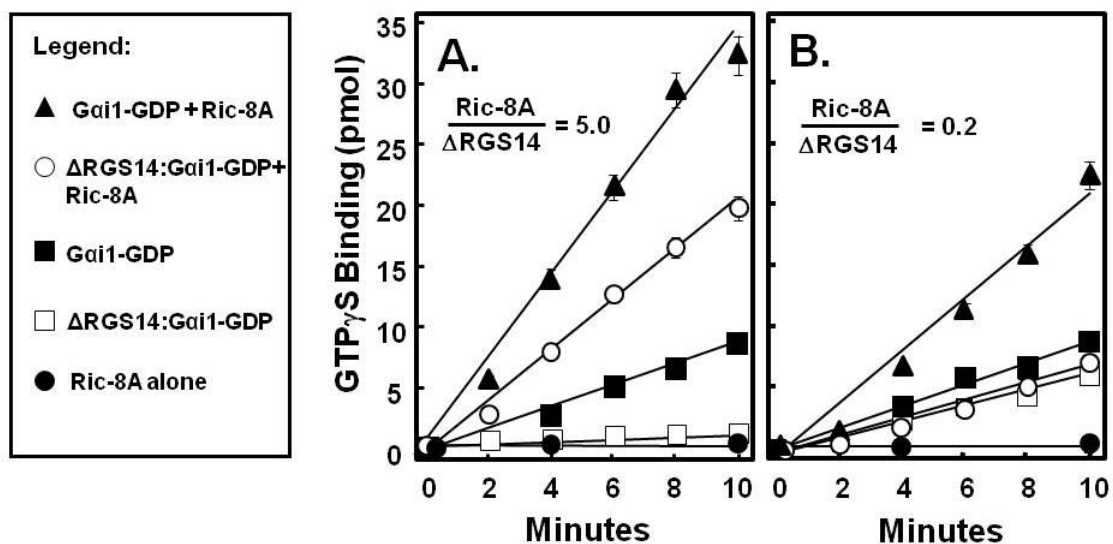


**Figure 2.5. Ric-8A reverses RGS14 inhibition of GTP $\gamma$ S binding to Gαi1.** The degree of RGS14-induced inhibition of Ric-8A nucleotide exchange activity toward Gαi1 is dependent on the molar ratio of Ric-8A to RGS14. ΔRGS14:Gαi1-GDP complex was incubated with either a 5-fold excess of YFP-Ric-8A to ΔRGS14 (A) or one-fifth the concentration of YFP-Ric-8A to ΔRGS14 (B) and then mixed with [ $^{35}$ S]GTP $\gamma$ S (2  $\mu$ M; 10,000 cpm/pmol) at 30°C in triplicate. The amount of [ $^{35}$ S]GTP $\gamma$ S bound to protein was quantified using scintillation counting. Measurements were converted to pmol [ $^{35}$ S]GTP $\gamma$ S bound, with background subtracted out. This figure is representative of three separate experiments for each condition, with data presented as mean  $\pm$  S.E.M.

*Ric-8A stimulates an increase in the steady-state GTPase activity of Gai1 in the presence of RGS14.* All GEFs act by increasing the rate of release of GDP bound to  $G\alpha$ , thereby greatly reducing the rate-limiting step in guanine nucleotide exchange and steady-state hydrolysis. Thus, GEF activity is reflected both as an increase in GTP $\gamma$ S binding and also as an increase in steady-state GTPase activity on the target  $G\alpha$  (50,151). Consistent with its reported role as a GEF, Ric-8A stimulates steady-state GTPase activity of Gai1 (46,50). Thus, in addition to examining Ric-8A effects on nucleotide binding (Fig. 2.5), we also examined its effects on Gai1 GTPase activity and the importance of RGS14 and its RGS domain on this activity. Assays of Gai1 steady-state GTPase activity were designed to include combinations of purified Ric-8A, Gai1-GDP, and either truncated  $\Delta$ RGS14 or full-length RGS14 (Fig. 2.6).  $\Delta$ RGS14 inhibits the GTPase activity of Gai1 2.8-fold (0.48 pmol/min compared to 1.37 pmol/min for Gai1 alone) (Fig. 2.6A). Ric-8A overcomes this inhibition, catalyzing an increase in Gai1 GTPase activity by 2.5-fold in the presence of  $\Delta$ RGS14 (1.20 pmol/min compared to 0.48 pmol/min). However, the capacity of Ric-8A to overcome this inhibition does not exceed the intrinsic GTP hydrolysis rate of Gai1 (1.37 pmol/min). Full-length RGS14 also inhibits the GTPase activity of Gai1 (0.62 pmol/min compared to 1.15 pmol/min for Gai1 alone) (Fig. 2.6B). Ric-8A overcomes this inhibition by 2.4-fold, however again only to the approximate rate of intrinsic Gai1 GTP hydrolysis.

To examine the effects of RGS14 on Gai1 GTPase activity more carefully, we tested a range of full-length RGS14 concentrations on Gai1 GTPase activity in the absence or presence of Ric-8A (Fig. 2.6C). We found that RGS14 inhibits Ric-8A-mediated increases in Gai1 GTPase activity in a concentration-dependent manner, with complete inhibition evident at 3  $\mu$ M RGS14 (Fig. 2.6C). This suggests that RGS14 competes with Ric-8A for Gai1 binding, as greater concentrations of RGS14 hinder Ric-8A from acting on Gai1.

*RGS14 and Ric-8A bind to distinct and overlapping sites of Gai1.* We next examined whether RGS14 and Ric-8A interact at the same or different sites of Gai1. A recent report suggests that Ric-8A binds to the extreme C-terminus of Gai1 since pertussis toxin disrupts Ric-

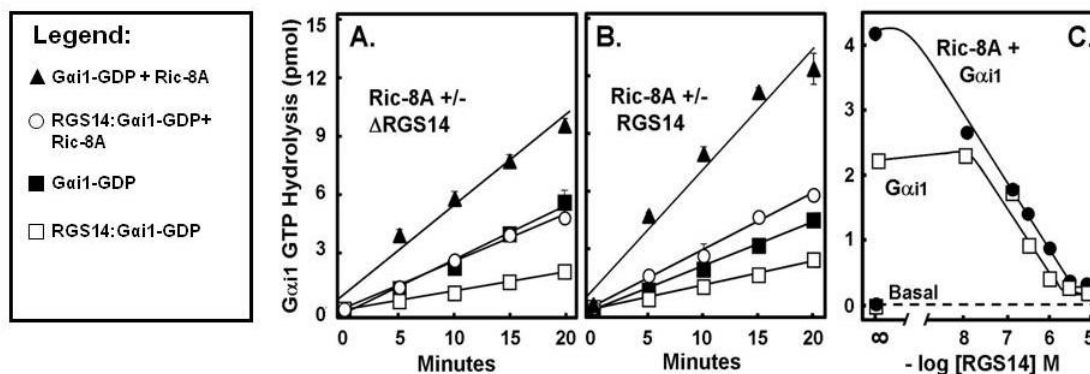


**Figure 2.6. Ric-8A reverses RGS14 inhibition of Gai1 steady-state GTPase activity.** Both full-length RGS14 and  $\Delta$ RGS14 inhibit the Ric-8A-catalyzed increase in steady-state GTPase activity of Gai1. Combinations of YFP-Ric-8A, His<sub>6</sub>-Gai1-GDP, and either pre-formed  $\Delta$ RGS14:Gai1-GDP complex (A) or full-length RGS14:Gai1-GDP complex (B) were used to analyze steady-state GTPase activity of Gai1. (C), YFP-Ric-8A and Gai1-GDP were mixed with increasing concentrations of full-length RGS14 as indicated. Protein combinations were mixed in triplicate with [ $\gamma$ -<sup>32</sup>P]GTP and the amount of [<sup>32</sup>P]i released in each sample was quantified using scintillation counting. Measurements were converted to pmol [ $\gamma$ -<sup>32</sup>P]GTP hydrolyzed, with background subtracted out. This figure is representative of three separate experiments for each condition, with data presented as mean  $\pm$  S.E.M.

8A interactions with G $\alpha$ i1 (52). Based on this observation, we generated a truncation of G $\alpha$ i1 (G $\alpha$ i1- $\Delta$ CT) that is missing the last 11 amino acids of the protein. We also made a single point mutation in G $\alpha$ i1 (N149I) that previously has been reported to block its binding to RGS14 (152,153). GTP $\gamma$ S binding studies illustrate that these proteins are functional and active (0.59 pmol/min, 0.75 pmol/min, and 0.68 pmol/min for wild-type G $\alpha$ i1, G $\alpha$ i1 (N149I), and G $\alpha$ i1- $\Delta$ CT, respectively). We examined the capacity of purified full-length TxHis<sub>6</sub>-RGS14 and YFP-Ric8A to form a stable complex with His<sub>6</sub>-G $\alpha$ i1- $\Delta$ CT, His<sub>6</sub>-G $\alpha$ i1 (N149I), and wild-type His<sub>6</sub>-G $\alpha$ i1 derived from *E. coli* lysates as assessed by immunoprecipitation (Fig. 2.7). Both Ric-8A and RGS14 bind wild-type G $\alpha$ i1, as expected (Fig. 2.7). Ric-8A interacts with G $\alpha$ i1 (N149I) whereas RGS14 does not, indicating a distinct site of interaction for the two proteins on G $\alpha$ i1 (Fig. 2.7). In contrast, Ric-8A fails to bind G $\alpha$ i1- $\Delta$ CT, which is consistent with a recent report (52) showing that pertussis toxin-mediated ADP-ribosylation of a cysteine (C351) within this deleted region of G $\alpha$ i1 blocks its functional interactions with Ric-8A. Surprisingly, RGS14 also fails to bind to this truncated form of G $\alpha$ i1, suggesting an overlapping binding region that is shared by Ric-8A and RGS14 within the last 11 amino acids of G $\alpha$ i1 (Fig. 2.7). These findings show that RGS14 and Ric-8A bind to both distinct sites and overlapping regions of G $\alpha$ i1.

*Ric-8A and RGS14 co-exist within the same hippocampal neurons.* Thus far, our findings provide evidence that Ric-8A can functionally regulate the RGS14:G $\alpha$ i1 complex. For this to be physiologically relevant, we would expect native RGS14 and Ric-8A to exist within the same cells. Since both RGS14 and Ric-8A are natively expressed in brain (115,118,154,155), we studied the localization patterns of each of these proteins within brain using IHC staining techniques and confocal microscopy of fixed tissue (Fig. 2.8). Consistent with our recent observations (124), we find that RGS14 is present in hippocampus, but with a protein expression pattern that is largely restricted to neurons and neurites of the CA2 and CA1 sub-regions (Fig. 2.8A). We find that Ric-8A protein is also highly expressed in neurons of the CA2 and CA1 regions of the hippocampus (Fig. 2.8A). Staining of RGS14 and Ric-8A with anti-RGS14 and



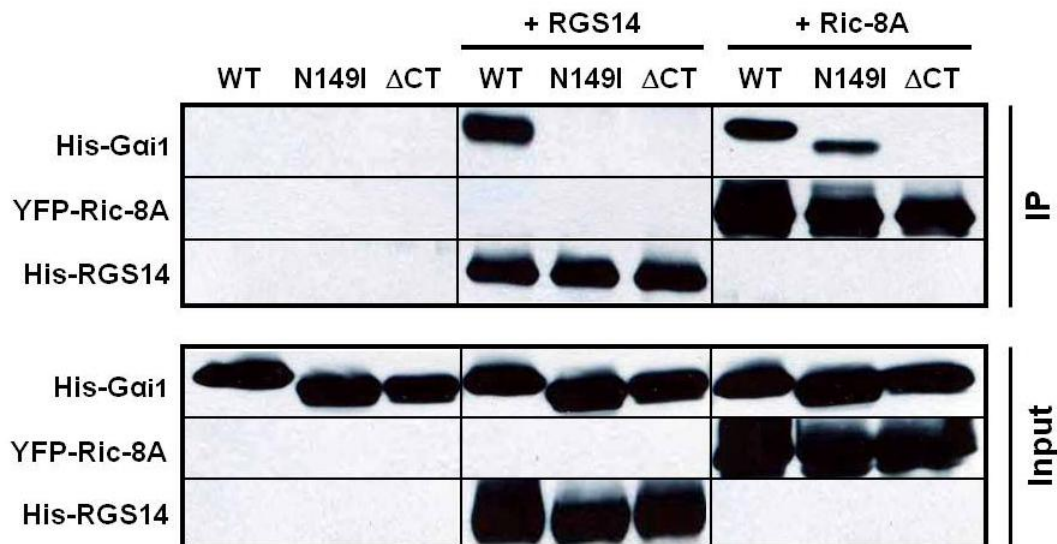


**Figure 2.7. RGS14 and Ric-8A bind to distinct and overlapping regions of G $\alpha$ i1.** RGS14 binds G $\alpha$ i1 distinct from Ric-8A at residue N149, whereas both RGS14 and Ric-8A share an overlapping binding region at the extreme C-terminus of G $\alpha$ i1. Wild-type His<sub>6</sub>-G $\alpha$ i1 (WT), His<sub>6</sub>-G $\alpha$ i1 (N149I) (N149I), and His<sub>6</sub>-G $\alpha$ i1-ΔCT (ΔCT) proteins derived from *E. coli* were mixed alone or with either purified full-length TxHis<sub>6</sub>-RGS14 or purified YFP-Ric-8A. Protein mixtures were subjected to either anti-RGS14 or anti-Ric-8A immunoprecipitation, SDS-PAGE, and immunoblot. Results are indicative of three replicate experiments.

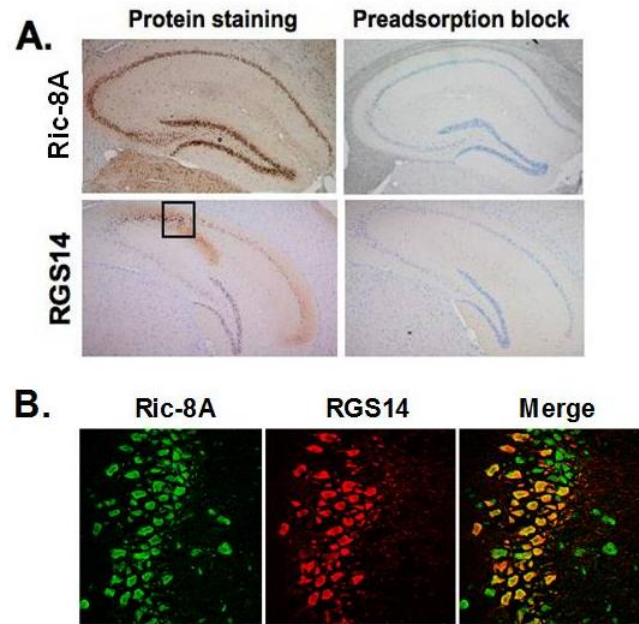


**Figure 2.8. RGS14 and Ric-8A co-exist and co-localize within the same hippocampal neurons.** RGS14 and Ric-8A co-localize within neurons of the hippocampus, specifically in the CA2 region of the hippocampus. (A), Mouse brain thin sections were subjected to immunohistochemistry and stained for RGS14 and Ric-8A. Control sections were incubated with antibody that was pre-adsorbed with RGS14 and Ric-8A pure protein (1:10 ratio of antibody to protein) (right panels). (B), Mouse brain thin sections were labeled with RGS14 and Ric-8A antibodies, followed by fluorescently-conjugated secondary IgG. Sections were analyzed by confocal microscopy as described in Experimental Procedures.

anti-Ric-8A antibodies is blocked by pre-adsorption of the antibodies with pure RGS14 and Ric-8A proteins, respectively (Fig. 2.8A; right panels). Most importantly, Ric-8A and RGS14 co-localize within the same CA2 hippocampal neurons as visualized by confocal imaging (corresponding to the area shown in the black box in Fig. 2.8A) (Fig. 2.8B). Ric-8A and RGS14 co-localize mainly to the cytosol of the soma of these neurons. These results further support the idea that Ric-8A and RGS14 are functionally linked within hippocampal neurons to regulate their functions.

## **2.4 Discussion**

RGS14 is a complex signaling protein that contains an RGS domain, tandem Ras/Rap-binding domains, and a GPR motif. Previous studies have focused largely on the presumed function of RGS14 as a regulator of GPCR/G protein signaling (115,116,118,142,143). However, findings here and elsewhere (43,117,152) strongly suggest that RGS14 serves as a scaffold that integrates unconventional G protein signaling events rather than as a conventional RGS protein. In support of this idea, we show that RGS14 functionally interacts with Ric-8A, a defined regulator of unconventional G protein signaling pathways (46,47,50). Our key findings indicate the following: 1) RGS14 and Ric-8A co-localize at the plasma membrane with wild-type  $G\alpha i1$ ; 2) RGS14 and Ric-8A interact with each other in cells; 3) Ric-8A stimulates dissociation of the RGS14: $G\alpha i1$ -GDP complex in cells and *in vitro*; 4) Ric-8A serves as a GEF to facilitate nucleotide exchange (*e.g.* GTP $\gamma$ S binding) on the  $G\alpha i1$  that it liberates from RGS14; 5) the capacity of Ric-8A to overcome the inhibitory effects of RGS14 on  $G\alpha i1$  nucleotide exchange and GTPase activity depends on the molar ratio of RGS14 relative to Ric-8A; 6) RGS14 and Ric-8A bind to both distinct and overlapping regions of  $G\alpha i1$ ; and 7) native RGS14 and Ric-8A co-exist within the same hippocampal neurons.

Our findings indicate that Ric-8A can functionally regulate the activation state of the RGS14: $G\alpha i1$ -GDP signaling complex, which may potentially play a role in hippocampal

signaling functions since RGS14 expression is highly restricted to this brain region. In this regard, RGS14 shows structural and mechanistic parallels with two other brain proteins, LGN (mPins) and AGS3. Like RGS14, these proteins contain GPR motifs that form stable complexes with G $\alpha$ i1-GDP, and LGN has been shown to be recruited to the plasma membrane in cells to form an LGN:G $\alpha$ i1-GDP complex (40,46,47). Similar to its effects on RGS14, Ric-8A also recognizes and induces dissociation of both the AGS3:G $\alpha$ i1-GDP and LGN:G $\alpha$ i1-GDP complexes, subsequently facilitating GTP binding to free G $\alpha$ i1 (46,47). As is the case with RGS14, excess amounts of both LGN and AGS3 have been shown to inhibit Ric-8A effects on G $\alpha$ i1, suggesting competition between these GPR proteins and Ric-8A for G $\alpha$ i1 binding (46,47). Taken together, our findings strongly suggest that RGS14 acts as a GPR protein as well as an RGS protein.

*RGS14 and Ric-8A co-localize with Gai1-GDP at the plasma membrane in cells.* Our cellular localization findings (Fig. 2.1) suggest that Ric-8A, RGS14, and G $\alpha$ i1 may functionally interact at the plasma membrane in cells. Since both Ric-8A and RGS14 directly bind to inactive G $\alpha$ i1 in cells (42,43,50,118), we examined the subcellular localization of both Ric-8A and RGS14 in the presence of wild-type G $\alpha$ i1. While a majority of Ric-8A is recruited to the plasma membrane in the presence of wild-type G $\alpha$ i1, almost all Ric-8A is recruited to the plasma membrane when expressed with both wild-type G $\alpha$ i1 and RGS14 (Fig. 2.1). The fact that Ric-8A and RGS14 co-localize at the same time with G $\alpha$ i1 at the plasma membrane supports the possibility that these proteins functionally interact together through sequential formations/dissociations of RGS14:G $\alpha$ i1 and Ric-8A:G $\alpha$ i1 complexes, and perhaps through formation of a transient ternary RGS14:G $\alpha$ i1-GDP:Ric-8A complex. Our data throughout support both the idea of the formation of RGS14:G $\alpha$ i1 and Ric-8A:G $\alpha$ i1 complexes and the concept that G $\alpha$ i1 is exchanged between RGS14 and Ric-8A before dissociation as free G $\alpha$ i1-GTP.

*Ric-8A induces dissociation of the RGS14:Gai1-GDP complex and subsequently facilitates nucleotide exchange on Gai1.* Mechanistically, our results show that Ric-8A interacts with the RGS14:Gai1 complex to regulate its activation state. In the absence of nucleotide, Ric-8A forces Gai1 dissociation from RGS14 to form a stable (and presumably nucleotide free (50)) Ric-8A:Gai1 complex. In the presence of GTP $\gamma$ S, Ric-8A-induced dissociation of RGS14:Gai1 allows Ric-8A to act as a GEF toward free Gai1, which results in a rapid uncoupling of the Ric-8A:Gai1 complex and formation of free Gai1-GTP $\gamma$ S. Our findings are consistent with previous reports describing Ric-8A regulation of other GPR:Gai1-GDP complexes both in the presence and absence of exogenous GTP (46,47). While these intermediate ternary biochemical complexes can be isolated under controlled experimental conditions, the lifetime of an RGS14:Gai1-GDP:Ric-8A complex in cells is likely very transient (47). This is reflected by our failure to observe a stable heterotrimeric RGS14:Gai1-GDP:Ric-8A complex in cells or as purified proteins; in both cases, Ric-8A seems to displace Gai1 from RGS14 (Figs. 2.2 and 2.3). However, such a transition complex must exist since Gai1 transfer occurs from RGS14 to Ric-8A (Fig. 2.3). We observed Ric-8A/RGS14 complex formation in cells (Fig. 2.2), but failed to observe this with purified proteins (Fig. 2.3, and data not shown). Reasons for the discrepancy between these two findings are unclear. We do not observe a stable Ric-8A/RGS14 complex when native RGS14 is co-immunoprecipitated from mouse brain (data not shown), though this does not definitively rule out such a complex. One possibility is that our observed cellular interactions are due to post-translation modifications (*e.g.* fatty acylation, phosphorylation) on either protein that promote a favorable conformation for binding. Alternatively, an intermediary protein may facilitate an interaction which may be independent of any Ric-8A effects on the RGS14:Gai1-GDP complex (as is the case with Frmpd1 and AGS3 (156)). Recovered Ric-8A bound to RGS14 (Fig. 2.2) may also be the result of native Gai1 bridging the two proteins together, however our dissociation data (Fig. 2.2B) does not support this idea. Such an intermediary protein bringing Ric-8A and RGS14 together may facilitate RGS14 to “switch”

from regulating G protein signaling to regulating H-Ras/Raf-1-mediated MAP kinase signaling (121) (or other unknown signaling pathways). The role of Ric-8A in this context remains to be studied.

*Ric-8A accelerates nucleotide exchange and GTPase activity of Gai1 following RGS14:Gai1-GDP dissociation.* We observe that Ric-8A accelerates both GTP $\gamma$ S binding to and the steady-state GTPase activity of Gai1 in the presence of RGS14, however these Ric-8A effects can be reversed by increasing concentrations of RGS14 (Figs. 2.4-2.6); this was the case for both full-length RGS14 and truncated RGS14 missing the RGS domain ( $\Delta$ RGS14). Even with a dominant GDI function, Ric-8A is able to overcome  $\Delta$ RGS14 inhibition of GTP $\gamma$ S binding to Gai1, stimulating over a 20-fold increase in Gai1 nucleotide binding when introduced to the  $\Delta$ RGS14:Gai1-GDP complex (Fig. 2.5A). A five-fold excess of  $\Delta$ RGS14 to Ric-8A completely inhibits this Ric-8A-induced GTP $\gamma$ S binding, indicating that  $\Delta$ RGS14 maintains Gai1 in an inactive state. Full-length RGS14 appears to be as effective as  $\Delta$ RGS14 at inhibiting Gai1-directed steady-state GTP hydrolysis, both alone and in the presence of Ric-8A (Fig. 2.6). The presence of the RGS domain and its GAP activity might be expected to enhance GTP hydrolysis. However, it is likely that nucleotide exchange, and not GTP hydrolysis, is rate-limiting under the experimental conditions used. In this case, the GAP activity of the RGS domain would not be apparent in this *in vitro* assay, but is necessarily important in the context of cellular signaling.

Like we observe with the GTP $\gamma$ S binding assay, Ric-8A is able to overcome RGS14 inhibition of steady-state Gai1 GTPase activity, catalyzing a 2.4-fold increase in Gai1 steady-state GTPase activity when introduced to the RGS14:Gai1-GDP complex (Fig. 2.6B). Again, increasing concentrations of RGS14 inhibit Ric-8A effects on Gai1 GTP hydrolysis (Fig. 2.6C). Since the GEF activity of Ric-8A serves to enhance GDP release and increase the velocity of and/or eliminate the rate-limiting step in nucleotide exchange and hydrolysis, enhanced RGS14 binding to Gai1-GDP would result in increased GDI activity reflected as an inhibition of GTP $\gamma$ S binding and steady-state GTPase activity that is more difficult for Ric-8A to overcome (as we

observe). Therefore, RGS14 may bind G $\alpha$ i1-GDP and hinder Ric-8A (by competitive or non-competitive inhibition) from binding and catalyzing G $\alpha$ i1-directed GTP binding and hydrolysis.

*Ric-8A and RGS14 bind Gai1 at both distinct and overlapping sites.* In studies designed to identify sites(s) of RGS14 and Ric-8A interactions on G $\alpha$ i1 (Fig. 2.7), we found that RGS14 and Ric-8A compete for an overlapping binding site on the extreme C-terminus of G $\alpha$ i1. Whereas residue N149 of G $\alpha$ i1 has been shown to interact with the GPR motif of RGS14 (152), identified binding sites on G $\alpha$ i1 for Ric-8A were previously unknown. A recent study suggests that Ric-8A binds to the extreme C-terminus of G $\alpha$ i1 since pertussis toxin-stimulated modification of C351 within this region inhibits Ric-8A activation of G $\alpha$ i1 in cells (52). By comparing the binding properties of G $\alpha$ i1 (N149I) (which does not bind RGS14 (153)) and G $\alpha$ i1- $\Delta$ CT (missing the last 11 amino acids including C351), we determined that Ric-8A and RGS14 share distinct and overlapping binding regions on G $\alpha$ i1 (Fig. 2.7). The presence of an overlapping binding region correlates with our other data (Figs. 2.5 and 2.6) that shows increasing concentrations of RGS14 block Ric-8A GEF activity toward G $\alpha$ i1. Taken together, these findings are consistent with the idea that RGS14 and Ric-8A compete for the exact same or very proximal residues within the extreme C-terminal 11 amino acids of G $\alpha$ i1. Since RGS14 binds N149 of G $\alpha$ i1 and Ric-8A does not, it is also possible that RGS14 and Ric-8A are acting on distinct and overlapping regions of G $\alpha$ i1 at the same time. RGS14 may interact with G $\alpha$ i1 at residue N149 to carry out additional functions and/or to affect Ric-8A:G $\alpha$ i1 interactions by allosteric modulation. These findings are the first to show any binding site for Ric-8A on G $\alpha$ i1, and also the first to show a second binding region on G $\alpha$ i1 for RGS14. Solved co-crystal structures of the RGS14:G $\alpha$ i1 and the Ric-8A:G $\alpha$ i1 complexes will be necessary to precisely define the binding interfaces between these proteins.

*Working model for how Ric-8A regulates the RGS14:Gai1-GDP signaling complex.* Since RGS14 was first identified as a Rap binding protein that contains an RGS domain (114,115), much of the previous work on this protein has focused on its presumed role as an RGS

protein that modulates GPCR/G protein signaling (115,116,118,142). However, our findings here combined with findings elsewhere (43,117,121,152) suggest that RGS14 may serve as a GPR protein that integrates unconventional Ric-8A/G protein signaling with Ras/Raf/MAP kinase signaling (43,115,121). These findings provide a framework for a working model (Fig. 2.9) to describe how these proteins and the functionally opposed RGS domains and GPR motifs work together to bind and modulate the functions of Ric-8A, inactive G $\alpha$ i-GDP, and active G $\alpha$ i-GTP. Our proposed model highlights the GPR motif as the first point of contact between G $\alpha$ i and RGS14 rather than the RGS domain. In its basal resting state, RGS14 exists in a stable complex with G $\alpha$ i1-GDP at the cell membrane. We postulate that following a signaling event (as yet undefined), Ric-8A recognizes the RGS14:G $\alpha$ i1-GDP complex to stimulate nucleotide exchange and GTP binding to G $\alpha$ i1, which then promotes dissociation of RGS14 (because the GPR motif does not bind G $\alpha$ -GTP). Of note, a role for a GPCR in this activation step cannot be ruled out. Once free from G $\alpha$ i1, RGS14 would be available to act on other downstream binding partners (*e.g.* active H-Ras and Raf kinases to modulate MAP kinase signaling) (43,115,121). In this model, we envision that the lifetime of this newly-formed RGS14 signaling complex is limited by the RGS domain, which acts on nearby G $\alpha$ i1-GTP to restore G $\alpha$ i1-GDP and to promote reformation of the G $\alpha$ i1-GDP:GPR-RGS14 complex. This event is coupled with dissociation of RGS14 from its binding partners and a return to the basal resting state. An attractive feature of this model is that the structural configuration of RGS14 that incorporates both the RGS domain and GPR motif into the same protein could serve to spatially restrict the function of the RGS domain toward the pre-bound G $\alpha$ , thus eliminating the need for strict intrinsic RGS/G $\alpha$  selectivity (*i.e.* even though the RGS domain is capable of acting on other G $\alpha$ , it will only act on the one that is nearby). This idea is consistent with earlier observations that the RGS domain is a non-selective GAP for G $\alpha$ i/o (115,116,118), while the GPR motif is specific for G $\alpha$ i1 and G $\alpha$ i3 (42,43,117). This proposed activation/deactivation cycle (Fig. 2.9) is entirely consistent with our



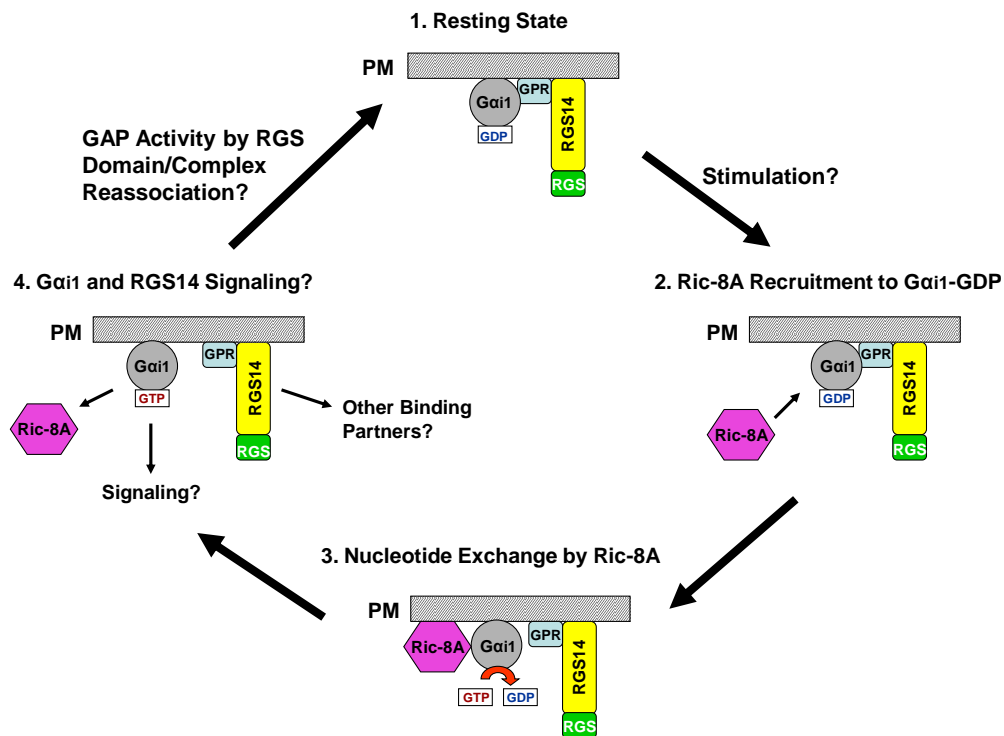


**Figure 2.9. Working model depicting Ric-8A regulation of the RGS14:Gai1-GDP complex.**

This visual model includes RGS14, Gai1, Ric-8A, and reference to speculative RGS14 binding partners localized at or near the plasma membrane (PM). Both the GPR (GPR) motif and RGS (RGS) domain of RGS14 are shown. The cycle begins at the “Resting State” and proceeds clockwise in the direction of the large bold and black arrows.

findings here and with previous findings (46,47,117,121), and future studies will examine untested steps in this model.

*RGS14 and Ric-8A are brain proteins important for hippocampal functions.* We find that native RGS14 and Ric-8A co-exist and co-localize within the same neurons of the CA2 and CA1 sub-regions of the hippocampus (Fig. 2.8). These findings highlight the likelihood for functional interplay between Ric-8A and RGS14 in hippocampal signaling pathways. Our findings here and those in previous reports (155,157) indicate that Ric-8A is widely expressed in brain, including but not limited to those hippocampal neurons that contain RGS14. Thus, Ric-8A must also serve roles in addition to regulation of the RGS14:G $\alpha$ i1-GDP signaling complex. In this regard, LGN/mPins, AGS3, and other proteins that contain GPR motifs are also highly enriched in various brain regions (38,158,159). Furthermore, we observe via size-exclusion chromatography that most of the Ric-8A in soluble brain lysates exists as an uncomplexed monomer (data not shown). Therefore, it is possible that Ric-8A acts as a master regulator of multiple GPR:G $\alpha$ i-GDP signaling complexes involved with brain signaling. Consistent with this idea, both LGN/mPins and AGS3 have each been reported to serve important roles in synaptic plasticity in brain (33,36,158,160). Genetic deletion of Ric-8A is reported to alter hippocampal learning behavior (154). Of particular relevance to these reports and our findings here, we observe that RGS14 is expressed almost exclusively in CA2 neurons of mouse hippocampus and that genetic deletion of RGS14 in mouse brain results in animals with a targeted enhancement of hippocampal-based learning and memory and synaptic plasticity in CA2 neurons (124). These studies, combined with our results here and other reports showing that the RGS14 binding partners H-Ras and Raf-1 are also important for hippocampal learning and memory (134,135,137,161-164) strongly suggest that RGS14 is a newly appreciated multifunctional GPR and RGS protein that integrates unconventional Ric-8A/G $\alpha$ i and MAP kinase signaling pathways important for hippocampal cognitive processing.

**CHAPTER 3:****G Protein-Coupled Receptors and Resistance to Inhibitors of Cholinesterase-8A (Ric-8A)****Both Regulate the Regulator of G Protein Signaling 14 (RGS14):G $\alpha$ i1 Complex in Live****Cells<sup>3</sup>**

<sup>3</sup> This chapter has been slightly modified from the published manuscript. Vellano CP, Maher EM, Hepler JR, and Blumer JB. (2011) G Protein-Coupled Receptors and Resistance to Inhibitors of Cholinesterase-8A (Ric-8A) Both Regulate the Regulator of G Protein Signaling 14(RGS14):G $\alpha$ i1 Complex in Live Cells. *J Biol. Chem.* 286: 38659-69.

### **3.1 Introduction**

Established models of G protein signaling suggest that heterotrimeric G proteins ( $G\alpha\beta\gamma$  subunits) are linked to specific G protein – coupled receptors (GPCRs), and that these receptors act as guanine nucleotide exchange factors (GEFs) toward the  $G\alpha$  subunit to promote nucleotide exchange and downstream signaling events (14,145). The regulators of G protein signaling (RGS) proteins act as GTPase accelerating proteins (GAPs) on the activated  $G\alpha$  subunit, catalyzing GTP hydrolysis to terminate G protein signaling (113,146,147).

Recent studies have explored novel unconventional G protein signaling pathways involved with cell division and synaptic signaling/plasticity that can operate independently of GPCRs (30-34,36,148,165). The hallmark of these unconventional G protein pathways are signaling complexes involving  $G\alpha$ -GDP bound to proteins containing one or more G protein regulatory (GPR) motifs. Resistance to inhibitors of cholinesterase-8A (Ric-8A) is a cytosolic GEF that directly promotes nucleotide exchange on  $G\alpha_i$ ,  $G\alpha_o$ , and  $G\alpha_q$  subunits in unconventional G protein signaling (50). Ric-8A also recognizes, binds, and regulates the formation/dissociation of some GPR: $G\alpha_i$ -GDP complexes, such as AGS3: $G\alpha_i$ -GDP, LGN: $G\alpha_i$ -GDP, and RGS14: $G\alpha_i$ -GDP (46-48).

RGS14 is a functionally and structurally complex signaling protein that is most highly expressed in the brain, but also present in spleen, thymus, and lymphocytes (114-116,118). Within brain, RGS14 is predominately localized in the CA2 subregion of the hippocampus, where it is involved in spatial memory, learning, and synaptic plasticity (124). The unique structure of RGS14, which includes an RGS domain, two Ras/Rap-binding domains, and a GPR (also known as GoLoco (37)) motif (114,115), suggests that RGS14 functions in the brain through a variety of signaling mechanisms which may involve both G protein and MAP kinase signaling cascades (121). In addition to possessing GAP activity toward activated  $G\alpha_{i/o}$ -GTP subunits, RGS14 also exhibits selective guanine nucleotide dissociation inhibitor (GDI) activity toward  $G\alpha_{i/3}$ -GDP subunits through direct binding of its GPR motif (42,43,115-118). In this regard, RGS14 shares

similarities with the family of Group II Activators of G protein Signaling (AGS) proteins that are characterized by one or more GPR motifs and mediate unconventional G protein signaling (151,166). Similar to AGS3 and LGN, which form stable complexes with G $\alpha$ i1-GDP via their GPR motifs (46,47), the RGS14:G $\alpha$ i1-GDP signaling complex is a substrate for Ric-8A-induced dissociation and nucleotide exchange on the resulting free G $\alpha$ i1 (48).

Recent evidence suggests that unconventional pathways involving GPR:G $\alpha$ -GDP complexes and conventional pathways involving GPCR:G protein complexes may be functionally linked. In particular, the GPR proteins AGS3 and AGS4 appear to interface with GPCRs in a G $\alpha$ i-dependent manner (144,167). Compelling evidence also indicates that RGS proteins directly and selectively interact with GPCRs to modulate G protein signaling (reviewed in (168)). Given that RGS14 is an RGS protein that interacts with G $\alpha$ i/o-GTP but contains a GPR motif that binds G $\alpha$ i1/3-GDP, we examined whether the RGS14:G $\alpha$ i1 complex can be regulated by a G $\alpha$ i/o-linked GPCR.

The non-receptor GEF Ric-8A regulates the RGS14:G $\alpha$ i1 complex (48), as well as certain GPCR signaling pathways (169,170). However, it remains unknown whether Ric-8A can modulate GPCR/G $\alpha$  interactions, especially in the presence of a GPR protein such as RGS14. Therefore, we also studied the effects of Ric-8A on RGS14/G $\alpha$ i1/GPCR complex formation, and whether RGS14 may be at the interface between conventional and unconventional G protein signaling pathways. Here we report the first evidence that the RGS14:G $\alpha$ i1-GDP complex is regulated in concert by both a G $\alpha$ i/o-linked GPCR and Ric-8A in live cells. We show that RGS14 forms a stable complex with G $\alpha$ i1 via its GPR motif, and that this complex is proximal to GPCRs as evidenced by the presence of specific bioluminescence resonance energy transfer (BRET) signals between RGS14 and the  $\alpha_{2A}$ -adrenergic receptor ( $\alpha_{2A}$ -AR) in the presence of G $\alpha$ i1. This RGS14: $\alpha_{2A}$ -AR complex partially dissociates/rearranges following receptor agonist treatment, and is further regulated by Ric-8A. Together, these findings illustrate that RGS14 functions together

in both conventional and unconventional G protein signaling, and that Ric-8A may recognize and act on GPCR:G $\alpha$ i:GPR complexes to further regulate G $\alpha$ i signaling.

### 3.2 Experimental Procedures

*Plasmids and antibodies:* The rat RGS14 cDNA used in this study (Genbank accession number U92279) was acquired as described (118). Rat RGS14 was used as a template in PCR reactions using *TaKaRa Taq* (Fisher, Pittsburgh, PA) to generate Luciferase (Luc) fusion protein constructs in the phRLucN2 vector graciously provided by Dr. Michel Bouvier (University of Montreal). The following oligonucleotides and restriction enzymes were used in the PCR amplification and subsequent digestion: RGS14 forward primer, 5'-GCT CTC GAG GCC ACC ATG CCA GGG AAG CCC AAG CAC-3', XhoI; reverse primer, 5'-CGC GGT ACC TGG TGG AGC CTC CTG AGA ACC-3', KpnI.

The RGS14-Luc GPR mutant, in which invariant glutamine and arginine residues (<sup>515</sup>Gln and <sup>516</sup>Arg) were both mutated to alanine, was generated by site-directed mutagenesis using a Stratagene Site Directed Mutagenesis kit according to the manufacturer's instructions, and is referred to as RGS14(*GPR-null*). Oligonucleotide primers used to create RGS14-Q515A/R516A-Luc (RGS14(*GPR-null*)) are as follows: RGS14(*GPR-null*) forward primer, 5'-GGG GCC CAT GAC GCC GCC GGA CTT CTT CGC AAA G-3'; reverse primer, 5'-CTT TGC GAA GTC CGG CGG CGT CAT GGG CCC C-3'. The RGS14-Luc RGS domain mutant, in which invariant glutamic acid and asparagine (<sup>92</sup>Glu and <sup>93</sup>Asn) residues were both mutated to alanine, was generated by site-directed mutagenesis using a Stratagene kit and is referred to as RGS14(*RGS-null*). Oligonucleotide primers used to create RGS14-E92A/N93A-Luc (RGS14(*RGS-null*)) are as follows: RGS14(*RGS-null*) forward primer, 5'-AAG GAA TTC AGC GCC GCC GCC GTA ACT TTC TGG CAA GC-3'; reverse primer, 5'-GCT TGC CAG AAA GTT ACG GCG GCG GCG CTG AAT TCC TT-3'. The RGS14-Luc RGS/GPR double mutant referred to as RGS14(*RGS/GPR-null*) was generated by using RGS14(*RGS-null*) as a template

and RGS14(*GPR-null*) primers in site-directed mutagenesis. In all cases, the plasmids were sequenced to confirm the fidelity of the PCR.

Wild-type AGS4-Luc was generated as previously described (144). Rat  $G\alpha i1$ -YFP ( $G\alpha i1$ -YFP) in pcDNA3.1 was generated by Dr. Scott Gibson (University of Texas Southwestern) (171) and was generously provided along with pcDNA3.1::Ric-8A plasmid by Dr. Gregory Tall (University of Rochester School of Medicine and Dentistry).  $G\alpha i1$ -N149I-YFP (referred to as  $G\alpha i1$ -GPRi),  $G\alpha i1$ -G183S-YFP (referred to as  $G\alpha i1$ -RGSi), and  $G\alpha i1$ -G183S/N149I-YFP (referred to as  $G\alpha i1$ -RGSi/GPRi) were generated using the QuickChange kit (Stratagene) previously described. pcDNA3.1:: $G\alpha i1$ -YFP was used as a template for oligonucleotide primers  $G\alpha i1$ -GPRi forward primer, 5'-GGG AGT ACC AGC TGC TCG ATT CGG CGG CGT A-3'; reverse primer, 5'-TAC GCC GCC GAA TCG ATC AGC TGG TAC TCC C-3' and  $G\alpha i1$ -RGSi forward primer, 5'-AGT GAA AAC GAC GTC AAT TGT GGA AA-3'; reverse primer, 5'-GGT TTC CAC AAT TGA CGT CGT TTT CA-3'. The  $G\alpha i1$ -RGSi/GPRi double mutant was constructed using the  $G\alpha i1$ -GPRi as a template for the  $G\alpha i1$ -RGSi primers. In all cases, the plasmids were sequenced to confirm the fidelity of the PCR.

$G\alpha s$ -YFP and  $G\alpha q$ -YFP constructs were obtained from Dr. Catherine Berlot (Geisenger Institute, Danville, PA). Glu-Glu (EE)-tagged recombinant  $G\alpha i1$  plasmid was purchased from UMR cDNA Resource Center (Rolla, Missouri).  $\alpha_{2A}$ -adrenergic receptor ( $\alpha_{2A}$ -AR) and  $\beta_2$ -adrenergic receptor ( $\beta_2$ -AR) plasmids were generated as described and provided by Dr. Michel Bouvier (University of Montreal) (172,173).

Anti-sera used include anti- $G\alpha i1$  (Millipore and Santa Cruz Biotechnologies, Inc.), anti- $G\alpha i2$  (Abcam), anti- $G\alpha i3$  and anti- $G\alpha s$  (gifts from Dr. Thomas Gettys at Pennington Biomedical Research Center, Baton Rouge, LA), anti-Flag (Sigma), anti-Ric-8A (provided by Dr. Gregory Tall, University of Rochester School of Medicine and Dentistry), anti- $G\alpha q$  (Santa Cruz Biotechnologies, Inc.), anti- $G\alpha o$  (Santa Cruz Biotechnologies, Inc.), Alexa 546 goat anti-rabbit secondary IgG (Invitrogen), Alexa 633 goat anti-mouse secondary IgG (Invitrogen), peroxidase-

conjugated goat anti-mouse IgG (Rockland Immunochemicals, Inc.), and peroxidase-conjugated goat anti-rabbit IgG (Bio-Rad).

*Cell Culture and Transfection:* HEK293 cells were maintained in Dulbecco's minimal essential medium (without phenol red) containing 10% fetal bovine serum (5% following transfection), 2 mM glutamine, 100 U/mL penicillin, and 100 mg/mL streptomycin. Cells were incubated at 37°C with 5% CO<sub>2</sub> in a humidified environment. Transfections were performed using previously described protocols with polyethyleneimine (PEI; Polysciences, Inc.) (144). For immunofluorescence, cells were seeded onto glass coverslips prior to transfection.

*BRET:* BRET experiments were performed as previously described (144,167). Briefly, HEK293 cells were transiently transfected with BRET donor and acceptor plasmids using PEI. Forty-eight hours after transfection, the culture medium was removed and cells were washed once with PBS and harvested with Tyrode's solution (140 mM NaCl, 5 mM KCl, 1 mM MgCl<sub>2</sub>, 1mM CaCl<sub>2</sub>, 0.37 mM NaH<sub>2</sub>PO<sub>4</sub>, 24 mM NaHCO<sub>3</sub>, 10 mM HEPES, and 0.1% glucose (w/v), pH 7.4). Each group of cells was distributed into gray 96-well optiplates (Perkin Elmer) in triplicate, with each well containing 1x10<sup>5</sup> cells. The acceptor (YFP/Venus-tagged) protein expression levels were evaluated by measuring total fluorescence using the TriStar LB 941 plate reader (Berthold Technologies) with excitation and emission filters at 485 and 535 nm, respectively. Data was analyzed using the MikroWin 2000 program. After fluorescence measurement, coelenterazine H (Nanolight Technology; 5 μM final concentration) was added and luminescence detected in the 480 +/- 20 and 530 +/- 20 nm windows for donor (Luc) and acceptor (YFP/Venus), respectively, by the TriStar LB 941 plate reader. BRET signals were determined by calculating the ratio of the light intensity emitted by the YFP/Venus divided by the light intensity emitted by Luc. Net BRET values were corrected by subtracting the background BRET signal detected from the expression of the donor fusion protein (Luc) alone. Agonists used were UK14304 (Sigma) and isoproterenol (Sigma). Immunoblots were performed as described previously (158).



*Immunofluorescence and confocal imaging:* Transfected HEK293 cells were treated with either vehicle or 10  $\mu$ M UK14304 diluted in serum-free DMEM for 5 mins at 37°C. Cells were then fixed at room temperature for 15 mins in buffer containing 3.7% paraformaldehyde diluted in PBS. Cells were washed in PBS and incubated for 8 mins with 0.4% TritonX-100 diluted in PBS. Cells were then blocked for 1 hour at room temperature in PBS containing 10% goat serum and 3% bovine serum albumin. Next, cells were incubated in this same buffer with a 1:1000 dilution of rabbit anti-Flag and/or mouse anti-G $\alpha$ i1 antibodies at room temperature for 2 hours. Cells were washed with PBS (3X) and incubated with 1:300 dilutions of Alexa 546 goat anti-rabbit and/or Alexa 633 goat anti-mouse secondary antibodies at room temperature for 1 hour. Cells were washed with PBS again (3X) and mounted with ProLong Gold Antifade Reagent (Invitrogen). Confocal images were taken using a 63x oil immersion objective from a LSM510 laser scanning microscope with AxioObserver Stand (Zeiss). Images were processed using the ZEN 2009 Light Edition software and Adobe Photoshop 7.0 (Adobe Systems).

### **3.3 Results**

*RGS14 interacts selectively with Gai1 through its GPR motif.* RGS14 has two distinct G $\alpha$ -binding domains. The RGS domain binds activated G $\alpha$ i/o subunits (115,116,118), whereas the GPR motif binds inactive G $\alpha$ i1 and G $\alpha$ i3 (42,43,117,118). Since RGS14 is recruited from the cytosol to the plasma membrane and co-localizes with wild-type G $\alpha$ i1 (Figs. 3.1A and (48,117)), it suggests that RGS14 forms a stable complex with G $\alpha$ i1 at the plasma membrane, which we sought to quantitatively measure using BRET. We therefore measured the strength and selectivity of a BRET signal between RGS14-Luc and various YFP-tagged G $\alpha$  subunits (171,174-176) (Fig. 3.1B). Of note, the YFP tag was inserted into the loop joining the  $\alpha$ B and  $\alpha$ C helices of each G $\alpha$  (171,174,176), preserving nucleotide binding and hydrolysis properties similar to the wild-type protein (171). Transfection of HEK cells with increasing amounts of G $\alpha$ -YFP plasmid and a fixed amount (5 ng) of RGS14-Luc plasmid showed a robust, saturable BRET signal in the

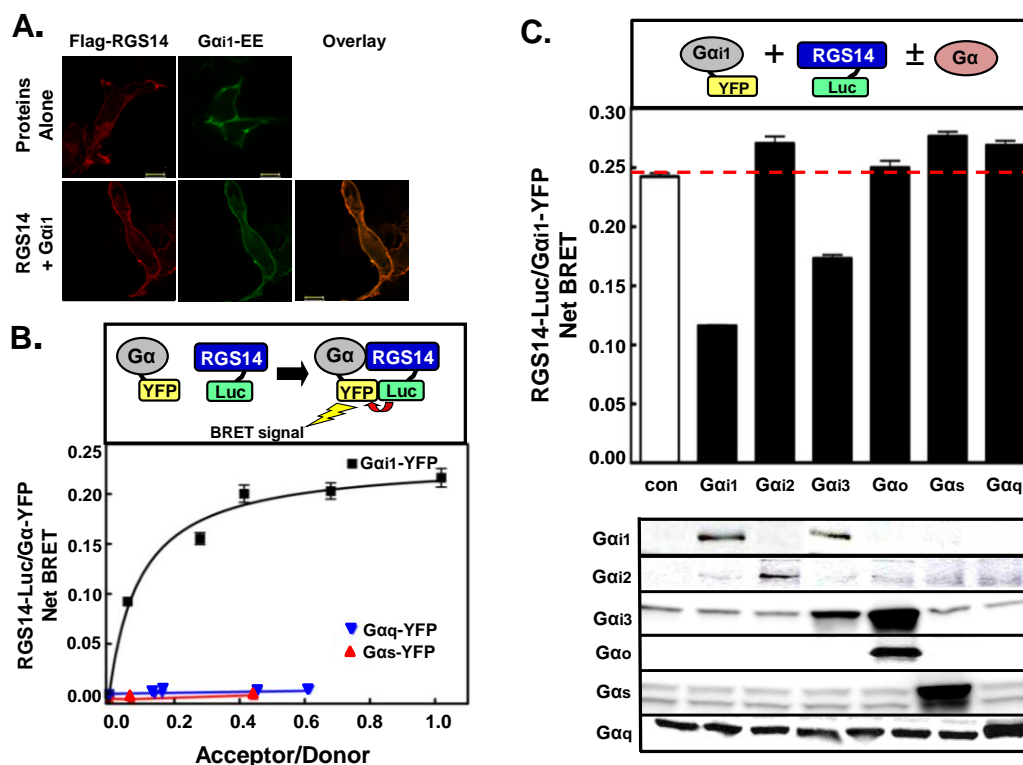


**Figure 3.1.** RGS14 selectively interacts with Gαi1 and Gαi3 in the basal state of live cells as observed by BRET. (A) Flag-RGS14 and Gαi1-EE plasmids were transfected into HEK cells alone and in combination. Cells were fixed, subjected to immunocytochemistry, and analyzed using confocal microscopy with a 63x objective as described in “Experimental Procedures.” Images are representative of cells observed in three separate experiments. Scale bars represent 10 μm. (B) *Top* – Diagram showing the principle of BRET using the RGS14-Luc/Gαi1-YFP pair. Non-radiative emission from the Luc tag excites the YFP if the donor/acceptor pairs are <math><100\text{\AA}</math>, which then emits at 535 nm. *Bottom* – HEK cells were transfected with 5ng RGS14-Luc plasmid alone or in combination with 10ng, 50ng, 100ng, 250ng, or 500ng of either Gαi1-YFP, Gαs-YFP, or Gαq-YFP plasmid. BRET signals (luminescence measured: Donor -  $480 \pm 20$  nm, Acceptor -  $530 \pm 20$  nm) were measured and net BRET was calculated by first calculating the  $530 \pm 20$  nm /  $480 \pm 20$  nm ratio and then subtracting the background BRET signal determined from cells transfected with the RGS14-Luc plasmid alone. (C) *Top panel* – HEK cells were transfected with

5ng RGS14-Luc and 250ng  $G\alpha i1$ -YFP plasmids alone (con) or in combination with 1 $\mu$ g of untagged  $G\alpha i1$ ,  $G\alpha i2$ ,  $G\alpha i3$ ,  $G\alpha o$ ,  $G\alpha s$ , or  $G\alpha q$  plasmid. Net BRET signals are shown between RGS14-Luc and  $G\alpha i1$ -YFP. *Bottom panel* – representative immunoblot of the different untagged  $G\alpha$  subunits used in the BRET experiment. All BRET graphs are representative of at least 3 separate experiments.

presence of  $G\alpha_{i1}$ -YFP, while no BRET signal was observed between RGS14-Luc paired with either  $G\alpha_s$ -YFP or  $G\alpha_q$ -YFP (Fig. 3.1B). This BRET signal saturation is indicative of a specific interaction between RGS14 and  $G\alpha_{i1}$  (177).

To further show BRET signal selectivity for RGS14-Luc interactions with  $G\alpha_{i1}$ -YFP, we performed a competition assay in cells co-expressing untagged  $G\alpha$  subunits (Fig. 3.1C) to determine which  $G\alpha$  subunits could displace  $G\alpha_{i1}$ -YFP from RGS14-Luc and disrupt the BRET signal. As expected, the previously reported RGS14 binding partners  $G\alpha_{i1}$  and  $G\alpha_{i3}$  each disrupted the RGS14/ $G\alpha_{i1}$  BRET signal, indicative of competition with  $G\alpha_{i1}$ -YFP for RGS14 binding. By contrast,  $G\alpha_{i2}$ ,  $G\alpha_o$ ,  $G\alpha_s$ , and  $G\alpha_q$  did not disrupt  $G\alpha_{i1}$ -YFP binding to RGS14. This selectivity for  $G\alpha_{i1}$  and  $G\alpha_{i3}$  binding is entirely consistent with earlier reports showing RGS14 binding to only  $G\alpha_{i1}$  and  $G\alpha_{i3}$ , but not other  $G\alpha$  through its GPR motif, further validating our BRET system (42,43,115-118).

Findings in Figure 3.1 suggested that the BRET signal we observed between RGS14 and  $G\alpha_{i1}$  occurs via the GPR motif. To test this hypothesis, we constructed mutants of RGS14-Luc that rendered it insensitive to binding  $G\alpha_{i1}$ -YFP through either the RGS domain (RGS14-E92A/N93A-Luc; *RGS-null*) (116), the GPR motif (RGS14-Q515A/R516A-Luc; *GPR-null*) (152,178), or both (RGS14-E92A/N93A/Q515A/R516A-Luc; *RGS/GPR-null*) (Fig. 3.2A-B). The BRET signal between wild-type RGS14 (WT) and  $G\alpha_{i1}$  was comparable to that between RGS14(*RGS-null*) and  $G\alpha_{i1}$ , suggesting that the majority of the observed BRET signal was not due to the RGS domain interacting with  $G\alpha_{i1}$ . However, the BRET signal between RGS14(*GPR-null*) and  $G\alpha_{i1}$  was approximately 5-fold lower than that of the RGS14-WT/ $G\alpha_{i1}$  pair. This indicates that the observed BRET signal between RGS14 and  $G\alpha_{i1}$  is primarily due to the GPR motif. As an additional approach, we generated  $G\alpha_{i1}$ -YFP mutants that were insensitive to binding either the RGS domain ( $G\alpha_{i1}$ -G183S-YFP; *RGSi*) (65), the GPR motif ( $G\alpha_{i1}$ -N149I-YFP; *GPRi*) (153,179), or both ( $G\alpha_{i1}$ -G183S/N149I-YFP; *RGSi/GPRi*) (Fig. 3.2C). Consistent

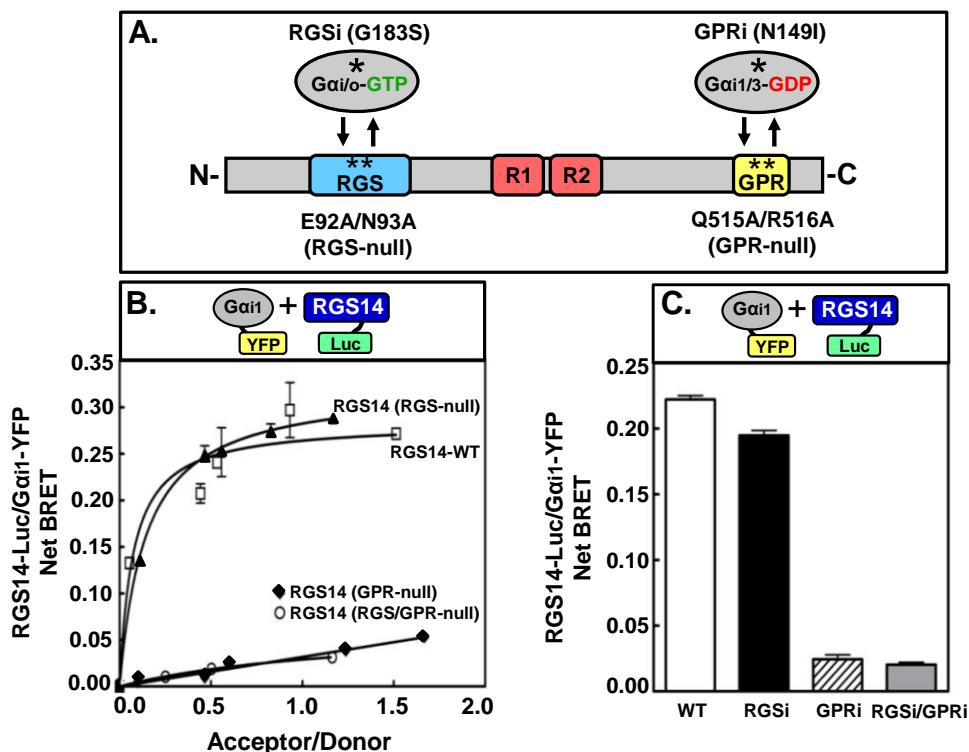


**Figure 3.2. RGS14 BRET signals with  $G\alpha i1$  in live cells are dependent on the GPR motif.**

(A) Illustration of the functional RGS14 and  $G\alpha i1$  mutants, with  $G\alpha i/o$ -RGSi incapable of binding the RGS domain,  $G\alpha i/3$ -GPRi incapable of binding the GPR motif, RGS14(*RGS-null*) incapable of binding active  $G\alpha i/o$ , and RGS14(*GPR-null*) incapable of binding inactive  $G\alpha i/3$ . (B) HEK cells were transfected with increasing amounts of  $G\alpha i1$ -YFP plasmid (10ng, 50ng, 100ng, 250ng, and 500ng) in combination with 5ng of either wild-type RGS14-Luc (RGS14-WT), RGS14(*RGS-null*)-Luc, RGS14(*GPR-null*)-Luc, or RGS14(*RGS/GPR-null*)-Luc plasmids. Net BRET was calculated by first calculating the  $530 \pm 20$  nm /  $480 \pm 20$  nm ratio and then subtracting the background BRET signal determined from cells transfected with the RGS14-Luc expression vector alone. Net BRET is shown between  $G\alpha i1$ -YFP and the different RGS14-Luc mutants. This figure is representative of at least three separate experiments with triplicate determinations. (C) HEK cells were transfected with 5ng wild-type RGS14-Luc and 250ng of either wild-type  $G\alpha i1$ -YFP (WT),  $G\alpha i1$ -RGSi-YFP,  $G\alpha i1$ -GPRi-YFP, or  $G\alpha i1$ -RGSi/GPRi-YFP plasmids. Net

BRET is shown between RGS14-Luc and the different G $\alpha$ i1-YFP mutants. This data is expressed as the mean of six separate experiments with triplicate determinations.

with findings in Fig. 3.2B, the BRET signal between RGS14 and  $G\alpha_{i1}$ -GPRi was substantially (~8-fold) lower than that generated by RGS14 paired with either wild-type  $G\alpha_{i1}$  (WT) or  $G\alpha_{i1}$ -RGSi. Taken together, these findings are entirely consistent with the idea that the majority of the BRET signals observed between RGS14 and  $G\alpha_{i1}$  are due to the interaction between the RGS14 GPR motif and  $G\alpha_{i1}$ .

*RGS14 forms a complex with the  $\alpha_{2A}$ -adrenergic receptor in a  $G\alpha_{i/o}$ -dependent manner.*

The GPR proteins AGS3 and AGS4 form  $G\alpha_{i}$ -dependent complexes with GPCRs that are regulated by receptor activation (144,167). Therefore, we sought to investigate whether the RGS14: $G\alpha_{i1}$  complex can also be regulated by GPCRs in cells. Subcellular localization data showed that while RGS14 remained predominately cytosolic in the presence of co-expressed  $\alpha_{2A}$ -AR, it was recruited to the plasma membrane in the presence of both overexpressed  $\alpha_{2A}$ -AR and  $G\alpha_{i1}$  in the absence of agonist (Fig. 3.3; left panel). This suggests formation of an RGS14: $G\alpha_{i1}$ : $\alpha_{2A}$ -AR complex at the plasma membrane. While RGS14 and  $G\alpha_{i1}$  remained at the plasma membrane, the  $\alpha_{2A}$ -AR internalized in the presence of agonist UK14304 (Fig. 3.3; right panel).

To further examine the regulatory effects of GPCRs on RGS14: $G\alpha_{i1}$  complexes, we analyzed the BRET signals between RGS14-Luc and Venus-tagged  $\alpha_{2A}$ -AR or  $\beta_2$ -AR (Fig. 3.4). As expected, little to no detectable BRET signal was observed between RGS14 and the  $G_s$ -linked  $\beta_2$ -AR in the absence or presence of both  $G\alpha_{i1}$  and the receptor agonist isoproterenol (Fig. 3.4A). Very low specific BRET signals were observed between RGS14 and  $\alpha_{2A}$ -AR both in the absence and presence of receptor agonist UK14304 (Fig. 3.4B; filled circles and open circles, respectively). However, a 3-fold increase in BRET signal was observed between  $\alpha_{2A}$ -AR and RGS14 in the presence of co-expressed  $G\alpha_{i1}$  (Fig. 3.4B; filled triangles). This signal was reduced by ~50% in the presence of UK14304 (Fig. 3.4B; open triangles). This agonist-induced reduction in BRET correlates with the lack of co-localization between RGS14 and the  $\alpha_{2A}$ -AR following agonist stimulation (Fig. 3.3; right panel). Furthermore, agonist-induced dissociation of the

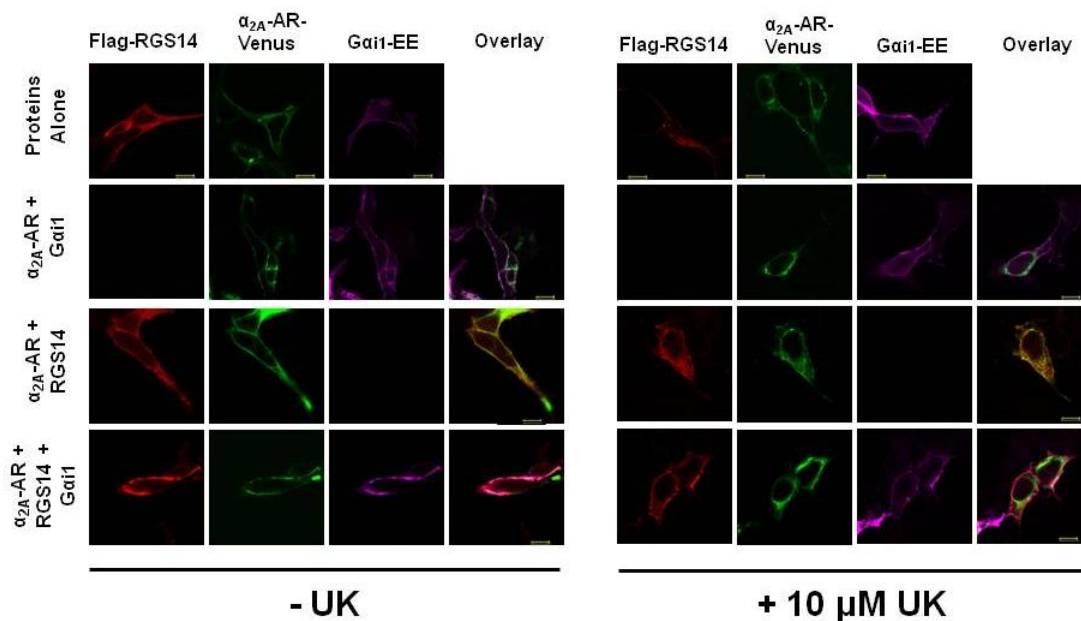


**Figure 3.3. RGS14 co-localization with Gai1 and the  $\alpha_{2A}$ -AR in live cells is regulated by receptor agonist.** Flag-RGS14, Gai1-EE, and  $\alpha_{2A}$ -AR-Venus were transfected into HEK cells alone and in combination. Cells were either unstimulated (-UK) or stimulated (+UK) with 10  $\mu$ M UK14304 for 5 mins. Cells were fixed, subjected to immunocytochemistry, and analyzed using confocal microscopy as described in “Experimental Procedures.” Images are representative of cells observed in three separate experiments. Scale bars represent 10  $\mu$ m.



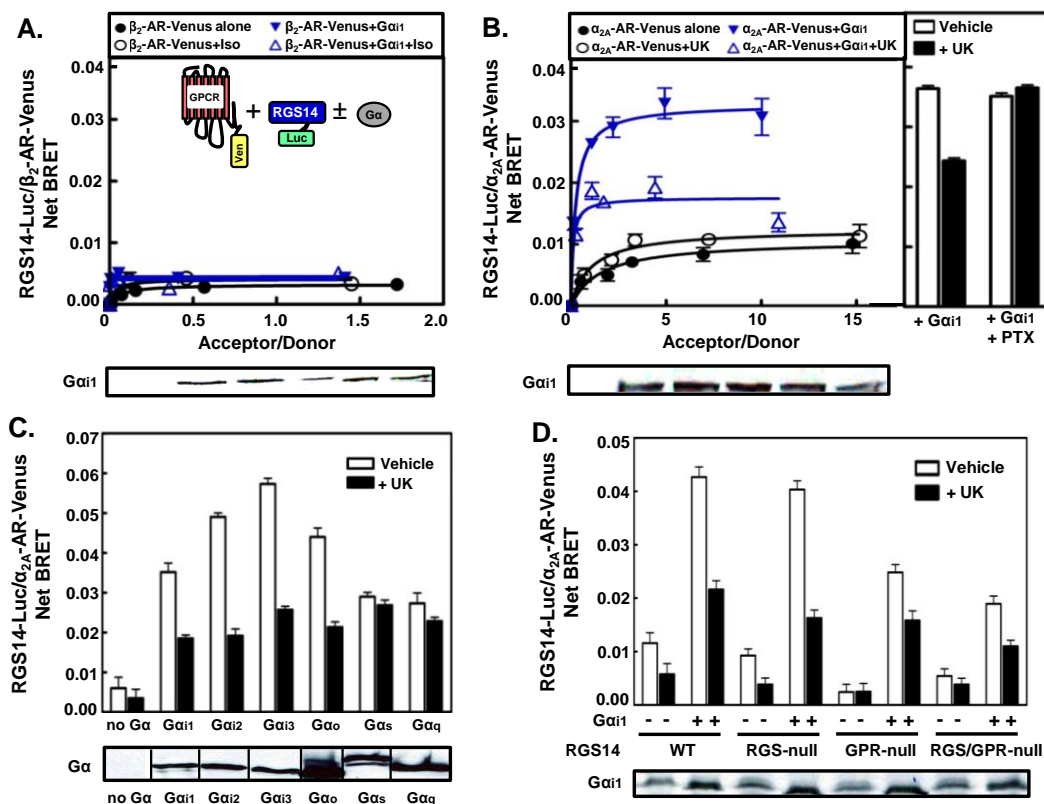


**Figure 3.4.** RGS14 forms a G*α*i/o-dependent complex with the  $\alpha_{2A}$ -AR in live cells. (A) Net BRET signals are shown from HEK cells transfected with 5ng RGS14-Luc, and 0ng, 10ng, 50ng, 100ng, 250ng, or 500ng  $\beta_2$ -AR-Venus plasmids in the presence or absence of 750ng pcDNA3::G*α*i1. Measurements were taken following treatment with either vehicle or isoproterenol (100  $\mu$ M) for 5 mins. A cartoon representing the BRET principal used in all experiments of Figure 4, which includes BRET measured between RGS14-Luc and a GPCR-Venus (Ven) in the presence or absence of untagged G*α*, is shown within the graph. (B) *Left panel* – Net BRET signals are shown from HEK cells transfected with 5ng RGS14-Luc, and either 0ng, 10ng, 50ng, 100ng, 250ng, or 500ng  $\alpha_{2A}$ -AR-Venus plasmid in the presence or absence of 750ng pcDNA3::G*α*i1. Measurements were taken following treatment with either vehicle or  $\alpha_{2A}$ -AR agonist UK14304 (10  $\mu$ M) for 5 mins. *Bottom panels* – representative immunoblots of untagged G*α*i1 subunits used in samples with transfected G*α*i1. *Right panel* – Net

RGS14-Luc/ $\alpha_{2A}$ -AR-Venus BRET signals are shown from HEK cells transfected with 5ng RGS14-Luc, 250ng  $\alpha_{2A}$ -AR-Venus, and 750ng  $G\alpha i1$  plasmids. Measurements were taken following treatment with UK14304 for 5 mins in the absence or presence of 100 ng/mL pertussis toxin that was applied 18 hours prior to agonist treatment, as indicated in the figure. Data is expressed as the mean of three separate experiments with triplicate determinations. (C) *Top panel* – HEK cells were transfected with 5ng RGS14-Luc and 100ng  $\alpha_{2A}$ -AR-Venus plasmids alone (no  $G\alpha$ ) or in combination with 750ng of either untagged  $G\alpha i1$ ,  $G\alpha i2$ ,  $G\alpha i3$ ,  $G\alpha o$ ,  $G\alpha s$ , or  $G\alpha q$  plasmids. Cells were either treated with vehicle or UK14304 (10  $\mu$ M) for 5 mins. The net BRET between RGS14-Luc and the  $\alpha_{2A}$ -AR-Venus under each condition is shown. Data is expressed as the mean of three separate experiments with triplicate determinations. *Bottom panel* – representative immunoblot of the different  $G\alpha$  subunits used. (D) Net BRET signals for the RGS14-Luc/ $\alpha_{2A}$ -AR-Venus pair are shown for HEK cells transfected with 100ng  $\alpha_{2A}$ -AR-Venus and combinations of 5ng RGS14-Luc mutant (WT, RGS-null, GPR-null, and RGS/GPR-null) plasmids in the absence or presence of 750ng untagged pcDNA3:: $G\alpha i1$ , and then treated with either vehicle or 10  $\mu$ M UK14304 for 5 mins. *Bottom panel* – representative immunoblot for  $G\alpha i1$  expression. Data is expressed as the mean of four separate experiments with triplicate determinations. The net BRET between RGS14-Luc and the GPCR-Venus pairs was calculated by first calculating the  $530 \pm 20$  nm /  $480 \pm 20$  nm ratio and then subtracting the background BRET signal determined from cells transfected with RGS14-Luc plasmid alone.

RGS14: $\alpha_{2A}$ -AR complex was completely blocked by pre-treatment with pertussis toxin (PTX) (Fig. 3.4B; right panel). The very low BRET signals observed between RGS14 and the  $\beta_2$ -AR in the presence of G $\alpha$ i1 (Fig. 3.4A) illustrate that the BRET signals observed between RGS14 and the  $\alpha_{2A}$ -AR are indeed specific and are not simply the result of “by-stander BRET,” i.e. RGS14 localizing at the plasma membrane with G $\alpha$ i1 and randomly interacting with the receptor.

The interaction between RGS14 and the  $\alpha_{2A}$ -AR was dependent on the presence of G $\alpha$ i/o family members (Fig. 3.4C). Specific BRET signals were observed between RGS14 and the  $\alpha_{2A}$ -AR in the presence of G $\alpha$ i1, G $\alpha$ i2, G $\alpha$ i3, and G $\alpha$ o, with lower signals observed in the presence of G $\alpha$ s and G $\alpha$ q. The agonist-mediated dissociation of the RGS14: $\alpha_{2A}$ -AR complex was observed in the presence of all four G $\alpha$ i/o family members tested, but not G $\alpha$ s or G $\alpha$ q (Fig. 3.4C).

To determine which domains of RGS14 are important for associating with the  $\alpha_{2A}$ -AR, we performed BRET experiments using the RGS14 constructs with mutations in the RGS domain and GPR motif as described in Fig. 3.2B (Fig. 3.4D). BRET signals observed between either RGS14-WT or RGS14(*RGS-null*) and the  $\alpha_{2A}$ -AR in the presence of co-expressed G $\alpha$ i1 were comparable, with similar reductions in response to receptor agonist UK14304. This suggests that the RGS domain of RGS14 is not required for the formation of the G $\alpha$ i1-dependent complex with the  $\alpha_{2A}$ -AR. In contrast, the BRET signals observed between the  $\alpha_{2A}$ -AR and RGS14(*GPR-null*) in the presence of G $\alpha$ i1 were reduced by approximately 50% in the absence of agonist compared to RGS14-WT, indicating that the GPR motif is critical to forming a complex with the  $\alpha_{2A}$ -AR in the presence of G $\alpha$ i1. Together, these results indicate that RGS14 forms a complex with the  $\alpha_{2A}$ -AR in the presence of a G $\alpha$ i/o protein, and that the GPR motif is critical in promoting the formation of this complex.

*The RGS14:G $\alpha$ i1 complex remains intact following  $\alpha_{2A}$ -AR stimulation.* Since the presence of G $\alpha$ i1 promotes the formation of an RGS14: $\alpha_{2A}$ -AR complex that is regulated by agonist, we examined the effects of  $\alpha_{2A}$ -AR stimulation on the RGS14:G $\alpha$ i1 complex (Fig. 3.5). To test this, we measured the BRET signal between RGS14-Luc and G $\alpha$ i1-YFP in the presence of

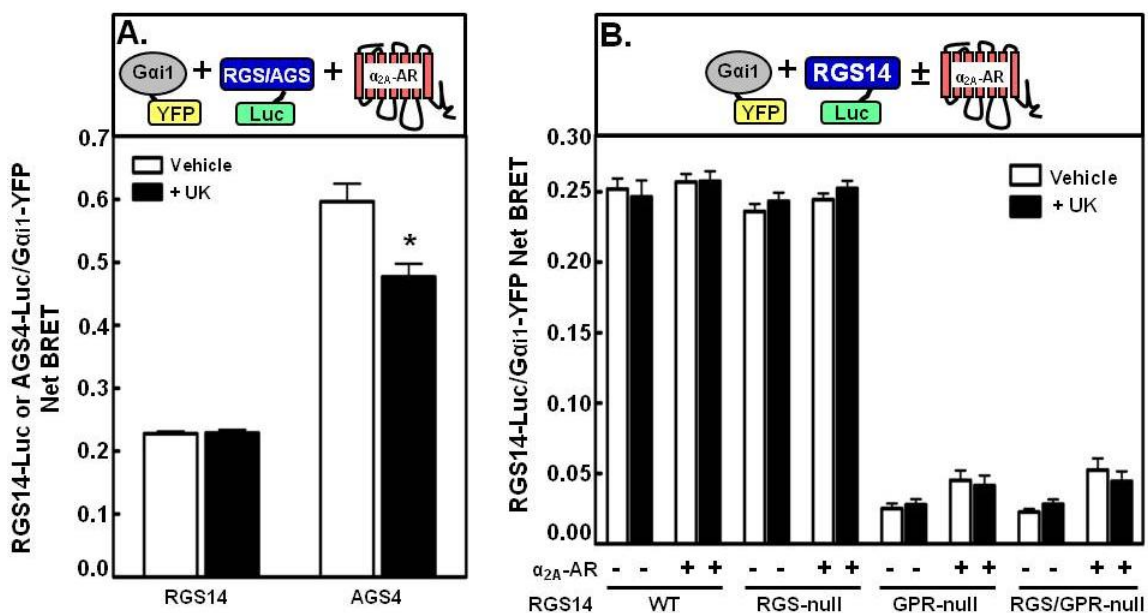


**Figure 3.5. RGS14 remains bound to Gαi1 following α<sub>2A</sub>-AR activation in live cells.** (A) HEK cells were transfected with 500ng untagged α<sub>2A</sub>-AR, 250ng Gαi1-YFP, and either 5ng RGS14-Luc or 2ng AGS4-Luc plasmids. Cells were treated with either vehicle or UK14304 (10 μM) for 5 mins. Net BRET generated from the RGS14-Luc/Gαi1-YFP or AGS4-Luc/Gαi1-YFP pairs was calculated by first calculating the  $530 \pm 20 \text{ nm} / 480 \pm 20 \text{ nm}$  ratio and then subtracting the background BRET signal determined from cells transfected with RGS14-Luc or AGS4-Luc plasmid alone, respectively. Data was analyzed using paired Student's *t*-test. \*,  $p < 0.05$  as compared with Vehicle control. (B) HEK cells were transfected with 250ng Gαi1-YFP and 5ng RGS14-Luc (WT, RGS-null, GPR-null, and RGS/GPR-null) plasmids with and without 500ng untagged α<sub>2A</sub>-AR plasmid and then treated with either vehicle or UK14304 (10 μM) for 5 mins. Net BRET generated from the RGS14-Luc/Gαi1-YFP pair was calculated as in (A). All data are expressed as the mean of three separate experiments with triplicate determinations.

untagged  $\alpha_{2A}$ -AR. The RGS14:G $\alpha$ i1 complex remains intact in the presence of the  $\alpha_{2A}$ -AR, regardless of receptor stimulation (Fig. 3.5A). This is in marked contrast to the decrease in BRET signal observed between AGS4-Luc and G $\alpha$ i1-YFP in the presence of stimulated  $\alpha_{2A}$ -AR (Fig. 3.5A and (144)). Together, these findings suggest that the  $\alpha_{2A}$ -AR dissociates from RGS14 following agonist stimulation, but that the dissociated RGS14 remains in complex with G $\alpha$ i1. This portrays a novel mechanism of GPR:G $\alpha$ i complex function with GPCRs that may be unique to RGS14 compared with other Group II AGS proteins.

The GPR motif is still critical for RGS14 interactions with G $\alpha$ i1 in the presence of the  $\alpha_{2A}$ -AR (Fig. 3.5B), as > 80% reductions in BRET signals were observed between G $\alpha$ i1 and both RGS14(*GPR-null*) and RGS14(*RGS/GPR-null*) regardless of the presence of receptor. This indicates that even the presence of a GPCR cannot facilitate RGS14 interactions with G $\alpha$ i1 in the absence of a functional GPR motif.

*Ric-8A promotes dissociation of the RGS14:G $\alpha$ i1 complex.* Since we observed Ric-8A regulation of RGS14:G $\alpha$ i1 complexes *in vitro* (48), we sought to quantitatively measure Ric-8A-mediated dissociation of RGS14:G $\alpha$ i1 complexes in live cells using BRET (Fig. 3.6A). As expected (48), increasing Ric-8A protein levels induced a decrease in BRET between RGS14-Luc and G $\alpha$ i1-YFP (Fig. 3.6C). Ric-8A-induced reductions in RGS14/G $\alpha$ i1 BRET were inhibited by pertussis toxin (+PTX) (Fig. 3.6C), which blocks Ric-8A binding and GEF activity toward G $\alpha$ i subunits (52). Expression of Ric-8A also induces an increase in G $\alpha$ i1-YFP protein expression levels (Fig. 3.6B), which is consistent with recent evidence showing that Ric-8A is important for the functional expression and stability of G $\alpha$  subunits (180). Interestingly, the effect of Ric-8A on G $\alpha$ i1-YFP expression levels was not blocked by pertussis toxin pre-treatment, suggesting that the effect of Ric-8A on G $\alpha$ i expression is independent from its GEF activity.

We next studied the effects of Ric-8A on RGS14:G $\alpha$ i1 complexes in the presence of the  $\alpha_{2A}$ -AR (Fig. 3.7A). In the absence of Ric-8A, RGS14:G $\alpha$ i1 complexes remained intact following receptor stimulation as before (see Fig. 3.5A). In the absence of receptor agonist, Ric-8A

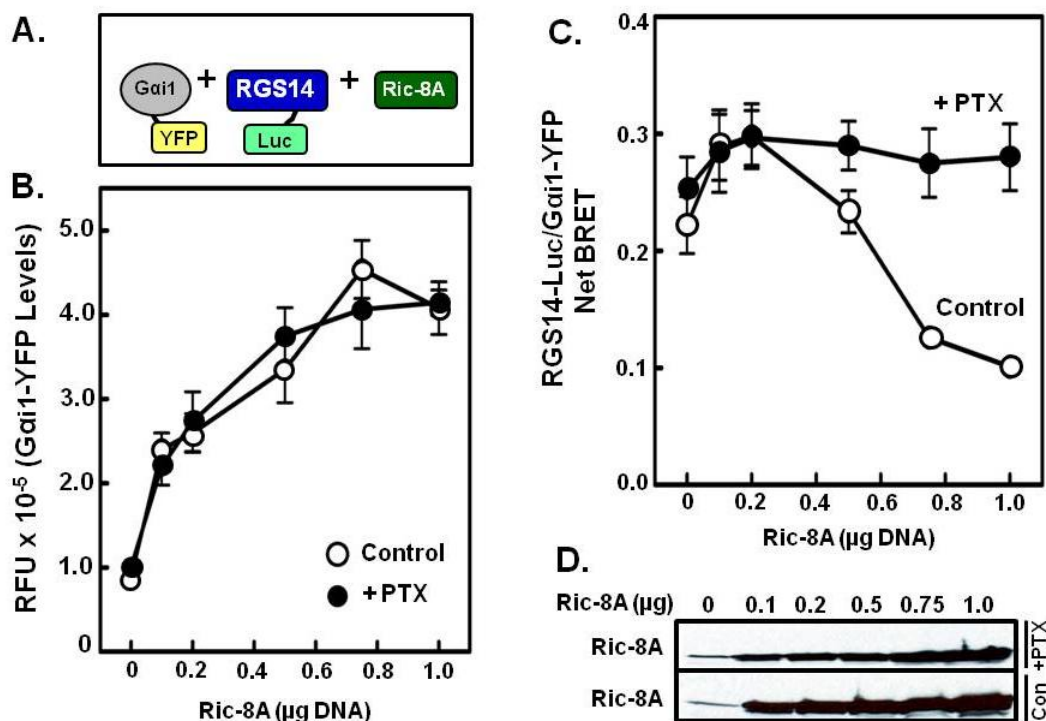


**Figure 3.6. Ric-8A facilitates dissociation of RGS14 from Gai1 in live cells.** (A) Diagram illustrating the BRET measured in this experiment between RGS14-Luc and Gai1-YFP in the presence of untagged Ric-8A. (B) HEK cells were transfected with 5ng RGS14-Luc, 250ng Gai1-YFP, and increasing amounts (0ng, 100ng, 200ng, 500ng, 750ng, or 1000ng) of Ric-8A plasmids. Cells were subsequently left untreated or pre-treated with 100 ng/mL pertussis toxin (+PTX) for 18 hours and then the Gai1-YFP fluorescence was measured. (C) HEK cells were transfected with 5ng RGS14-Luc, 250ng Gai1-YFP, and increasing amounts (0ng, 100ng, 200ng, 500ng, 750ng, or 1000ng) of Ric-8A plasmids. Cells were subsequently left alone or pre-treated with 100 ng/mL pertussis toxin (+PTX) for 18 hours and then the net BRET between RGS14-Luc and Gai1-YFP was measured and calculated. (D) Representative immunoblot of Ric-8A in each sample left alone (Con) or treated with PTX (+PTX). Measurements in panels (B) and (C) were taken from the exact same samples. Data is expressed as the mean of three separate experiments with triplicate determinations.

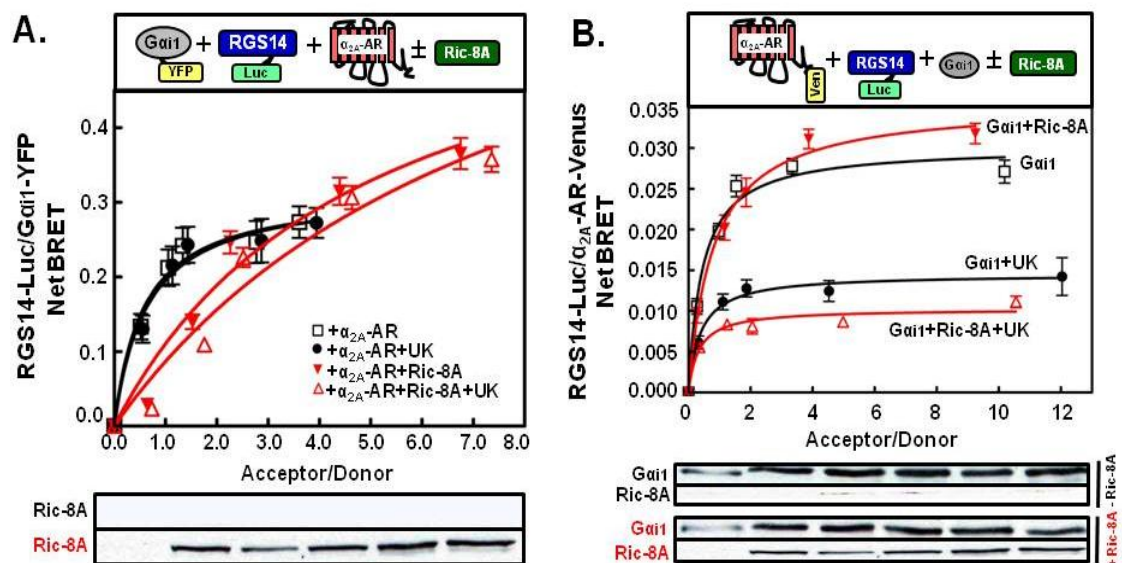


**Figure 3.7. Ric-8A induces dissociation of both Gαi1 and the α<sub>2A</sub>-AR from RGS14 following receptor stimulation.** (A) *Top panel* – Net BRET signals generated from the RGS14-Luc/Gαi1-YFP pair in HEK cells transfected with combinations of 5ng RGS14-Luc, 500ng α<sub>2A</sub>-AR, 200ng Ric-8A, and increasing amounts of Gαi1-YFP (0ng, 10ng, 50ng, 100ng, 250ng, and 500ng) plasmids. Cells were treated with either vehicle or UK14304 (10 μM) for 5 mins before BRET signals were measured. *Bottom panel* – representative immunoblot of Ric-8A expression for all 6 amounts of Gαi1-YFP plasmid transfected. “Ric-8A” and “Ric-8A” represent lysates from cells without transfected Ric-8A (top immunoblot) or cells with transfected Ric-8A (bottom immunoblot), respectively. Data are expressed as the mean of three separate experiments with triplicate determinations. (B) *Top panel* – Net BRET signals generated from the RGS14-Luc/α<sub>2A</sub>-AR-Venus (Ven) pair in HEK cells transfected with combinations of 5ng RGS14-Luc, 100ng Gαi1, 200ng Ric-8A, and increasing amounts of α<sub>2A</sub>-AR-Venus (0ng, 10ng, 50ng, 100ng, 250ng, and 500ng) plasmids. Cells were treated with either vehicle or UK14304 (10 μM) for 5 mins before BRET signals were measured. *Bottom panel* – representative immunoblot of Ric-8A and Gαi1 expression for all 6 amounts of α<sub>2A</sub>-AR-Venus transfected. Data are expressed as the mean of three separate experiments with triplicate determinations.

promoted a decrease in the RGS14/G $\alpha$ i1 BRET signal. In the presence of agonist, Ric-8A induced an even greater decrease in the BRET signal (Fig. 3.7A). These findings suggest that Ric-8A can recognize and act on RGS14:G $\alpha$ i1 complexes in the presence of GPCRs, and even more so in the presence of activated receptors.

*Ric-8A potentiates dissociation of the RGS14: $\alpha$ <sub>2A</sub>-AR complex caused by receptor agonist.* Since Ric-8A induced dissociation of G $\alpha$ i1 from RGS14 in the presence of the  $\alpha$ <sub>2A</sub>-AR, we next investigated the effect of Ric-8A on the RGS14: $\alpha$ <sub>2A</sub>-AR complex in the presence of G $\alpha$ i1 (Fig. 3.7B). Ric-8A had little effect on the RGS14: $\alpha$ <sub>2A</sub>-AR complex in the presence of co-expressed G $\alpha$ i1 in the absence of agonist. However, BRET signals between RGS14 and the  $\alpha$ <sub>2A</sub>-AR in the presence of G $\alpha$ i1 and receptor agonist were further reduced by ~25% in the presence of Ric-8A (red lines) compared with the absence of Ric-8A (black lines) (Fig. 3.7B). These findings suggest that Ric-8A acts to facilitate dissociation of RGS14 from activated  $\alpha$ <sub>2A</sub>-AR in the presence of G $\alpha$ i1.

### **3.4 Discussion**

RGS14 is unusual among RGS protein family members in that it possesses two distinct G $\alpha$  binding domains: an RGS domain that accelerates GTP hydrolysis on activated G $\alpha$ i/o subunits (115,116,118), and a GPR motif that forms a tight complex with inactive G $\alpha$ i1/3 subunits (43,48,117,118,152). RGS14 also belongs to a second family of signaling proteins, the Group II AGS proteins, that are characterized by the presence of one or more GPR motifs that mediate newly appreciated “unconventional” G protein signaling events (166,181). Recent studies of AGS3 and AGS4 demonstrate that these GPR domain-containing proteins interact with G $\alpha$ i to form complexes with G $\alpha$ i/o-linked GPCRs in cells (144,167). Our results with RGS14 support those findings, but also highlight some important differences that will be discussed. Overall, our findings indicate the following: 1) RGS14 selectively interacts with G $\alpha$ i1/3 in live cells through its GPR motif; 2) RGS14 forms a G $\alpha$ i/o-dependent complex with the Gi/o-linked  $\alpha$ <sub>2A</sub>-AR in live cells;



3) RGS14 dissociates from the  $\alpha_{2A}$ -AR following agonist treatment, but remains bound to G $\alpha$ i1; 4) Ric-8A potentiates agonist-stimulated dissociation of the RGS14: $\alpha_{2A}$ -AR complex; and 5) Ric-8A induces dissociation of G $\alpha$ i1 and  $\alpha_{2A}$ -AR from RGS14, having a greater effect in the presence of stimulated  $\alpha_{2A}$ -AR. Taken together, these findings suggest that RGS14 integrates both unconventional Ric-8A/G protein signaling and conventional GPCR/G protein signaling. A summary and interpretation of these findings is shown in Figs. 3.8 and 3.9.

*RGS14 selectively interacts with inactive G $\alpha$ i1/3 in live cells through its GPR motif.* Our BRET analysis and confocal imaging indicate that the interaction of RGS14 with inactive G $\alpha$ i1/3 occurs at the plasma membrane of live cells (Fig. 3.1). Consistent with previous studies (42,43,116-118), the capacity of both G $\alpha$ i1 and G $\alpha$ i3 (but not G $\alpha$ i2, G $\alpha$ o, G $\alpha$ s, or G $\alpha$ q) to disrupt the BRET between RGS14-Luc and G $\alpha$ i1-YFP indicates that the observed BRET signal is specific for interactions between RGS14 and G $\alpha$ i1/3 (Fig. 3.1C).

To clarify which RGS14 domains are involved in the RGS14:G $\alpha$ i1 interaction, we measured the BRET signal between mutant forms of RGS14-Luc and G $\alpha$ i1-YFP that specifically blocked RGS and/or GPR motif functions (Fig. 3.2). These studies show that the majority of the observed RGS14:G $\alpha$ i1 interaction is conferred by the GPR motif of RGS14 interacting with G $\alpha$ i1. The fact that the BRET signal was never completely abolished in the presence of the RGS14 and G $\alpha$ i1 double mutants that ablate G $\alpha$  binding to both the GPR and RGS domains (Fig. 3.2B-C) is consistent with the existence of a third G protein binding site on RGS14, as has been postulated (143).

*RGS14 selectively interacts with the  $\alpha_{2A}$ -AR receptor in a G $\alpha$ i/o-dependent manner.* Since RGS14 interacts with G $\alpha$ i/o family members, we examined whether RGS14 can be regulated by a G $\alpha$ i/o-linked GPCR, specifically the  $\alpha_{2A}$ -AR. RGS14, G $\alpha$ i1, and the  $\alpha_{2A}$ -AR co-localized at the plasma membrane when all three proteins were expressed together in cells (Fig. 3.3; left panel), consistent with the possibility that a ternary protein complex forms at the plasma membrane. Following treatment with the  $\alpha_{2A}$ -AR agonist UK14304, RGS14 and G $\alpha$ i1 remained at the plasma

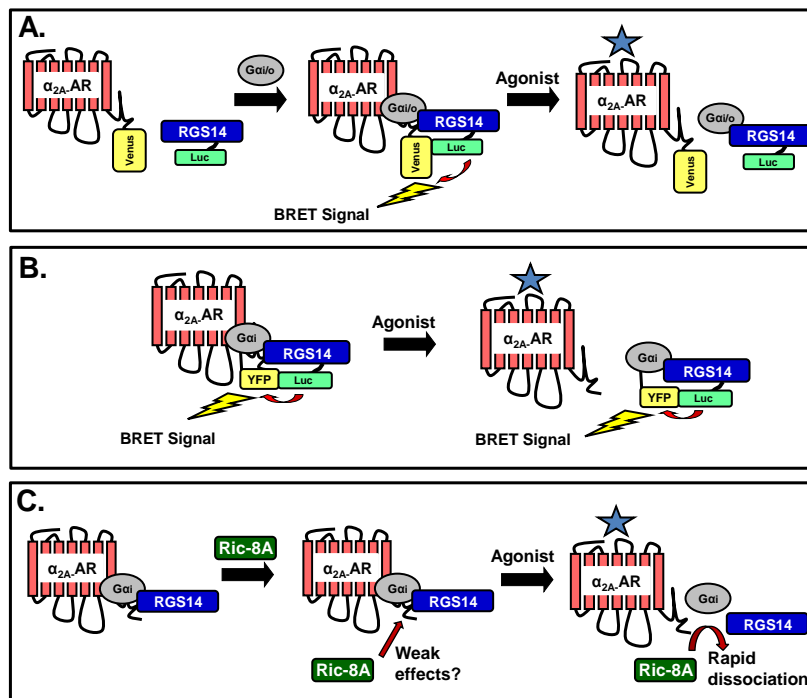


**Figure 3.8. Working model for regulation of RGS14 complexes with Gai1 and  $\alpha_{2A}$ -AR.**

Diagrams are shown illustrating our findings from experiments measuring BRET signals between RGS14-Luc and  $\alpha_{2A}$ -Venus in the presence and absence of both untagged Gai1 and receptor agonist (A), as well as RGS14-Luc and Gai1-YFP in the presence and absence of both untagged  $\alpha_{2A}$ -AR and receptor agonist (B). (C) Summary of findings when Ric-8A was expressed with RGS14, Gai1, and  $\alpha_{2A}$ -AR in live cells in both the absence and presence of receptor agonist.

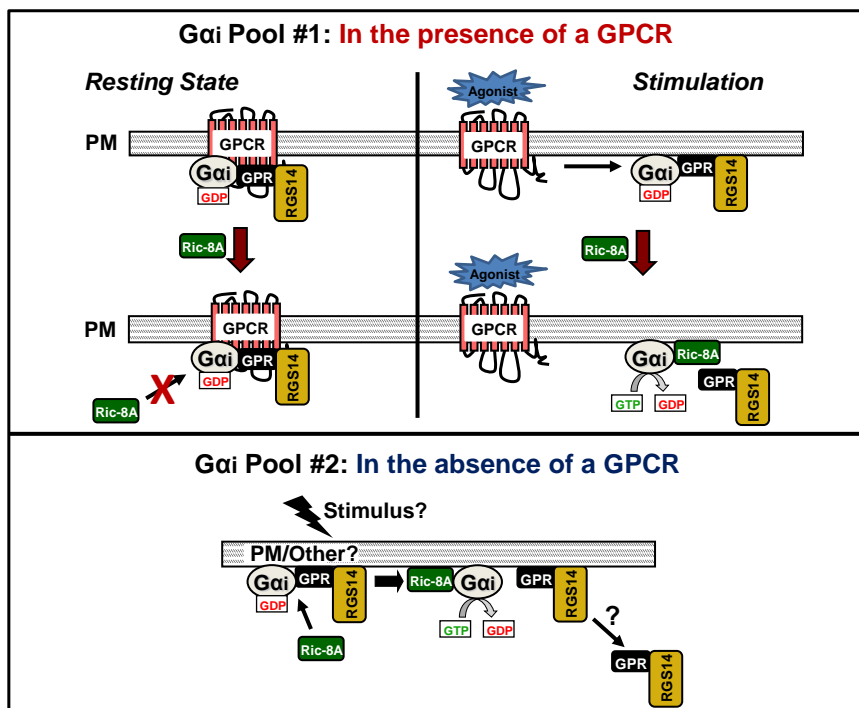


**Figure 3.9. Working model depicting Ric-8A regulation of the  $\alpha_{2A}$ -AR:Gαi1:RGS14 complex.** This visual model includes RGS14, Gαi1,  $\alpha_{2A}$ -AR, and Ric-8A localized at or near the plasma membrane (PM). We propose that two pools of Gαi exist in cells. *Top* – One pool localizes with GPCRs and Gβγ/GPR proteins at the plasma membrane (PM) to participate in conventional GPCR-dependent G protein signaling. In the resting state (left) of our model, a GPCR:Gαi:RGS14 complex forms and remains intact. Ric-8A has little effect on this complex in the absence of stimulation. Upon receptor stimulation (right), the RGS14:Gαi complex dissociates from the GPCR, where it can be further acted upon by Ric-8A. *Bottom* – The second Gαi pool forms complexes with GPR proteins at the plasma membrane in the absence of a GPCR to participate in unconventional GPCR-independent signaling. According to our findings, RGS14 forms a complex with Gαi through its GPR motif. Ric-8A can recognize this RGS14:Gαi complex, catalyze GTP exchange on Gαi, and induce dissociation of the complex.

membrane, whereas the  $\alpha_{2A}$ -AR partially internalized (Fig. 3.3; right panel), suggesting that the ternary complex dissociates. This hypothesis was supported in our BRET experiments. Co-expression of  $G\alpha i1$  resulted in an approximate 3-fold increase in RGS14/ $\alpha_{2A}$ -AR BRET compared to RGS14 and  $\alpha_{2A}$ -AR alone (Fig. 3.4B). The  $G\alpha i1$ -dependent RGS14/ $\alpha_{2A}$ -AR BRET signal was reduced ~50% following receptor activation by agonist, and this agonist effect was blocked by pertussis toxin pre-treatment (Figure 3.4B; right panel). This implies that functional coupling of the  $\alpha_{2A}$ -AR to  $G\alpha i1$  disrupts the RGS14: $\alpha_{2A}$ -AR complex. It is possible that the interacting sites between GPCR/ $G\alpha i$  are different between the inactive and active states, the latter being sensitive to PTX. This is suggested by previous work on the phenomenon of guanine nucleotide-sensitive agonist binding to GPCRs, and more recent work demonstrating preformed complexes of GPCRs and G proteins (15).

As expected, RGS14 interaction with the  $\alpha_{2A}$ -AR is dependent on the presence of  $G\alpha i/o$  since  $G\alpha q$  and  $G\alpha s$  failed to elicit a robust RGS14/ $\alpha_{2A}$ -AR BRET signal. Somewhat unexpectedly, RGS14: $\alpha_{2A}$ -AR association is promoted indiscriminately by the presence of any  $G\alpha i/o$  family member ( $G\alpha i1$ ,  $G\alpha i2$ ,  $G\alpha i3$ , and  $G\alpha o$ ) (Fig. 3.4C). This is surprising given that the RGS14: $\alpha_{2A}$ -AR interaction was highly dependent on the GPR motif (Fig. 3.4D), which only interacts with  $G\alpha i1$  and  $G\alpha i3$  in the absence of receptor. One possible explanation may be that RGS14 recognizes a receptor if the receptor is bound to any  $G\alpha i/o$  protein, reflecting the promiscuity of RGS14 GAP activity toward activated  $G\alpha i/o$  subunits. In this regard, RGS14 is similar to RGS2. In the absence of receptor, RGS2 acts specifically on  $G\alpha q$  (74). However, RGS2 is capable of interacting with  $G\alpha i$  in the presence of a  $G i/o$ -linked GPCR (89), albeit with 30-fold lower affinity than for  $G\alpha q$  (182). We note that RGS14 complexes with receptor are dependent on both the G protein and the receptor because the  $G_s$ -linked  $\beta_2$ -AR failed to interact with RGS14 in the presence of  $G\alpha i1$  (Fig. 3.4A).

The GPR motif interaction with  $G\alpha i1$  is important in promoting formation of the RGS14: $\alpha_{2A}$ -AR complex (Fig. 3.4D). The RGS14/ $\alpha_{2A}$ -AR BRET signal was greatly reduced in

the presence of RGS14(*GPR-null*) compared to RGS14-WT, indicating that G $\alpha$ i1 has a reduced capacity to bring RGS14 and the  $\alpha_{2A}$ -AR in close proximity when it cannot bind the GPR motif. Even when G $\alpha$ i1 could no longer bind either the RGS domain or GPR motif, there was still a slight BRET signal between RGS14(*RGS/GPR-null*) and the  $\alpha_{2A}$ -AR. Several possibilities exist to explain these results: 1) there may be another (undefined) G $\alpha$ i1 binding site on RGS14 (143); 2) RGS14 may be bound to G $\alpha$ i1 at a distinct site on the extreme C-terminus of G $\alpha$ i1 (48); or 3) an unknown binding partner/scaffold may facilitate an RGS14: $\alpha_{2A}$ -AR interaction.

*RGS14 remains bound to G $\alpha$ i1 after dissociating from the  $\alpha_{2A}$ -AR.* Although RGS14 dissociated from the  $\alpha_{2A}$ -AR following agonist treatment in the presence of co-expressed G $\alpha$ i1 (Fig. 3.4), it remained in complex with G $\alpha$ i1 via the GPR motif (Fig. 3.5). This finding is unexpected and differs from previous observations that show AGS3 and AGS4 dissociating from G $\alpha$ i following receptor activation (Fig. 3.5A and (144,167)). Our result suggests that RGS14 and G $\alpha$ i1 remain bound following receptor activation. This result is reminiscent of other findings showing that, in contrast to established models of G protein signaling (14), G $\beta\gamma$  may not necessarily always dissociate from G $\alpha$ . In some cases G $\beta\gamma$  may rearrange relative to G $\alpha$ -GTP following receptor activation (15), although in others G $\beta\gamma$  does appear to dissociate ((16,17) and (183)). Irrespective of the mechanism involved, our findings represent a novel mechanism of action for GPCR/G $\alpha$ /RGS complexes, where the active conformation of the  $\alpha_{2A}$ -AR favors release of an RGS14:G $\alpha$ i1 complex that may then be able to function as a signaling complex on its own or with other binding partners (such as potential MAP kinase signaling partners (121)). This complex may be regulated and function independently of the GPCR.

*Ric-8A is a key regulator of the GPCR:G $\alpha$ i1:RGS14 complex.* Although Ric-8A has been shown to influence GPCR signaling (169,170,184), little is known mechanistically about if or how Ric-8A may directly interact with and regulate GPCR/G protein complexes. We recently demonstrated that Ric-8A induces dissociation of RGS14 from G $\alpha$ i1 *in vitro* (48). In this study we sought to quantitatively measure the dissociative effects of Ric-8A on RGS14:G $\alpha$ i1 complexes

in live cells using BRET (Fig. 3.6). Pertussis toxin blocked Ric-8A mediated dissociation of the RGS14:G $\alpha$ i1 complex (Fig. 3.6C-D), consistent with recent reports showing that pertussis toxin inhibits Ric-8A GEF activity on G $\alpha$ i1 and that Ric-8A binds to G $\alpha$ i1 at a region overlapping with the pertussis toxin binding site (48,52). In the absence of pertussis toxin, Ric-8A facilitated RGS14:G $\alpha$ i1 complex dissociation (Fig. 3.6C-D). Ric-8A also induced dissociation of the RGS14:G $\alpha$ i1 complex in the presence of the  $\alpha_{2A}$ -AR, even in the absence of  $\alpha_{2A}$ -AR stimulation (Fig. 3.7A). This may be explained by Ric-8A effects on G $\alpha$ i1 expression levels. Since Ric-8A overexpression also induced an increase in G $\alpha$ i1 expression (Fig. 3.6B), it may be that there is an overabundance of G $\alpha$ i1 that is free to bind RGS14. The number of RGS14:G $\alpha$ i1 complexes may therefore outnumber the number of  $\alpha_{2A}$ -ARs, resulting in free RGS14:G $\alpha$ i1 complexes on which Ric-8A may act in the absence of receptor activation.

Ric-8A did not induce dissociation of the RGS14: $\alpha_{2A}$ -AR complex in the absence of receptor stimulation (Fig. 3.7B). This is in contrast to its effects on the RGS14:G $\alpha$ i1 complex in the presence of unstimulated receptor. It is possible that Ric-8A is facilitating dissociation of RGS14:G $\alpha$ i1 complexes that are not associated with receptors, accounting for the decrease in RGS14/G $\alpha$ i1 BRET seen in the presence of unstimulated receptor (Fig. 3.7A). In a cellular signaling context, Ric-8A may function similarly to the Arr4 protein in yeast that serves a feed-forward facilitatory role in pheromone receptor-G protein signaling mating responses (185). Consistent with this idea is that Ric-8A potentiates taste-receptor signaling by a potential feed-forward mechanism (169).

Taken together, these studies show that RGS14 can associate with a GPCR:G $\alpha$ i/o complex in a regulated fashion, and that Ric-8A is a regulatory partner in this process (see Fig. 3.8). Although Ric-8A potentiated dissociation of RGS14:G $\alpha$ i1 complexes from the  $\alpha_{2A}$ -AR in both the absence and presence of receptor stimulation, it had no effect on dissociating the RGS14: $\alpha_{2A}$ -AR complex itself in the absence of stimulation. We postulate that two pools of RGS14:G $\alpha$ i1 complexes may exist (Fig. 3.9). One subset resides at membranes (plasma and

others?) in the absence of a GPCR, and the other directly complexes to a cell surface receptor. Ric-8A acts differently on the RGS14:G $\alpha$ i1 complex depending on whether or not the complex is coupled to a GPCR. In the absence of a GPCR (Fig. 3.9; bottom), Ric-8A can recognize and induce dissociation of the RGS14:G $\alpha$ i1 complex. When the RGS14:G $\alpha$ i1 complex is associated with a GPCR (Fig. 3.9; top), Ric-8A may not affect RGS14:G $\alpha$ i1 complexes unless the receptor is activated. In this case, Ric-8A induces dissociation of G $\alpha$ i1 from RGS14 and subsequently RGS14 from receptor.

Our findings demonstrate that RGS14 functions in a unique mechanism to integrate both conventional GPCR/G protein signaling and unconventional GPCR-independent G protein signaling. These results highlight newly appreciated roles of GPR proteins at the interface of G protein signaling pathways, making them significant targets in the study of non-canonical G protein regulation and function.

**CHAPTER 4:****G*α*i1 and G Protein-Coupled Receptors Regulate Regulator of G Protein Signaling 14****(RGS14) Interactions with H-Ras in Live Cells**



#### 4.1 Introduction

Canonical G protein signaling pathways include a G protein-coupled receptor (GPCR) coupled to a heterotrimeric G protein ( $G\alpha\beta\gamma$ ), which acts as a GTPase timing switch. Upon GPCR activation, the receptor acts as a guanine nucleotide exchange factor (GEF) and facilitates GDP release and subsequent GTP binding to the  $G\alpha$  subunit, which is followed by  $G\beta\gamma$  dissociation/rearrangement from  $G\alpha$ -GTP. Free  $G\beta\gamma$  and  $G\alpha$ -GTP are now able to engage downstream effectors and regulate signaling events (14,145). Recent studies have examined the function of the regulators of G protein signaling (RGS) proteins in conventional G protein signaling, specifically how they act as GTPase accelerating proteins (GAPs) toward activated  $G\alpha$  subunits. The conserved RGS domain binds and enhances the intrinsic rate of  $G\alpha$  nucleotide hydrolysis, resulting in GPCR/G protein signal termination (113,146,147).

The Regulator of G protein Signaling 14 (RGS14) is a complex RGS protein grouped in the R12 subfamily of RGS proteins along with its closest relatives, RGS10 and RGS12 (62,113). Predominately expressed in the hippocampus of brain (118,124), RGS14 has been implicated in hippocampal-based learning, memory, and cognition (124). The molecular mechanisms underlying these effects of RGS14, however, remain largely unknown. The highly unusual sequence and domain structure of RGS14 suggests it serves as a multifunctional scaffold in both G protein and MAP kinase signaling (114). In addition to the conserved RGS domain that confers GAP activity toward  $G\alpha_{i/o}$  subunits (115,116,118), RGS14 also possesses two tandem Ras/Rap-binding domains (RBDs) and a G protein regulatory (GPR) motif that binds selectively to  $G\alpha_{i1}$  and  $G\alpha_{i3}$  subunits and prevents them from becoming activated (42,43,117). Recent work has also shown that RGS14 participates in newly-appreciated unconventional G protein signaling networks, which involve G protein activation in the absence of GPCRs (30-34,36,148,165). Specifically, the RGS14: $G\alpha_{i1}$ -GDP complex is regulated by the non-receptor GEF Ric-8A (48), both in the absence and presence of a coupled GPCR (186). This highlights a novel mechanism

of action for an RGS protein, shedding light onto how RGS14 may function within hippocampal neurons to regulate their signaling.

Although RGS14 may function within the brain through binding  $G\alpha_{i/3}$  and participating in Ric-8A-mediated unconventional G protein signaling pathways, evidence also suggests that RGS14 regulates MAP kinase signaling through binding H-Ras and Raf-1 via its RBDs (121). RGS14 binds directly to H-Ras via its first RBD (122), preferring to bind the activated form of H-Ras (121). By binding activated H-Ras, RGS14 inhibits PDGF-mediated ERK activation. Interestingly, this effect is dependent on the presence of  $G\alpha_{i1}$ . When RGS14 is bound to  $G\alpha_{i1}$ , it can no longer bind Raf-1, and therefore can no longer regulate PDGF signaling (121). These results suggest that RGS14 acts as a molecular switch from binding Ras/Raf-1 and regulating MAP kinase signaling to binding  $G\alpha_i$  and regulating G protein signaling. What remains unknown is whether a GPCR is involved in promoting this switch mechanism, as studies have shown that GPCRs can transactivate growth factor receptors to stimulate Ras-mediated MAP kinase signaling (97-99).

Here, I wanted to investigate how RGS14/H-Ras interactions are regulated in live cells, specifically examining the effects of both active and inactive  $G\alpha_i$  and GPCRs on this interaction. Using bioluminescence resonance energy transfer (BRET), I show that RGS14 binds preferentially to activated H-Ras in live cells, and that this interaction is greatly facilitated by inactive  $G\alpha_{i1}$ . Also, activation of the  $G_i$ -linked  $\alpha_{2A}$ -adrenergic receptor ( $\alpha_{2A}$ -AR) induces dissociation of RGS14:H-Ras complexes, further supporting a link between GPCRs and MAP kinase signaling. These results suggest that GPCR activation may promote the switch mechanism for RGS14 and allow it to participate in G protein signaling, which may ultimately underlie the function of RGS14 in suppressing synaptic plasticity within hippocampal neurons (124).

## 4.2 Experimental Procedures

*Plasmids and antibodies:* The rat RGS14 cDNA used in this study (Genbank accession number U92279) was acquired as described (118). Wild-type (WT) and *GPR-null* rat RGS14 Luciferase (Luc) constructs were generated as previously described (186) using the phRLucN2 vector graciously provided by Dr. Michel Bouvier (University of Montreal).

Venus-tagged H-Ras constructs were made from the parental H-Ras cDNA purchased from the UMR cDNA Resource Center (Rolla, Missouri). Venus tagged-wild-type H-Ras (H-Ras-WT-Venus) was generated by digesting the parental H-Ras-WT plasmid at EcoRI and SacII restriction sites, and ligating the resulting product into Venus-C1 vector (graciously provided by Stephen Ikeda and Steven Vogel, National Institutes of Health). Constitutively activated H-Ras(G/V)-Venus was generated by mutating the G12 residue of H-Ras-WT-Venus to V12 using the QuickChange kit (Stratagene) and the following oligonucleotide primers: forward primer, 5'- AAT ATA AGC TGG TGG TGG TGG GCG CCG TCG GTG TGG GCA AGA GT-3'; reverse primer, 5'- ACT CTT GCC CAC ACC GAC GGC GCC CAC CAC CAC CAG CTT ATA TT - 3'. The H-Ras CaaX box mutants were made using the QuickChange kit (Stratagene) and the following oligonucleotide primers: forward primer, 5'- GGC TGC ATG AGC TGC AAG TCT GTG CTC TCC-3'; reverse primer, 5'- GGA GAG CAC AGA CTT GCA GCT CAT GCA GCC- 3'. The RGS14-R333L-Luc mutant was constructed using the QuickChange kit (Stratagene) and the following oligonucleotide primers: forward primer, 5'- CTG TGA GAA GAG TTG CCT CTC TCT ACC-3'; reverse primer, 5'- GGT AGA GAG AGG CAA CTC TTC TCA CAG-3'. Rat G $\alpha$ i1-YFP (G $\alpha$ i1-YFP) in pcDNA3.1 was generated by Dr. Scott Gibson (University of Texas Southwestern) (171) and was generously provided along with pcDNA3.1::G $\alpha$ i1-Q204L plasmid by Dr. Joseph Blumer (Medical University of South Carolina).  $\alpha_{2A}$ -adrenergic receptor ( $\alpha_{2A}$ -AR) plasmids were generated as described and provided by Dr. Michel Bouvier (University of Montreal) (172,173).

Anti-sera used include anti-G $\alpha$ i1 (Santa Cruz Biotechnologies, Inc.), anti-H-Ras (Abcam), peroxidase-conjugated goat anti-mouse IgG (Rockland Immunochemicals, Inc.), and peroxidase-conjugated goat anti-rabbit IgG (Bio-Rad).

*Cell Culture and Transfection:* HEK293 cells were maintained in Dulbecco's minimal essential medium (without phenol red) containing 10% fetal bovine serum (5% following transfection), 2 mM glutamine, 100 U/mL penicillin, and 100 mg/mL streptomycin. Cells were incubated at 37°C with 5% CO<sub>2</sub> in a humidified environment. Transfections were performed using previously described protocols with polyethyleneimine (PEI; Polysciences, Inc.) (144).

*BRET:* BRET experiments were performed as previously described (144,167). Briefly, HEK293 cells were transiently transfected with BRET donor and acceptor plasmids using PEI. Twenty-four hours after transfection, the culture medium was removed and cells were washed once with PBS and harvested with Tyrode's solution (140 mM NaCl, 5 mM KCl, 1 mM MgCl<sub>2</sub>, 1mM CaCl<sub>2</sub>, 0.37 mM NaH<sub>2</sub>PO<sub>4</sub>, 24 mM NaHCO<sub>3</sub>, 10 mM HEPES, and 0.1% glucose (w/v), pH 7.4). Each group of cells was distributed into gray 96-well optiplates (Perkin Elmer) in triplicate, with each well containing 1x10<sup>5</sup> cells. The acceptor (YFP/Venus-tagged) protein expression levels were evaluated by measuring total fluorescence using the TriStar LB 941 plate reader (Berthold Technologies) with excitation and emission filters at 485 and 535 nm, respectively. Data was analyzed using the MikroWin 2000 program. After fluorescence measurement, Coelenterazine H (Nanolight Technology; 5  $\mu$ M final concentration) was then added and luminescence detected in the 480 +/- 20 and 530 +/- 20 nm windows for donor (Luc) and acceptor (YFP/Venus), respectively, by the TriStar LB 941 plate reader. In samples containing overexpressed  $\alpha_{2A}$ -AR, cells were left untreated or were stimulated with 10  $\mu$ M UK14304 (Sigma) prior to addition of coelenterazine. BRET signals were determined by calculating the ratio of the light intensity emitted by the YFP/Venus divided by the light intensity emitted by Luc. Net BRET values were corrected by subtracting the background BRET signal detected from

the expression of the donor fusion protein (Luc) alone. Immunoblots were performed as described previously (158).

### 4.3 Results

*RGS14 preferentially interacts with activated H-Ras via the first RBD.* Since RGS14 has been shown to bind Ras both *in vitro* (122) and in cells through co-immunoprecipitation (121), we sought to quantitatively measure this interaction in live cells using BRET. We therefore measured the strength and selectivity of a BRET signal between RGS14-Luc and either H-Ras-WT-Venus or constitutively activated H-Ras(G12V)-Venus (referred to as H-Ras(G/V)-Venus) (Fig. 4.1A). Transfection of HEK cells with increasing amounts of Venus-tagged H-Ras plasmids and a fixed amount (5 ng) of RGS14-Luc plasmid showed a robust, saturable BRET signal in the presence of H-Ras(G/V)-Venus, while an approximate 2-fold decrease in the signal was observed in the presence of H-Ras-WT-Venus (Fig. 4.1A). To determine the specificity of this interaction, H-Ras(G/V) was co-expressed with either wild-type (WT) RGS14 or the RGS14-R333L mutant of RGS14 (Fig. 4.1B), which does not bind H-Ras(G/V) in cell lysates (121). As in Fig. 4.1A, there is a strong BRET signal between RGS14-WT and H-Ras(G/V). This signal is reduced more than 4-fold in the presence of RGS14-R333L; however, the signal is not completely ablated (Fig. 4.1B).

*Gai1 facilitates RGS14 interactions with activated H-Ras.* Since our previous work suggests that RGS14 acts as a molecular switch for regulating MAP kinase and G protein signaling, we next tested the effects of Gai1 on RGS14/H-Ras(G/V) BRET signals. The BRET signal between RGS14-Luc and increasing amounts of H-Ras(G/V)-Venus was measured in the absence or presence of Gai1 (Fig. 4.2A). The observed RGS14/H-Ras(G/V) BRET signal was greatly enhanced in the presence of overexpressed Gai1 (Fig. 4.2A), indicating Gai1-mediated regulation of this complex. To test whether Gai1 remained bound to RGS14 in the presence of H-

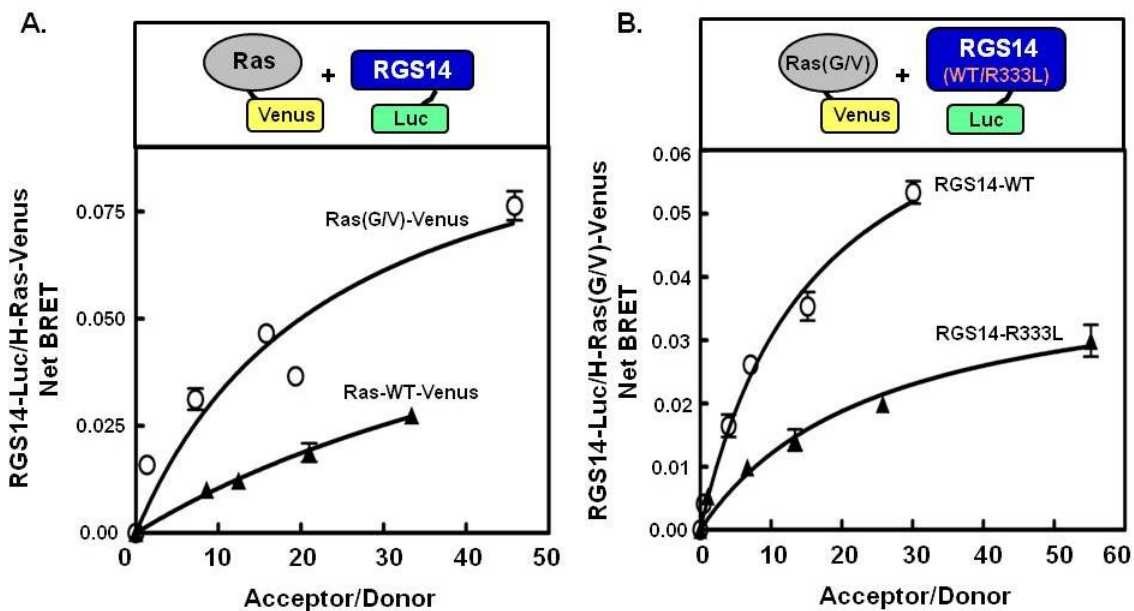


**Figure 4.1. RGS14 selectively interacts with activated H-Ras in live cells as observed by BRET.** (A) *Top* – Diagram showing the RGS14-Luc/H-Ras-Venus BRET pair used. *Bottom* – HEK cells were transfected with 5ng RGS14-Luc plasmid alone or in combination with 10ng, 50ng, 100ng, 250ng, or 500ng of either H-Ras-WT-Venus or H-Ras(G/V)-Venus plasmid. BRET signals (luminescence measured: Donor -  $480 \pm 20$  nm, Acceptor -  $530 \pm 20$  nm) were measured and net BRET was calculated by first calculating the  $530 \pm 20$  nm /  $480 \pm 20$  nm ratio and then subtracting the background BRET signal determined from cells transfected with the RGS14-Luc plasmid alone. (B) *Top* – Diagram showing the RGS14-Luc/H-Ras(G/V)-Venus BRET pair used. *Bottom* – HEK cells were transfected with 5ng wild-type RGS14-Luc (WT) or RGS14-R333L-Luc plasmid alone or in combination with 10ng, 50ng, 100ng, 250ng, or 500ng of H-Ras(G/V)-Venus plasmid. BRET signals were measured and net BRET was calculated as in A. All data are expressed as the mean of three separate experiments with triplicate determinations.

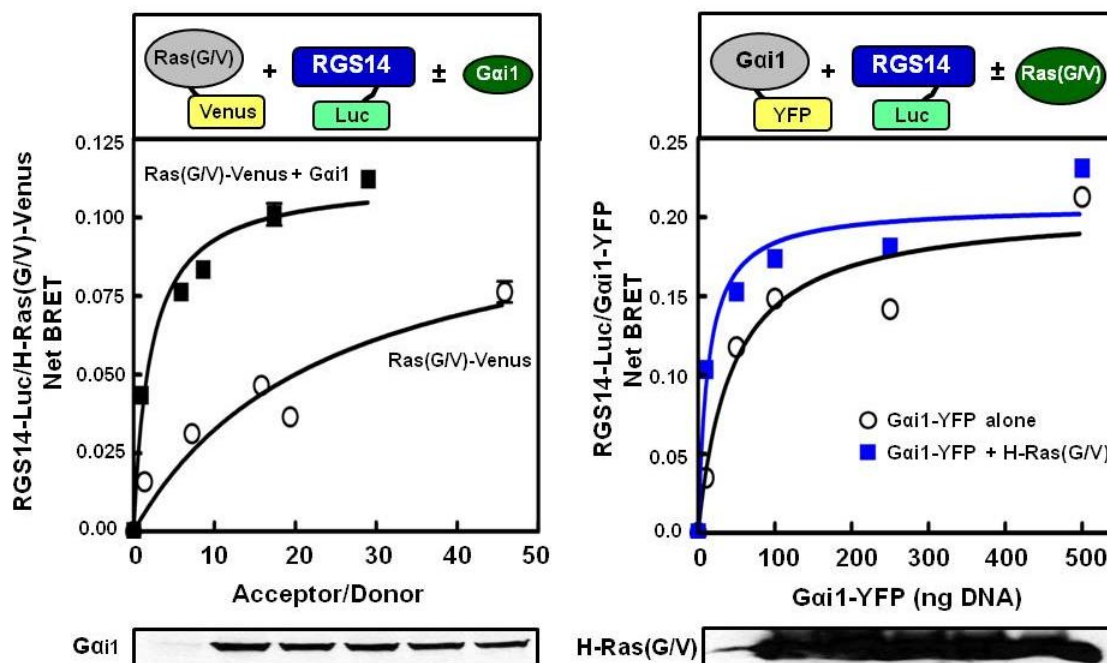


**Figure 4.2. RGS14 interactions with activated H-Ras in live cells are facilitated by Gai1.**

(A) *Top* – Diagram showing the RGS14-Luc/H-Ras(G/V)-Venus BRET pair used. *Bottom* – HEK cells were transfected with 5ng RGS14-Luc plasmid and either 0ng, 10ng, 50ng, 100ng, 250ng, or 500ng of H-Ras(G/V)-Venus plasmid in the absence or presence of 750ng untagged Gai1 plasmid. BRET signals (luminescence measured: Donor -  $480 \pm 20$  nm, Acceptor -  $530 \pm 20$  nm) were measured and net BRET was calculated by first calculating the  $530 \pm 20$  nm /  $480 \pm 20$  nm ratio and then subtracting the background BRET signal determined from cells transfected with the RGS14-Luc plasmid alone. *Bottom panel* – representative immunoblot for Gai1 expression. (B) *Top* – Diagram showing the RGS14-Luc/Gai1-YFP BRET pair used. *Bottom* – HEK cells were transfected with 5ng RGS14-Luc and either 0ng, 10ng, 50ng, 100ng, 250ng, or 500ng Gai1-YFP plasmid in the absence or presence of 750ng untagged H-Ras(G/V) plasmid. BRET signals were measured and net BRET was calculated as in A. *Bottom panel* – representative immunoblot for H-Ras(G/V) expression. All data are expressed as the mean of three separate experiments with triplicate determinations.

Ras(G/V), the BRET signals between RGS14-Luc and increasing amounts of G $\alpha$ i1-YFP were measured in the absence or presence of untagged H-Ras(G/V) (Fig. 4.2B). The BRET between RGS14 and G $\alpha$ i1 remains unchanged in the presence of H-Ras(G/V) (Fig. 4.2B; compare blue and black lines), suggesting that RGS14 may bind both activated H-Ras and G $\alpha$ i1 at the same time. Of note, the YFP tag was inserted into the loop joining the  $\alpha$ B and  $\alpha$ C helices of G $\alpha$  (171,174,176), preserving nucleotide binding and hydrolysis properties similar to the wild-type protein (171). To determine whether this G $\alpha$ i1-mediated effect on RGS14/H-Ras(G/V) interactions was dependent on the G $\alpha$ i1 activation state, the BRET between H-Ras(G/V) and RGS14-Q515A/R516A (referred to as RGS14(*GPR-null*)), which cannot bind inactive G $\alpha$ i1 (152,178), was measured (Fig. 4.3A). The G $\alpha$ i1-facilitated BRET between H-Ras(G/V) and RGS14-WT was abolished in the presence of RGS14(*GPR-null*) (Fig. 4.3A). The effects of mutating G $\alpha$ i1 in the presence of H-Ras(G/V) and wild-type RGS14 were also examined (Fig. 4.3B). The BRET signals observed between RGS14 and H-Ras(G/V) were enhanced by wild-type G $\alpha$ i1(WT), but remained unchanged in the presence of untagged constitutively active G $\alpha$ i1-Q204L (Fig. 4.3B).

Next, I determined the effects of G $\alpha$ i1 expression on the BRET between H-Ras(G/V) and the RGS14-R333L mutant. In the presence of wild-type (WT) RGS14, the BRET signal between RGS14 and H-Ras(G/V) is enhanced by co-expressed G $\alpha$ i1 (Fig. 4.4). The RGS14-R333L mutant exhibits an approximately 50% reduction in BRET with H-Ras(G/V) compared to RGS14-WT; however, this signal is enhanced in the presence of co-expressed G $\alpha$ i1 (Fig. 4.4). The presence of G $\alpha$ i1 thus induces an approximate 30-35% increase in RGS14/H-Ras(G/V) BRET signals regardless of which form of RGS14 is present (WT or R333L) (Fig. 4.4). The fact that there is still observable BRET signals between RGS14-R333L and H-Ras(G/V) (Figs 4.1 and 4.4), and that the presence of G $\alpha$ i1 enhances these signals (Fig. 4.4), indicates that some of the observed RGS14-R333L/H-Ras(G/V) BRET signals may be the result of “by-stander BRET,” (i.e. RGS14 localizing at the plasma membrane and randomly interacting with H-Ras because it too is at the



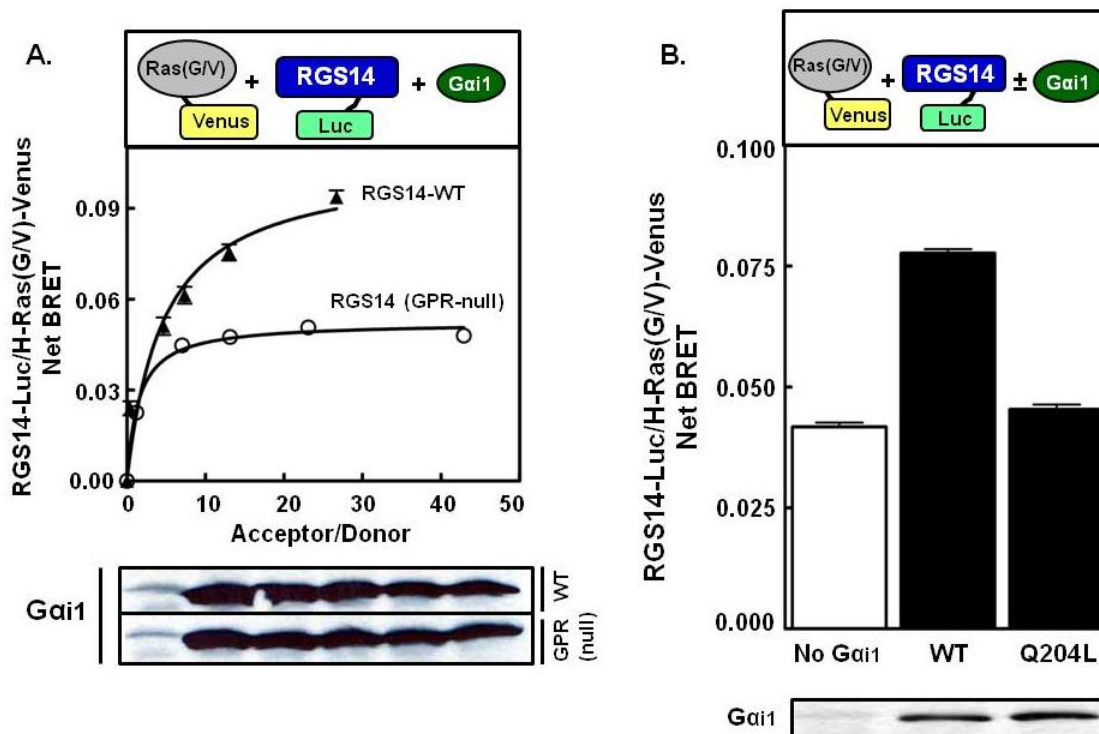


**Figure 4.3. RGS14/H-Ras(G/V) interactions depend on the Gai1 activation state.** (A) *Top* – Diagram showing the RGS14-Luc/H-Ras(G/V)-Venus BRET pair used. *Bottom* – HEK cells were transfected with 5ng wild-type (WT) or *GPR-null* RGS14-Luc plasmid and either 0ng, 10ng, 50ng, 100ng, 250ng, or 500ng of H-Ras(G/V)-Venus plasmid in the presence of 750ng untagged Gai1 plasmid. BRET signals (luminescence measured: Donor -  $480 \pm 20$  nm, Acceptor -  $530 \pm 20$  nm) were measured and net BRET was calculated by first calculating the  $530 \pm 20$  nm /  $480 \pm 20$  nm ratio and then subtracting the background BRET signal determined from cells transfected with the RGS14-Luc plasmid alone. *Bottom panel* – representative immunoblot for Gai1 expression. (B) *Top* – Diagram showing the RGS14-Luc/H-Ras(G/V)-Venus BRET pair used. *Bottom* – HEK cells were transfected with 5ng RGS14-Luc and 500ng H-Ras(G/V)-Venus plasmid in the presence of 750ng untagged wild-type (WT) or constitutively active (Q204L) Gai1 plasmid. BRET signals were measured and net BRET was calculated as in A. *Bottom panel* – representative immunoblot for Gai1 expression. All data are expressed as the mean of three separate experiments with triplicate determinations.

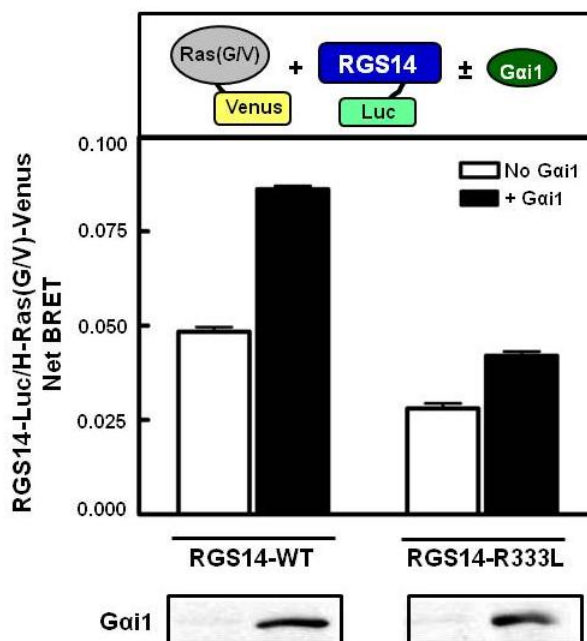


**Figure 4.4. RGS14 interactions with activated H-Ras are only partially inhibited by the R333L mutation.** *Top* – Diagram showing the RGS14-Luc/H-Ras(G/V)-Venus BRET pair used. *Bottom* – HEK cells were transfected with 5ng wild-type (WT) or R333L RGS14-Luc plasmid and 500ng of H-Ras(G/V)-Venus plasmid in the absence or presence of 750ng untagged G $\alpha$ i1 plasmid. BRET signals (luminescence measured: Donor -  $480 \pm 20$  nm, Acceptor -  $530 \pm 20$  nm) were measured and net BRET was calculated by first calculating the  $530 \pm 20$  nm /  $480 \pm 20$  nm ratio and then subtracting the background BRET signal determined from cells transfected with the RGS14-Luc plasmid alone. *Bottom panel* – representative immunoblot for G $\alpha$ i1 expression. All data are expressed as the mean of three separate experiments with triplicate determinations.

membrane). To test this idea, mutations in the CaaX boxes of both wild-type H-Ras and H-Ras(G/V) were generated to prevent membrane localization (187-189). Specifically, a C186S mutation was introduced into both H-Ras-WT-Venus and H-Ras(G/V)-Venus that prohibits the addition of lipid modifications that target the proteins to the plasma membrane. The observed BRET signal between RGS14 and both H-Ras-WT and H-Ras(G/V) was almost completely ablated in the presence of the C186S H-Ras mutants (Fig. 4.5A). Even the co-expression of G $\alpha$ i1 could not overcome the loss of BRET signal generated by the H-Ras-C186S mutants (Fig. 4.5B), indicating that RGS14/H-Ras interactions and all generated BRET signals are dependent on the membrane localization of H-Ras.

*RGS14 interactions with activated H-Ras are regulated by the  $\alpha_{2A}$ -AR.* To further examine the effects of regulatory proteins on RGS14:H-Ras(G/V) complexes, the BRET signals between RGS14-Luc and H-Ras(G/V)-Venus were analyzed in the presence of both G $\alpha$ i1 and a GPCR, specifically the  $\alpha_{2A}$ -AR (Fig. 4.6A). In the absence of receptor agonist, RGS14/H-Ras(G/V) BRET signals are similar to those seen in the presence of G $\alpha$ i1 only (Figs. 4.2-4.4). These signals decreased by ~35% in the presence of the  $\alpha_{2A}$ -AR agonist UK14304 (UK), suggesting that activation of the GPCR induces dissociation of RGS14:H-Ras(G/V) complexes. To expand on this idea, the BRET signal was measured between RGS14-Luc and the  $\alpha_{2A}$ -AR-Venus either in the absence or presence of untagged G $\alpha$ i1 and H-Ras(G/V) (Fig. 4.6B) to see if H-Ras(G/V) could regulate receptor interactions with RGS14. As previously observed (186), there is no detectable BRET signal generated between RGS14 and the  $\alpha_{2A}$ -AR when these two proteins are co-expressed in cells in the absence of G $\alpha$ i. The addition of H-Ras(G/V) alone has little effect on RGS14/ $\alpha_{2A}$ -AR BRET signals regardless of the presence of receptor agonist. However, a 4-fold increase in the BRET signal was observed between the  $\alpha_{2A}$ -AR and RGS14 in the presence of co-expressed G $\alpha$ i1 alone (Fig. 4.6B), as previously observed (186). This signal was reduced by over 50% in the presence of UK14304, which is similar to previously observed results (186).

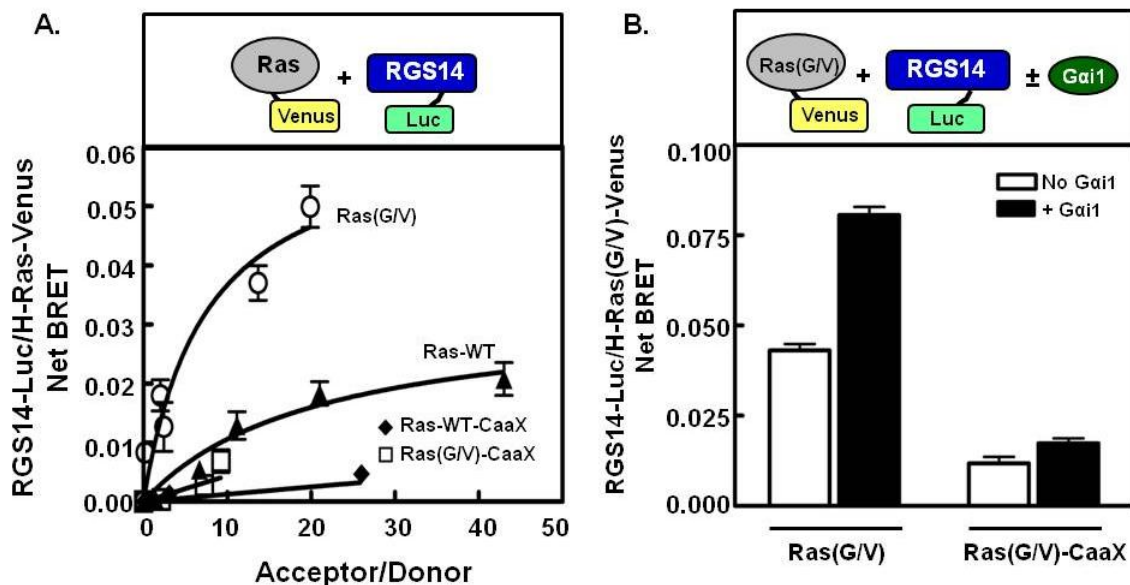


**Figure 4.5. RGS14/H-Ras(G/V) interactions depend on H-Ras(G/V) membrane localization.**

(A) *Top* – Diagram showing the RGS14-Luc/H-Ras-Venus BRET pair used. *Bottom* – HEK cells were transfected with 5ng RGS14-Luc plasmid and either 0ng, 10ng, 50ng, 100ng, 250ng, or 500ng of either Venus-tagged H-Ras(G/V), wild-type (WT) H-Ras, H-Ras(G/V)-C186S (CaaX), or H-Ras-WT-C186S (CaaX) plasmid. BRET signals (luminescence measured: Donor -  $480 \pm 20$  nm, Acceptor -  $530 \pm 20$  nm) were measured and net BRET was calculated by first calculating the  $530 \pm 20$  nm /  $480 \pm 20$  nm ratio and then subtracting the background BRET signal determined from cells transfected with the RGS14-Luc plasmid alone. (B) *Top* – Diagram showing the RGS14-Luc/H-Ras(G/V)-Venus BRET pair used. *Bottom* – HEK cells were transfected with 5ng RGS14-Luc and 500ng of either H-Ras(G/V)-Venus or H-Ras(G/V)-C186S (CaaX) plasmid in the presence or absence of 750ng untagged Gai1 plasmid. BRET signals were measured and net BRET was calculated as in A. All data are expressed as the mean of three separate experiments with triplicate determinations.

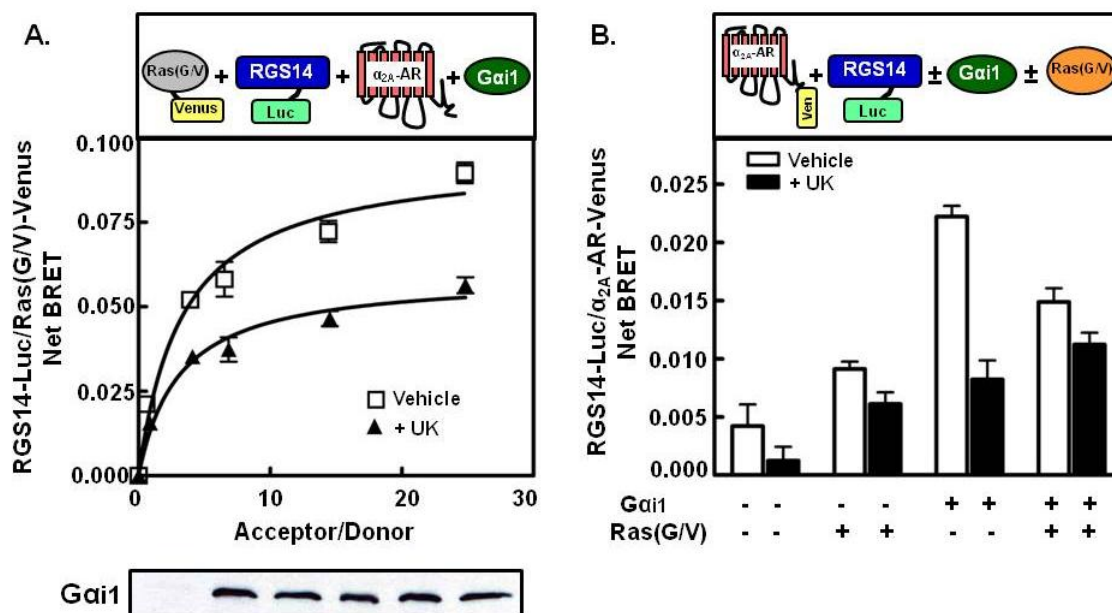


**Figure 4.6. H-Ras(G/V) and the  $\alpha_{2A}$ -AR regulate one another's interactions with RGS14.**

(A) *Top* – Diagram showing the RGS14-Luc/H-Ras(G/V)-Venus BRET pair used. *Bottom* – HEK cells were transfected with 5ng RGS14-Luc plasmid and either 0ng, 10ng, 50ng, 100ng, 250ng, or 500ng of H-Ras(G/V)-Venus in the presence of 750ng untagged Gαi1 and 500ng untagged  $\alpha_{2A}$ -AR. Cells were treated with either vehicle or 10  $\mu$ M UK14304 for 5 mins. BRET signals (luminescence measured: Donor - 480  $\pm$  20 nm, Acceptor - 530  $\pm$  20 nm) were then measured and net BRET was calculated by first calculating the 530  $\pm$  20 nm / 480  $\pm$  20 nm ratio and then subtracting the background BRET signal determined from cells transfected with the RGS14-Luc plasmid alone. *Bottom panel* – representative immunoblot for Gαi1 expression. (B) *Top* – Diagram showing the RGS14-Luc/ $\alpha_{2A}$ -AR-Venus (Ven) BRET pair used. *Bottom* – HEK cells were transfected with 5ng RGS14-Luc and 500ng of  $\alpha_{2A}$ -AR-Venus plasmid in the presence or absence of 750ng untagged Gαi1 and 500ng untagged H-Ras(G/V) plasmids. BRET signals were measured and net BRET was calculated as in A. All data are expressed as the mean of three separate experiments with triplicate determinations.

These  $G\alpha i1$  effects were partially blocked in the presence of untagged H-Ras(G/V) (Fig. 4.6B; far right). In the absence of agonist, H-Ras(G/V) inhibited the  $G\alpha i1$ -mediated BRET signal between RGS14 and the  $\alpha_{2A}$ -AR by ~30%. In addition, H-Ras(G/V) blocked the agonist-induced decrease in RGS14/ $\alpha_{2A}$ -AR BRET signals that was observed in the presence of  $G\alpha i1$ . Together, these results suggest that both H-Ras(G/V) and the  $\alpha_{2A}$ -AR regulate one another's interactions with RGS14 in a  $G\alpha i1$ -dependent manner.

#### **4.4 Discussion**

RGS14 is unusual among RGS protein family members because aside from possessing an RGS domain that accelerates GTP hydrolysis on activated  $G\alpha i/o$  subunits (115,116,118), RGS14 also contains a GPR motif that binds to inactive  $G\alpha i1/3$  subunits (48,117,118,146,147) and tandem RBDs that bind to activated Ras and Raf-1 (114,121,122). As much of the work on RGS14 has dealt with its interactions with  $G\alpha i/o$  subunits, recent work has shown that RGS14 signals through H-Ras and Raf-1 to mediate MAP kinase signaling. Importantly, RGS14's effects on H-Ras/Raf-1-mediated MAP kinase signaling are dependent on its interactions with  $G\alpha i1$ , suggesting that RGS14 switches from regulating MAP kinase signaling to regulating G protein signaling (121). The exact molecular mechanics behind this switch mechanism are largely unknown, and evidence showing RGS14 interactions with GPCRs (186) and GPCR-induced transactivation of growth factor receptors (98,99) indicates that both G proteins and GPCRs may be involved in promoting this switch. Our results with RGS14 support these ideas, and highlight specific molecular mechanisms underlying the regulation of RGS14 interactions with H-Ras. Overall, our findings indicate the following: 1) RGS14 selectively interacts with activated H-Ras (H-Ras(G/V)) via the first RBD in live cells; 2) RGS14 interactions with activated H-Ras depend on the membrane localization of H-Ras; 3)  $G\alpha i1$  greatly facilitates RGS14/H-Ras(G/V) interactions depending on the  $G\alpha i1$  activation state; 4) Activation of the  $\alpha_{2A}$ -AR promotes dissociation of RGS14:H-Ras(G/V) complexes in the presence of  $G\alpha i$ ; and 5) Activated H-Ras induces dissociation of

RGS14: $\alpha_{2A}$ -AR complexes in the presence of G $\alpha$ i1. Taken together, these findings suggest that RGS14 integrates both G protein signaling and MAP kinase signaling through a unique mechanism that includes GPCRs.

*RGS14 preferentially interacts with activated H-Ras in a G $\alpha$ i1-regulated manner.* The BRET analysis indicates that RGS14 preferentially binds to activated H-Ras in cells (Fig. 4.1A). Consistent with previous studies (121,122), this interaction takes place via the first RBD of RGS14 (Fig. 4.1B). Surprisingly, this interaction was greatly facilitated by G $\alpha$ i1 (Fig. 4.2A), as the presence of overexpressed G $\alpha$ i1 induced an approximate 2.5-fold increase in the initial RGS14/H-Ras(G/V) BRET signals (summarized in Fig. 4.7A). The fact that G $\alpha$ i1 remains bound to RGS14 in the presence of H-Ras(G/V) (Fig. 4.2B) indicates that RGS14 can bind activated H-Ras and G $\alpha$ i1 at the same time in live cells, as has been postulated (121). Like other GPR proteins (40), RGS14 may form a clamshell-like structure that is regulated by its binding partners. G $\alpha$ i1 binding to RGS14 may promote a conformational change in RGS14 that allows it to bind activated H-Ras more freely, thereby promoting a platform where RGS14 can switch from regulating G protein signaling to regulating MAP kinase signaling. How or if G $\alpha$ i1 ever dissociates from RGS14 upon H-Ras binding remains to be studied; however, our results indicate that, for at least some time, RGS14 binds both G $\alpha$ i1 and activated H-Ras at the same time.

Critical to this mechanism is that only inactive G $\alpha$ i1 can facilitate H-Ras(G/V) binding to RGS14, since G $\alpha$ i1 that was unable to bind the GPR motif of RGS14 could not enhance RGS14:H-Ras(G/V) complex formation (Fig. 4.3A; compare RGS14-WT and RGS14(*GPR-null*)). Furthermore, activated G $\alpha$ i1 could not facilitate RGS14/H-Ras(G/V) interactions at all (Fig. 4.3B), indicating that the RGS14 interaction with inactive G $\alpha$ i1 through the GPR motif is essential in facilitating activated H-Ras/RGS14 interactions. It's possible that only G $\alpha$ i bound to the GPR motif can create a favorable conformation that opens up the first RBD for H-Ras binding. The importance of the GPR motif in promoting RGS14 interactions with other non-G $\alpha$

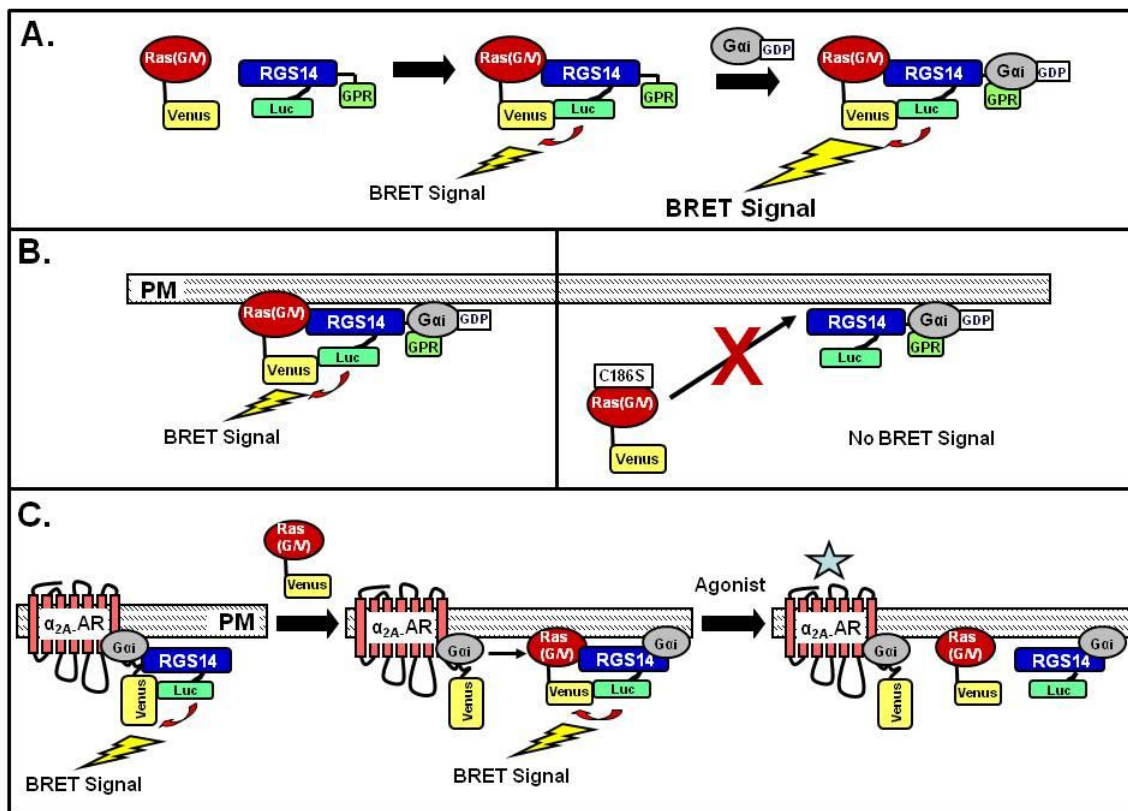


**Figure 4.7. Working model for regulation of RGS14 complexes with activated H-Ras,  $G\alpha i$ , and  $\alpha_{2A}$ -AR.** Diagrams are shown illustrating our findings from experiments measuring BRET signals between RGS14-Luc and H-Ras(G/V)-Venus in the presence and absence of untagged  $G\alpha i$  (A), as well as RGS14-Luc and either wild-type or C186S CaaX box mutant H-Ras(G/V)-Venus in the presence of untagged  $G\alpha i$  (B). (C) Summary of findings when BRET signals were measured separately between RGS14-Luc and either the  $\alpha_{2A}$ -Venus or H-Ras(G/V)-Venus in the presence of untagged  $G\alpha i$  and H-Ras(G/V) or untagged  $\alpha_{2A}$ -AR and  $G\alpha i$ , respectively. Findings are summarized both in the absence and presence of  $\alpha_{2A}$ -AR agonist.



binding partners is not a new phenomenon, as the GPR motif is critical in promoting complex association between RGS14 and the  $\alpha_{2A}$ -AR (186). Therefore, it is likely that G $\alpha$ i1 bound to the GPR motif may promote a stabilized and open conformation of RGS14, illustrating a mechanism that may shed new light onto the structure and function of RGS14.

*RGS14 interactions with H-Ras depend on H-Ras membrane localization.* Results showing a detectable BRET signal generated between H-Ras(G/V) and RGS14-R333L, which should not bind H-Ras(G/V) (121), indicates that some of this residual RGS14/H-Ras(G/V) BRET signal may be due to “by-stander” BRET at the plasma membrane. The fact that G $\alpha$ i1 enhanced the BRET signal between H-Ras(G/V) and RGS14-R333L (Fig. 4.4) suggests that this non-specific “by-stander” BRET is most likely occurring at the plasma membrane since more RGS14 protein is localized at the plasma membrane in the presence of co-expressed G $\alpha$ i1 (48,117,186). To test this, C186S mutations of H-Ras within its CaaX box were created to inhibit membrane localization (187-189). The BRET signal between RGS14 and H-Ras(G/V) was almost completely eliminated in the presence of the H-Ras(G/V) CaaX box mutation (Fig. 4.5A and Fig. 4.7B). Importantly, G $\alpha$ i1 had no effect on the BRET signal between RGS14 and H-Ras(G/V)-CaaX (Fig. 4.5B), illustrating that regardless of G $\alpha$ i1 binding, RGS14 cannot bind to activated H-Ras if H-Ras is not localized at the plasma membrane. These results show that although most of the BRET signals between RGS14 and H-Ras(G/V) are specific, small amounts may be due to random interactions at the plasma membrane that are completely blocked by mutating the CaaX box of H-Ras. Aside from the “by-stander” BRET effect, some of the residual BRET signals seen between H-Ras(G/V) and RGS14-R333L in the presence of G $\alpha$ i1 (Fig. 4.4) may be due to the effects of a third G $\alpha$ i binding site on RGS14, as has been postulated (143). In this case, RGS14 bound to this putative third site may expose residues of RGS14 not previously known to bind H-Ras.

*Activated H-Ras and the  $\alpha_{2A}$ -AR regulate one another's interactions with RGS14.* Since GPCRs have been shown to transactivate growth factor receptors (97,99) and since RGS14 has

been shown to interact with GPCRs (186), the BRET signals between H-Ras(G/V) and RGS14 were examined in the presence of the G $\alpha$ <sub>i</sub>-linked  $\alpha_{2A}$ -AR (Fig. 4.6A). The decrease in RGS14/H-Ras(G/V) BRET observed in the presence of G $\alpha$ <sub>i</sub>1 due to stimulated  $\alpha_{2A}$ -AR (Fig. 4.6A) indicates that activated receptor induces dissociation of RGS14:H-Ras(G/V) complexes. Agonist-binding to the receptor induces activation of G $\alpha$ <sub>i</sub>, which may attract RGS14 to bind and exhibit GAP activity via its RGS domain. In this case, RGS14 would dissociate from H-Ras(G/V) since activated G $\alpha$ <sub>i</sub> cannot facilitate interactions between RGS14 and H-Ras (Fig. 4.3B).

Another attractive model is that there are two pools of RGS14:G $\alpha$ <sub>i</sub>1 complexes in cells, as our data shows and as has been postulated (186). One population of RGS14:G $\alpha$ <sub>i</sub>1 complexes may be localized at the plasma membrane and coupled to GPCRs, as implied by the G $\alpha$ <sub>i</sub>1-dependent BRET signal observed between RGS14 and the  $\alpha_{2A}$ -AR (Fig. 4.6B and (186)). The other RGS14:G $\alpha$ <sub>i</sub>1 complex pools may be localized at the plasma membrane but do not interact with GPCRs, which allows them to bind other proteins such as activated H-Ras. This is supported by the decrease in G $\alpha$ <sub>i</sub>1-dependent RGS14/ $\alpha_{2A}$ -AR BRET signals observed in the presence of untagged activated H-Ras (Fig. 4.6B). In the absence of overexpressed H-Ras(G/V), there is an abundance of RGS14:G $\alpha$ <sub>i</sub>1 complexes that couple to the  $\alpha_{2A}$ -AR. When H-Ras(G/V) is introduced into cells, some of these RGS14:G $\alpha$ <sub>i</sub>1 complexes uncouple from receptors and bind to activated H-Ras. In this case, GPCR stimulation may induce dissociation of this pool of RGS14 bound to activated H-Ras, allowing H-Ras to activate Raf-1 and transduce signals through MEK and ERK (see Fig. 4.7C). This would support previous findings showing that RGS14 acts as a suppressor of growth factor receptor signaling through binding to Ras and Raf, an effect that is reversed by binding to G $\alpha$ <sub>i</sub>1 (121). Taken together, these findings highlight a potential mechanism for RGS14 involvement in GPCR transactivation of Ras-mediated MAP kinase signaling. Activation of a GPCR may induce dissociation of RGS14 from activated H-Ras, thereby reversing RGS14's inhibitory effect on H-Ras and allowing it to bind Raf-1 and potentiate signaling.

These results demonstrate that RGS14 functions in a unique mechanism to integrate both G protein and Ras-mediated MAP kinase signaling. These results highlight newly-appreciated roles of RGS14 at the interface of G protein and MAP kinase signaling pathways, particularly its capacity to act as a molecular switch between regulating these two pathways. It also suggests a means by which RGS14 may function to potentiate GPCR-mediated transactivation of growth factor receptor and Ras/Raf MAP kinase signaling. These molecular mechanisms may ultimately underlie how RGS14 functions physiologically within the brain to regulate hippocampal signaling pathways.

**CHAPTER 5:****Discussion<sup>4</sup>**

<sup>4</sup>A portion of this chapter has been published. Vellano CP, Lee SE, Dudek SM, and Hepler JR. (2011) RGS14 at the interface of hippocampal signaling and synaptic plasticity. *Trends Pharmacol. Sci.* 32: 666-74.

## **5.1 RGS14 Participates in Unconventional G Protein Signaling: Experimental Limitations and Future Directions**

The evidence in Chapter 2 indicates that RGS14 participates in newly-appreciated “unconventional” signaling pathways with  $G\alpha i1$ . In this case, RGS14 is similar to other GPR proteins that form tight complexes with inactive  $G\alpha i1$ -GDP (46,47). The non-receptor GEF Ric-8A is a focal point in these GPCR-independent signaling networks, acting as the GPCR to facilitate nucleotide exchange on  $G\alpha i$  (see Fig. 1.1). With respect to RGS14, we show that RGS14 and Ric-8A interact in cells (Fig. 2.2) and that Ric-8A is able to induce dissociation of RGS14: $G\alpha i1$ -GDP complexes both in cells (Fig. 2.2B) and *in vitro* (Fig. 2.3) using purified proteins. Ric-8A is then capable of exhibiting GEF activity on the free  $G\alpha i1$  (Figs. 2.4-2.6). These results highlight a novel mechanism of RGS proteins toward  $G\alpha$  subunits, and are the first to illustrate that RGS14 functions as both an RGS protein and a GPR protein in cells.

The results discussed above regarding RGS14 and Ric-8A were observed in recombinant systems. Cell culture experiments relied upon overexpressed proteins, as we were unable to work with native cell/tissue systems. This is an obvious limitation for these studies and must be addressed when interpreting the results. We understand that using native hippocampal neurons would be ideal for these co-immunoprecipitation studies since RGS14 is almost exclusively expressed within these neurons (118,124); however, this is technically challenging because RGS14 is only expressed within neurons of the small CA2 hippocampal subregion (124). We have successfully immunoprecipitated RGS14 out of mouse brain lysates; however, we only recover limiting amounts of the protein and are unable to detect other protein binding partners via Western blot (data not shown). We have been unable to detect RGS14 co-immunoprecipitating with Ric-8A in brain cell lysates, which may be due to the limiting amounts of recovered RGS14 and/or the harsh experimental conditions that may disrupt any transient or weak interactions. Ric-8A must bind RGS14 to facilitate exchange of  $G\alpha i1$  from RGS14 to Ric-8A (Fig. 2.3), and

this is supported by results showing that the GPR protein AGS3 also forms a ternary protein complex with both G $\alpha$ i1 and Ric-8A (47).

Another limitation worth discussing is that we only used G $\alpha$ i1 derived from *E. coli* for our *in vitro* experiments. A drawback to using this G $\alpha$ i1 is that it does not contain its natural lipid modifications; therefore, it is not presented exactly as it would be in cells. The presence of lipid modifications has indeed influenced previous experimental results, as Ric-8A binds and acts on myristoylated G $\alpha$ i1 with much greater affinity than unmodified G $\alpha$ i1 in the presence of the GPR protein LGN (46). Use of myristoylated G $\alpha$ i1 in our studies may have resulted in different effects than the unmodified G $\alpha$ i1, specifically with respect to the concentration of Ric-8A used in our studies. Less Ric-8A pure protein may have been able to induce dissociation of the RGS14:G $\alpha$ i1-GDP complex if myristoylated G $\alpha$ i1 was used, and perhaps greater concentrations of RGS14 would have been needed to overcome Ric-8A GEF activity on G $\alpha$ i1. Regardless of the forms of G $\alpha$ i1 used, we believe that increasing concentrations of RGS14 inhibit Ric-8A GEF activity on G $\alpha$ i1 and that RGS14 and Ric-8A may compete for binding to G $\alpha$ i1. RGS14 and Ric-8A clearly share an overlapping binding region on the extreme C-terminus of G $\alpha$ i1 (Fig. 2.7), which is likely independent of any G $\alpha$ i1 myristoylation.

Future experiments can be done to elucidate the role of native Ric-8A on RGS14. Hippocampal CA2 neurons can be isolated and cultured for use in biochemical studies. Specifically, conditions can be optimized for immunoprecipitating large quantities of RGS14 from these neurons and blotting for both G $\alpha$ i1 and Ric-8A. These immunoprecipitation experiments can be done in the absence or presence of stimulatory agents (i.e. growth factors) that promote synaptic plasticity (reviewed in (190)) in order to identify factors that regulate Ric-8A action on RGS14:G $\alpha$ i1 complexes. Also, *in vitro* experiments looking at Ric-8A GEF activity on G $\alpha$ i1 in the presence of RGS14 can be performed using myristoylated G $\alpha$ i1 pure protein derived from Sf9 insect cells. Studies with lipid-modified G $\alpha$ i1 protein may elucidate how well Ric-8A can recognize RGS14:G $\alpha$ i1 complexes in a more native environment, and also how

strongly it can compete with RGS14 for G $\alpha$ i1 binding. Finally, similar experiments can be done using other non-receptor GEFs, such as G $\alpha$ -interacting vesicle-associated protein (GIV), since it too has been shown to regulate GPR:G $\alpha$ i-GDP complexes (55).

Taken together, these results show that RGS14:G $\alpha$ i1-GDP complexes are substrates for Ric-8A, as Ric-8A can induce dissociation of these complexes and subsequently facilitate GTP exchange onto G $\alpha$ i1. It's possible that this mechanism may underlie RGS14 effects on mitosis since Ric-8 has been implicated in regulating cell division in *C. elegans* (191) and mammalian cells (52). The inconclusive postulated role of RGS14 in mitosis (125,127) and the fact that a majority of native RGS14 is expressed specifically in non-dividing hippocampal neurons (118,124) suggests that Ric-8A may also regulate RGS14:G $\alpha$ i1 complexes in certain hippocampal signaling pathways independent of mitosis. Supporting this idea is the fact that Ric-8A is expressed throughout the hippocampus (48,155) and that heterozygous *ric-8A*<sup>-/+</sup> mice display impaired spatial memory (154), an effect opposite of our RGS14-KO mice (124). It's possible that RGS14 binds inactive G $\alpha$ i and acts as a GDI to prevent G $\alpha$ i from becoming activated in signaling pathways important for promoting learning, memory, and synaptic plasticity. A yet-to-be-determined trigger may recruit Ric-8A to this RGS14:G $\alpha$ i1-GDP "inhibitory" complex, whereby Ric-8A induces complex dissociation and GTP binding to G $\alpha$ i1 (see Fig. 2.9). Activated G $\alpha$ i1 may then be free to signal on its own and couple to effector proteins that promote memory and synaptic plasticity.

## **5.2 RGS14 Links Both Conventional GPCR-dependent and Unconventional GPCR-independent G Protein Signaling Pathways**

The fact that RGS14 has an RGS domain that binds activated G $\alpha$ i/o subunits and confers GAP activity (115,116,118) indicates that it is most likely involved in regulating conventional GPCR-dependent signaling. Results in Chapter 3 using the  $\alpha$ <sub>2A</sub>-AR indicate that RGS14 can interact with GPCRs in a G $\alpha$ i/o-dependent manner, and that RGS14 dissociates from the receptor

following receptor activation (Fig. 3.4). Interestingly, RGS14 remains bound to G $\alpha$ i1 through its GPR motif following receptor activation and subsequent dissociation from the receptor (Fig. 3.5). This provides evidence for a unique mechanism of G protein signaling that links both unconventional GPCR-independent signaling to conventional GPCR-dependent signaling. Further supporting this idea is that Ric-8A recognizes and acts on RGS14:G $\alpha$ i1 complexes following GPCR activation (Fig. 3.7).

It's important to note that these observations in our live cell BRET system were discovered using overexpressed proteins in cells. Although not ideal for testing protein/protein interactions, the use of recombinant proteins is required to generate Luciferase- and Venus/YFP-tagged constructs that can be used in the BRET system. Use of live cell BRET does not require the use of harsh chemical buffers, such as those used in immunoprecipitation assays, that may disrupt transient or weak interactions. Also, agonist effects of protein/protein interactions can be detected in real-time in intact cells, which is critical to understanding how proteins function physiologically. Immunoprecipitations would complement these BRET findings, however. We could not detect a three protein complex including RGS14, G $\alpha$ i1, and the  $\alpha$ <sub>2A</sub>-AR in cells through co-immunoprecipitation; however, this is most likely due to the fact that this three protein complex is transient and may have been disrupted by the harsh experimental conditions. Future work can be done to optimize immunoprecipitation conditions with the use of cross-linkers. Also, pure protein BRET experiments can be performed with Luciferase- and Venus/YFP-tagged RGS14, G $\alpha$ i1, Ric-8A, and intracellular portions of the  $\alpha$ <sub>2A</sub>-AR. These experiments would elucidate some of the binding mechanisms seen in the live cell BRET assays, allowing direct interactions to be observed. Finally, the RGS14-KO mice can be utilized to determine the effects of RGS14 on  $\alpha$ <sub>2A</sub>-AR signaling since native  $\alpha$ <sub>2A</sub>-AR has been linked to CA2 hippocampal function (192). Wild-type and RGS14-KO mouse brain thin sections should be isolated and stained for RGS14, G $\alpha$ i1, Ric-8A, and the  $\alpha$ <sub>2A</sub>-AR to confirm that these proteins co-exist within the same neurons. Thin sections from wild-type and RGS14-KO mice can also be compared,



using phosphorylated ERK IHC staining or Western blotting as a readout, following treatment with the  $\alpha_{2A}$ -AR specific agonist UK14304 to determine if RGS14 affects  $\alpha_{2A}$ -AR signaling in the brain. In addition, studies can be aimed at determining whether native RGS14 can modulate signaling of other Gi-linked GPCRs in the CA2 subregion, such as adenosine receptors (193).

Taken together, these data support the idea that RGS14 links both GPCR/G protein signaling with unconventional Ric-8A/G protein signaling. This provides the first evidence that a GPR protein can directly link these two pathways, and illustrates that there may be two pools of G $\alpha_i$  within cells (Fig. 3.9). One pool is targeted to the plasma membrane to couple with GPCRs and either G $\beta\gamma$  or GPR proteins (like RGS14), and the second pool is targeted to the plasma membrane (or others) and binds GPR proteins in the absence of GPCRs. In this case, stimulation of a GPCR will result in G $\alpha_i$ :GPR protein complex dissociation from the receptor. This GPR:G $\alpha_i$  complex can then be recognized by a non-receptor GEF (like Ric-8A), resulting in G $\alpha_i$  activation. It's possible that RGS14 acts as a switch to regulate both of these populations. As such, RGS14 may be bound to G $\alpha_i$  and other binding partners, like activated H-Ras, as results in Chapter 4 suggest. RGS14 may also bind G $\alpha_{i1}$  and couple to GPCRs, such as G $\alpha_i$ -linked adenosine receptors, within dendritic spines of CA2 hippocampal neurons (Fig. 5.1). Loss of RGS14 and the capacity of its RGS domain to limit G $\alpha_i/o$  signaling may alter postsynaptic cAMP levels to affect LTP and learning. A particularly robust calcium extrusion system normally suppresses LTP in proximal and middle regions of CA2 dendrites (128,129,194); therefore, an increase in intracellular calcium would enhance LTP. Since GPR motifs can, in some cases, compete with G $\beta\gamma$  for G $\alpha_i$  binding (41), then loss of RGS14 may allow activated G $\beta\gamma$  to bind free G $\alpha_i$  to form an inactive complex, thus terminating any G $\beta\gamma$ -mediated effects on calcium channels. Ric-8A may act on RGS14:G $\alpha_{i1}$  complexes within spines to potentiate synaptic plasticity signaling pathways through activated G $\alpha_{i1}$  and G $\beta\gamma$ -mediated effects on calcium channels. Ric-8A function may also free up RGS14 to bind H-Ras and Raf-1 to modulate MAP kinase signaling

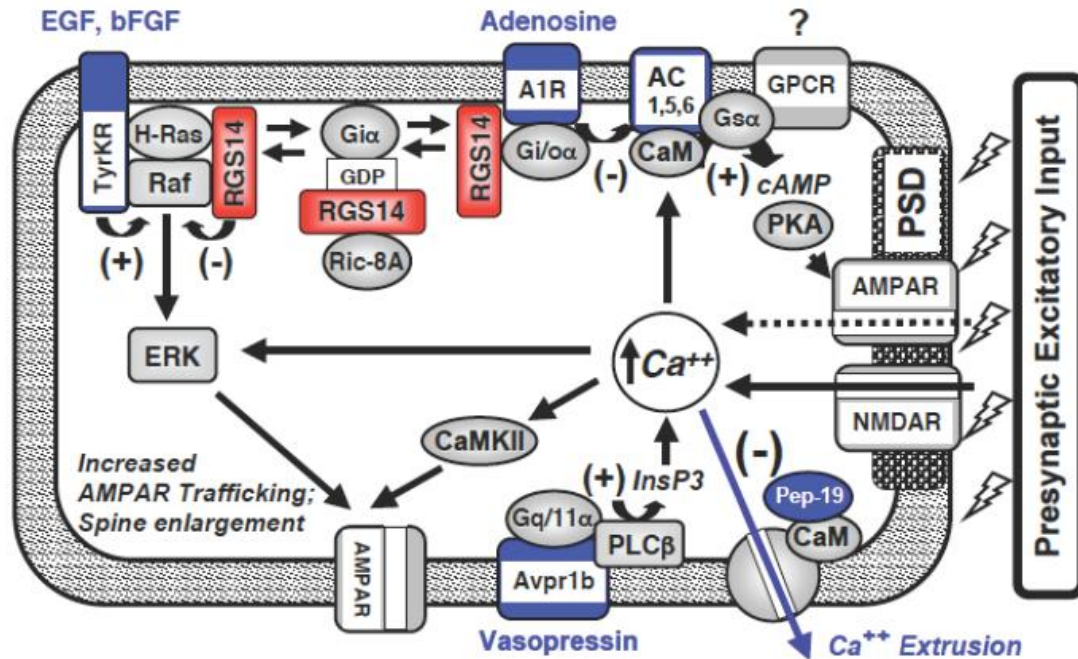


**Figure 5.1. Possible role for RGS14 in suppressing LTP in CA2 hippocampal neurons.**

Cartoon model of a dendritic spine from CA2 neurons that express RGS14, and potential roles for RGS14 in the negative regulation of CA2 synaptic plasticity. Shown are distinct properties and signaling proteins that are uniquely or highly expressed in CA2 neurons (blue), additional signaling proteins that are involved in synaptic plasticity (gray), and proposed roles for RGS14 (red).

(Fig. 5.1). Future studies are aimed at elucidating which specific pathways are activated during LTP.

### **5.3 Working Model for RGS14 Integration of Both G Protein and MAP Kinase Signaling**

To summarize our findings, RGS14 is a multifunctional scaffolding protein in brain that binds Ric-8A, active G $\alpha$ i/o, inactive G $\alpha$ i1/3, active H-Ras, and Raf kinases. RGS14 localizes to dendritic spines and possibly the PSD of CA2 hippocampal neurons, and is important for hippocampal synaptic plasticity, learning, and memory. However, the molecular mechanisms whereby RGS14 and its binding partners integrate unconventional G protein and MAP kinase signaling to modulate synaptic plasticity remain uncertain. Even so, sufficient information is now available to propose a testable working model (Figure 5.2) that describes how the RGS domain and GPR motif of RGS14 work together to bind and modulate the functions of a soluble GEF, such as Ric-8A, G $\alpha$ i, H-Ras, and Raf kinases in a coordinated signaling event.

In contrast to other RGS protein signaling models, our proposed model for RGS14 highlights the GPR motif rather than the RGS domain as the first point of contact between RGS14 and G $\alpha$ i. In the basal resting state (Figure 5.2; Step 1), we propose that RGS14 exists in a stable complex with G $\alpha$ i-GDP at the plasma membrane, or perhaps at the PSD within CA2 hippocampal neurons. We postulate that following a signaling event (as yet undefined) (Figure 5.2; Step 2), a soluble GEF, such as Ric-8A, recognizes and stimulates nucleotide exchange and GTP binding to G $\alpha$ i, subsequently promoting dissociation of the RGS14:G $\alpha$ i-GDP complex because the GPR motif cannot bind G $\alpha$ -GTP. Of note, a role for a G $\alpha$ i-linked GPCR or tyrosine kinase receptor in this activation step cannot be ruled out (144,167,186,195). Once released from G $\alpha$ i (Figure 5.2; Step 3), RGS14 would be free to interact with other downstream binding partners (*e.g.* active H-Ras and Raf kinases). RGS14 may sequester H-Ras and Raf-1 in a signaling complex to passively inhibit and/or modulate MAP kinase signaling involved with LTP and synaptic plasticity (Figure 5.2; Step 4). We postulate that the lifetime of this RGS14 signaling complex is

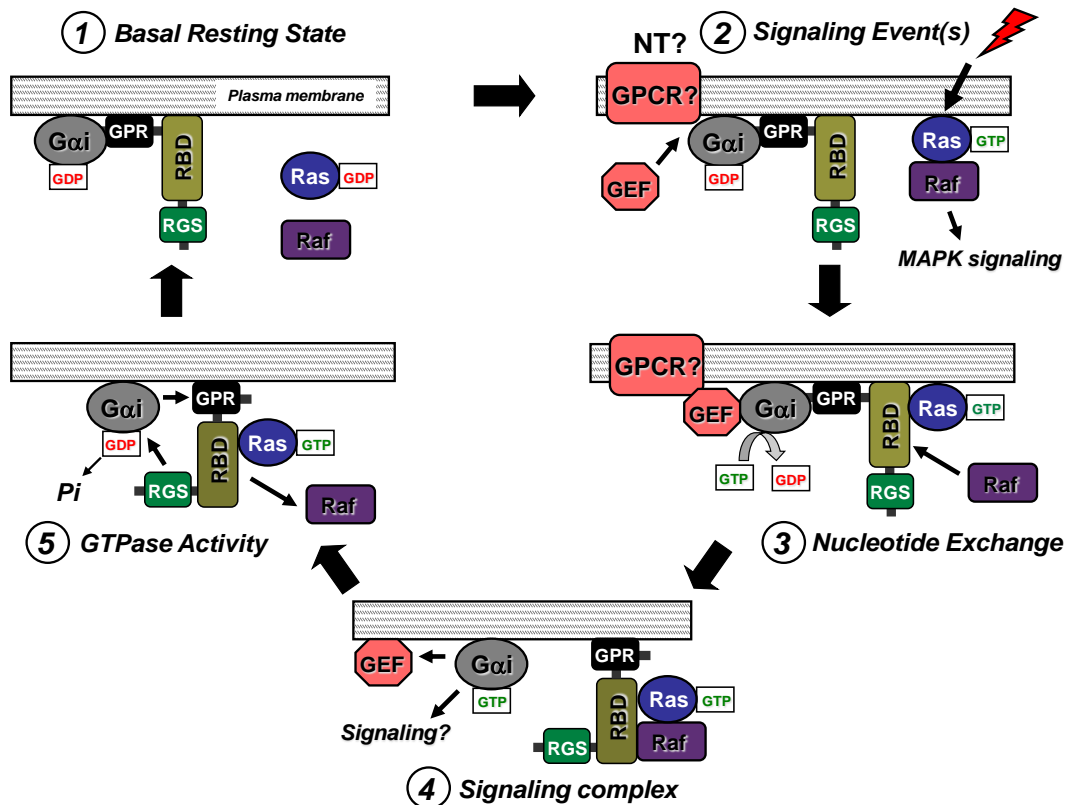


**Figure 5.2. Proposed working model of how the RGS, RBD, and GPR domains of RGS14 may function coordinately to regulate Gαi signaling.** The proposed model for RGS14 signaling proceeds clockwise from top left. (1) RGS14 pre-exists in complex with inactive Gαi-GDP via its GPR motif (and possibly a GPCR) at the plasma membrane in its basal resting state. (2) An unknown stimulation event, perhaps through a receptor tyrosine kinase to stimulate Ras and/or neurotransmitter (NT) activation of a GPCR, induces recruitment of a GEF to the RGS14:Gαi-GDP complex. (3) After binding the RGS14:Gαi-GDP complex, the GEF catalyzes nucleotide exchange on and GTP binding to the Gαi, thereby releasing RGS14 which is now free to bind activated Ras/Raf via its RBDs. (4) Active Gαi-GTP dissociates from RGS14, allowing it to serve as a scaffold to assemble Ras and Raf in a signaling complex. (5) In some regulated fashion, the adjacent RGS domain recognizes the active Gαi to accelerate Gα-GTP hydrolysis, resulting in signal termination. The nearby GPR motif re-binds Gαi-GDP and causes Raf and Ras

to dissociate, leading to reformation of the inactive RGS14:G $\alpha$ -GDP complex and a return to the basal resting state (1).

limited by the RGS domain (Figure 5.2; Step 5), which would act on the nearby G $\alpha$ i-GTP to restore G $\alpha$ i-GDP and promote reformation of the RGS14:G $\alpha$ i-GDP complex via the GPR motif. We speculate that G $\alpha$ i-GDP binding to RGS14 is coupled with dissociation of H-Ras and Raf-1 and a return to the basal resting state (Figure 5.2; Step 1).

Although speculative, this proposed activation/deactivation cycle is entirely consistent with reported findings, though many steps remain to be tested. One attractive feature of this model is that it reconciles the need for the RGS domain and GPR motif within RGS14, and also highlights the possibility that other GPR proteins and RGS proteins can work together in specific cellular contexts. This model also accounts for the idea that the RGS domain and GPR motif are functioning together to limit the presence of activated G $\alpha$ i subunits, favoring the accumulation of G $\alpha$ i-GDP. Furthermore, having the GPR motif and RGS domain built into the same protein could serve to spatially restrict the RGS domain GAP activity toward the pre-bound G $\alpha$ , thus the RGS domain would exhibit GAP activity toward the activated G $\alpha$  that is released from the GPR motif. This would be a logical point for tight regulation, for example, by a reversible phosphorylation step, as RGS14 is a target of phosphorylation by both PKA and ERK (119,196). Future studies will examine this idea and other untested steps in this model. Although this model addresses the mechanics of how RGS14 might integrate G protein and MAP kinase signaling pathways, it does not address how RGS14 integrates these signaling steps at the PSD of dendritic spines to modulate synaptic plasticity. This will be a focus of future studies examining the function(s) of RGS14.

#### **5.4 RGS14 Exhibits Similarities and Differences with its Closest Relative, RGS12**

When proposing roles for RGS14 in regulating G protein and MAP kinase signaling, it is important to discuss the similarities and differences between RGS14 and its closest relative, RGS12. Like RGS14, RGS12 is highly expressed within brain; however, it is mostly expressed within the caudate nucleus and cerebellum and has no known effects *in vivo*. Also, RGS12

possesses PDZ and PTB domains in addition to its RGS, GPR, and Ras/Rap-binding domains, suggesting both similar and unique functions between these two proteins (197). The fact that RGS12 also selectively binds  $G\alpha_i$  via its GPR motif and acts as a GDI toward  $G\alpha_i$  (and not  $G\alpha_o$ ) suggests that RGS12 may be serving similar functions as RGS14 in unconventional G protein signaling (42). RGS12 may also be serving to inhibit  $G\alpha_i$  activation in cells, thereby limiting  $G\alpha$  signaling and perhaps switching to regulate growth factor receptor signaling (123,198). RGS14 and RGS12 may serve similar roles in regulating MAP kinase signaling, since both proteins bind activated H-Ras and B-Raf to regulate PDGF signaling (121,123,198). A main difference for these two proteins regarding their capacity to regulate PDGF-R signaling may be attributed to that fact that RGS12 binds directly to the PDGF $\beta$ -R via its PDZ domain and inhibits PDGF-induced ERK activation (198). Since RGS14 cannot co-localize with the PDGF $\beta$ -R (198) and since there is no evidence showing RGS14 directly binds to the PDGF $\beta$ -R, RGS14 effects on PDGF-induced MAP kinase signaling are most likely dependent on the capacity of RGS14 to bind H-Ras and Raf-1, and not the PDGF-R. Related to CNS signaling, RGS12 binds the NGF receptor TrkA and migrates out of endosomes in the presence of activated TrkA. In addition, RGS12 induces sustained ERK activation and neurite outgrowth in PC12 cells following NGF treatment, indicating that RGS12 can scaffold TrkA, H-Ras, and B-Raf to regulate downstream NGF signaling (123). Again, no evidence has been found showing that RGS14 directly binds TrkA or any NGF receptors.

Although RGS12, and not RGS14, has been found to interact with growth factor receptors, both proteins have been shown to interact with GPCRs. Specifically, RGS14 interacts with MORs (142) and the  $\alpha_{2A}$ -AR (186), while RGS12 binds directly to the CXCR2 chemokine receptor via its PDZ domain (197). RGS14 has also been shown to inhibit IL-8 receptor signaling in cells, suggesting an important role in immune system signaling within spleen and lymphocytes where it is expressed (116). RGS12 interactions with CXCR2 may highlight roles for RGS12 in

immune system signaling pathways within the spleen and thymus, which links RGS14 and RGS12 in regulating GPCR-mediated immune system signaling pathways and immune function.

Together, RGS14 and RGS12 are similar with respect to binding GPCRs and regulating GPCR signaling. Also, both proteins bind H-Ras and Raf and form scaffolding complexes; however, RGS12 can bind both the PDGF $\beta$ -R and TrkA via its PDZ domain to regulate MAP kinase signaling, while studies indicate that RGS14 may not. This highlights an important mechanistic difference between RGS14 and RGS12 with regard to regulating growth factor signaling, as the presence of a PDZ domain may allow RGS12 to bind directly to activated H-Ras, Raf, and receptor at the same time to modulate MAP kinase signaling. RGS12 may prevent the RTKs from interacting with or inducing H-Ras activation. In the absence of a PDZ domain, RGS14 may only bind activated H-Ras and Raf-1 and inhibit their association with growth factor receptors. Studies are aimed to elucidate RGS14 interactions with H-Ras, Raf-1, and potential RTKs.

## **5.5 Concluding Remarks**

Compelling evidence now indicates that RGS14 is a multifunctional scaffold that integrates G protein and MAP kinase signaling pathways important for synaptic plasticity in CA2 hippocampal neurons. Although much is known about RGS14 binding partners and how they interact, more studies are needed to examine how these proteins and RGS14 may work together to suppress hippocampal synaptic plasticity in CA2 neurons. RGS14 can be added to a growing list of genes/proteins that have been linked to enhanced cognition (199). The challenge going forward will be to determine how RGS14 fits into these key pathways to suppress LTP, and how this process is regulated. Besides these signaling proteins involved with enhanced cognition, other GPR proteins that share similarities with RGS14 are also important for brain function. The *mammalian partner of inscutable* (mPins, aka LGN) and AGS3 both are enriched in brain, contain GPR motifs that bind G $\alpha$ i/o-GDP to stabilize their association with membranes, and are regulated



by Ric-8A. AGS3 is localized within neurons throughout most of the CNS, including the hippocampus (158). In the prefrontal cortex and nucleus accumbens, AGS3 is reported to be important for cocaine-seeking and ethanol-seeking relapse behavior, respectively (200,201). LGN is enriched in synaptic membranes of CA1 hippocampal neurons, where it associates with PSD-95 and MAGUK scaffolding proteins in a *Gai1*-dependent manner to influence membrane trafficking, NMDA receptor surface expression, and dendritic remodeling (36). RGS14 and its binding partners in CA2 neurons likely serve roles mechanistically similar to, though functionally distinct from those of LGN and AGS3 in brain physiology. Together, these proteins and RGS14 represent a newly appreciated class of G protein binding partners important for brain physiology/disease that could serve as future therapeutic targets for a range of CNS pathologies.

## References

1. Lander ES, Linton LM, Birren B, Nusbaum C, Zody MC, et al. 2001. Initial sequencing and analysis of the human genome. *Nature*. 409:860-921
2. Fredriksson R, Lagerström MC, Lundin L-G, Schiöth HB. 2003. The G-protein-coupled receptors in the human genome form five main families. Phylogenetic analysis, paralogon groups, and fingerprints. *Mol. Pharmacol.* 63:1256-72
3. Venter JC, Adams MD, Myers EW, Li PW, Mural RJ, et al. 2001. The sequence of the human genome. *Science* 291:1304-51
4. Wettschureck N, Offermanns S. 2005. Mammalian G proteins and their cell type specific functions. *Physiol. Rev.* 85:1159-204
5. Fatakia SN, Costanzi S, Chow CC. 2011. Molecular evolution of the transmembrane domains of G protein-coupled receptors. *PLoS ONE*. 6:e27813
6. Perez DM. 2003. The evolutionarily triumphant G-protein-coupled receptor. *Mol. Pharmacol.* 63:1202-5
7. Fredriksson R, Schiöth HB. 2005. The repertoire of G-protein-coupled receptors in fully sequenced genomes. *Mol. Pharmacol.* 67:1414-25
8. Insel PA, Tang C-M, Hahntow I, Michel MC. 2007. Impact of GPCRs in clinical medicine: monogenic diseases, genetic variants and drug targets. *Biochim. Biophys. Acta.* 1768:994-1005
9. David L S. 2006. What makes a good anti-inflammatory drug target? *Drug Discov. Today.* 11:210-9
10. Panetta R, Greenwood MT. 2008. Physiological relevance of GPCR oligomerization and its impact on drug discovery. *Drug Discov. Today.* 13:1059-66
11. Hebert TE, Moffett S, Morello J-P, Loisel TP, Bichet DG, et al. 1996. A peptide derived from a  $\beta$ 2-adrenergic receptor transmembrane domain inhibits both receptor dimerization and activation. *J. Biol. Chem.* 271:16384-92
12. Jordan BA, Devi LA. 1999. G-protein-coupled receptor heterodimerization modulates receptor function. *Nature.* 399:697-700
13. Waldhoer M, Fong J, Jones RM, Lunzer MM, Sharma SK, et al. 2005. A heterodimer-selective agonist shows in vivo relevance of G protein-coupled receptor dimers. *Proc. Natl. Acad. Sci. U.S.A.* 102:9050-5
14. Gilman AG. 1987. G proteins: transducers of receptor-generated signals. *Annu. Rev. Biochem.* 56:615-49
15. Bünemann M, Frank M, Lohse MJ. 2003. Gi protein activation in intact cells involves subunit rearrangement rather than dissociation. *Proc. Natl. Acad. Sci. U.S.A.* 100:16077-82
16. Digby GJ, Lober RM, Sethi PR, Lambert NA. 2006. Some G protein heterotrimers physically dissociate in living cells. *Proc. Natl. Acad. Sci. U.S.A.* 103:17789-94
17. Hollins B, Kuravi S, Digby GJ, Lambert NA. 2009. The c-terminus of GRK3 indicates rapid dissociation of G protein heterotrimers. *Cell. Signal.* 21:1015-21
18. Oldham WM, Hamm HE. 2008. Heterotrimeric G protein activation by G-protein-coupled receptors. *Nat. Rev. Mol. Cell Biol.* 9:60-71
19. Yanamadala V, Negoro H, Denker BM. 2009. Heterotrimeric G proteins and apoptosis: intersecting signaling pathways leading to context dependent phenotypes. *Curr. Mol. Med.* 9:527-45
20. Chikumi H, Vázquez-Prado J, Servitja J-M, Miyazaki H, Gutkind JS. 2002. Potent activation of RhoA by G $\alpha$ q and Gq-coupled receptors. *J. Biol. Chem.* 277:27130-4
21. Lutz S, Freichel-Blomquist A, Yang Y, Rumenapp U, Jakobs KH, et al. 2005. The guanine nucleotide exchange factor p63RhoGEF, a specific link between Gq/11-coupled receptor signaling and RhoA. *J. Biol. Chem.* 280:11134-9

22. Hepler JR, Gilman AG. 1992. G proteins. *Trends Biochem. Sci.* 17:383-7
23. Hawes BE, Luttrell LM, van Biesen T, Lefkowitz RJ. 1996. Phosphatidylinositol 3-kinase is an early intermediate in the G $\beta\gamma$ -mediated mitogen-activated protein kinase signaling pathway. *J. Biol. Chem.* 271:12133-6
24. Lopez-Illasaca M, Crespo P, Pellici PG, Gutkind JS, Wetzker R. 1997. Linkage of G protein-coupled receptors to the MAPK signaling pathway through PI 3-kinase  $\gamma$ . *Science.* 275:394-7
25. McCudden CR, Hains MD, Kimple RJ, Siderovski DP, Willard FS. 2005. G-protein signaling: back to the future. *Cell. Mol. Life Sci.* 62:551-77
26. Ferguson SSG. 2001. Evolving concepts in G protein-coupled receptor endocytosis: the role in receptor desensitization and signaling. *Pharmacol. Rev.* 53:1-24
27. Zhang J, Ferguson SSG, Barak LS, Bodduluri SR, Laporte SA, et al. 1998. Role for G protein-coupled receptor kinase in agonist-specific regulation of  $\mu$ -opioid receptor responsiveness. *Proc. Natl. Acad. Sci. U.S.A.* 95:7157-62
28. Ma L, Pei G. 2007.  $\beta$ -arrestin signaling and regulation of transcription. *J. Cell Sci.* 120:213-8
29. Reiter E, Lefkowitz RJ. 2006. GRKs and  $\beta$ -arrestins: roles in receptor silencing, trafficking and signaling. *Trends Endocrinol. Metab.* 17:159-65
30. Sato M, Blumer JB, Simon V, Lanier SM. 2006. Accessory proteins for G proteins: partners in signaling. *Annu. Rev. Pharmacol. Toxicol.* 46:151-87
31. Willard FS, Kimple RJ, Siderovski DP. 2004. Return of the GDI: the GoLoco motif in cell division. *Annu. Rev. Biochem.* 73:925-51
32. Colombo K, Grill SW, Kimple RJ, Willard FS, Siderovski DP, Gonczy P. 2003. Translation of polarity cues into asymmetric spindle positioning in *Caenorhabditis elegans* embryos. *Science.* 300:1957-61
33. Groves B, Gong Q, Xu Z, Huntsman C, Nguyen C, et al. 2007. A specific role of AGS3 in the surface expression of plasma membrane proteins. *Proc. Natl. Acad. Sci. U.S.A.* 104:18103-8
34. Hampoelz B, Knoblich JA. 2004. Heterotrimeric G proteins: new tricks for an old dog. *Cell.* 119:453-6
35. Reynolds NK, Schade MA, Miller KG. 2005. Convergent, RIC-8-dependent Galpha signaling pathways in the *Caenorhabditis elegans* synaptic signaling network. *Genetics.* 169:651-70
36. Sans N, Wang PY, Du Q, Petralia RS, Wang Y-X, et al. 2005. mPins modulates PSD-95 and SAP102 trafficking and influences NMDA receptor surface expression. *Nat. Cell. Biol.* 7:1179-90
37. Siderovski DP, Diversé-Pierluissi MA, De Vries L. 1999. The GoLoco motif: a G[alpha]i/o binding motif and potential guanine-nucleotide exchange factor. *Trends Biochem. Sci.* 24:340-1
38. Takesono A, Cismowski MJ, Ribas C, Bernard M, Chung P, et al. 1999. Receptor-independent activators of heterotrimeric G-protein signaling pathways. *J. Biol. Chem.* 274:33202-5
39. Du Q, Taylor L, Compton DA, Macara IG. 2002. LGN blocks the ability of NuMA to bind and stabilize microtubules: a mechanism for mitotic spindle assembly regulation. *Curr. Biol.* 12:1928-33
40. Du Q, Macara IG. 2004. Mammalian Pins is a conformational switch that links NuMA to heterotrimeric G proteins. *Cell.* 119:503-16
41. Ghosh M, Peterson YK, Lanier SM, Smrcka AV. 2003. Receptor- and nucleotide exchange-independent mechanisms for promoting G protein subunit dissociation. *J. Biol. Chem.* 278:34747-50

42. Kimple RJ, De Vries L, Tronchere H, Behe CI, Morris RA, et al. 2001. RGS12 and RGS14 GoLoco motifs are G-alpha-i interaction sites with guanine nucleotide dissociation inhibitor activity. *J. Biol. Chem.* 276:29275-81
43. Mittal V, Linder ME. 2004. The RGS14 GoLoco domain discriminates among G{alpha}i isoforms. *J. Biol. Chem.* 279:46772-8
44. Natochin M, Gasimov KG, Artemyev NO. 2001. Inhibition of GDP/GTP exchange on G alpha subunits by proteins containing G-protein regulatory motifs. *Biochemistry.* 40:5322-8
45. Peterson YK, Bernard ML, Ma H, Hazard S 3<sup>rd</sup>, Graber SG, Lanier SM. 2000. Stabilization of the GDP-bound conformation of Galpha by a peptide derived from the G-protein regulatory motif of AGS3. *J. Biol. Chem.* 275:33193-6
46. Tall GG, Gilman AG. 2005. Resistance to inhibitors of cholinesterase 8A catalyzes release of Galphai-GTP and nuclear mitotic apparatus protein (NuMA) from NuMA/LGN/Galphai-GDP complexes. *Proc. Natl. Acad. Sci. U.S.A.* 102:16584-9
47. Thomas CJ, Tall GG, Adhikari A, Sprang SR. 2008. Ric-8A catalyzes guanine nucleotide exchange on G{alpha}i1 Bound to the GPR/GoLoco exchange inhibitor AGS3. *J. Biol. Chem.* 283:23150-60
48. Vellano CP, Shu F-j, Ramineni S, Yates CK, Tall GG, Hepler JR. 2010. Activation of the Regulator of G Protein Signaling 14–Gai1-GDP signaling complex is regulated by Resistance to Inhibitors of Cholinesterase-8A. *Biochemistry.* 50:752-62
49. Miller KG, Emerson MD, McManus JR, Rand JB. 2000. RIC-8 (Synembryn): a novel conserved protein that is required for G(q)alpha signaling in the *C. elegans* nervous system. *Neuron.* 27:289-99
50. Tall GG, Krumins AM, Gilman AG. 2003. Mammalian Ric-8A (synembryn) is a heterotrimeric Galpha protein guanine nucleotide exchange factor. *J. Biol. Chem.* 278:8356-62
51. Chan P, Gabay M, Wright FA, Tall GG. 2011. Ric-8B Is a GTP-dependent G Protein  $\alpha$ s Guanine Nucleotide Exchange Factor. *J. Biol. Chem.* 286:19932-42
52. Woodard GE, Huang N-N, Cho H, Miki T, Tall GG, Kehrl JH. Ric-8A and Gi{alpha} recruit LGN, NuMA, and dynein to the cell cortex to help orient the mitotic spindle. *Mol. Cell. Biol.* 30:3519-30
53. Garcia-Marcos M, Ghosh P, Farquhar MG. 2009. GIV is a nonreceptor GEF for Gai with a unique motif that regulates Akt signaling. *Proc. Natl. Acad. Sci. U.S.A.* 106:3178-83
54. Le-Niculescu H, Niesman I, Fischer T, DeVries L, Farquhar MG. 2005. Identification and characterization of GIV, a novel Gai/s -interacting protein found on COPI, endoplasmic reticulum-golgi transport vesicles. *J. Biol. Chem.* 280:22012-20
55. Garcia-Marcos M, Ear J, Farquhar MG, Ghosh P. 2011. A GDI (AGS3) and a GEF (GIV) regulate autophagy by balancing G protein activity and growth factor signals. *Mol. Biol. Cell.* 22:673-86
56. Arshavsky VY, Pugh Jr EN. 1998. Lifetime regulation of G protein–effector complex: emerging importance of RGS proteins. *Neuron.* 20:11-4
57. Dohlman HG, Apaniesk D, Chen Y, Song J, Nusskern D. 1995. Inhibition of G-protein signaling by dominant gain-of-function mutations in Sst2p, a pheromone desensitization factor in *Saccharomyces cerevisiae*. *Mol. Cell. Biol.* 15:3635-43
58. De Vries L, Mousli M, Wurmser A, Farquhar MG. 1995. GAIP, a protein that specifically interacts with the trimeric G protein G alpha i3, is a member of a protein family with a highly conserved core domain. *Proc. Natl. Acad. Sci. U.S.A.* 92:11916-20
59. Koelle MR, Horvitz HR. 1996. EGL-10 regulates G protein signaling in the *C. elegans* nervous system and shares a conserved domain with many mammalian proteins. *Cell.* 84:115-25

60. Siderovski DP, Heximer SP, Forsdyke DR. 1994. A human gene encoding a putative basic helix–loop–helix phosphoprotein whose mRNA increases rapidly in cycloheximide-treated blood mononuclear cells. *DNA Cell Biol.* 13:125-47
61. Druey KM, Blumer KJ, Kang VH, Kehrl, JH. 1996. Inhibition of G-protein-mediated MAP kinase activation by a new mammalian gene family. *Nature.* 379:742-6
62. Kimple AJ, Bosch DE, Giguère PM, Siderovski DP. 2011. Regulators of G-protein signaling and their G $\alpha$  substrates: promises and challenges in their use as drug discovery targets. *Pharmacol. Rev.* 63:728-49
63. Willars GB. 2006. Mammalian RGS proteins: multifunctional regulators of cellular signalling. *Semin. Cell Dev. Biol.* 17:363-76
64. Tesmer JJ, Berman DM, Gilman AG, Sprang SR. 1997. Structure of RGS4 bound to AlF<sub>4</sub>–activated G $\alpha$ 1: stabilization of the transition state for GTP hydrolysis. *Cell.* 89:251-61
65. Lan K-L, Sarvazyan NA, Taussig R, Mackenzie RG, DiBello PR, et al. 1998. A point mutation in G $\alpha$ o and G $\alpha$ i1 blocks interaction with regulator of G protein signaling proteins. *J. Biol. Chem.* 273:12794-7
66. Moratz C, Kang VH, Druey KM, Shi C-S, Scheschonka A, et al. 2000. Regulator of G Protein Signaling 1 (RGS1) markedly impairs G $\alpha$  signaling responses of B lymphocytes. *J. Immunol.* 164:1829-38
67. Moratz C, Hayman JR, Gu H, Kehrl JH. 2004. Abnormal B-cell responses to chemokines, disturbed plasma cell localization, and distorted immune tissue architecture in Rgs1<sup>-/-</sup> mice. *Mol. Cell. Biol.* 24:5767-75
68. Oliveira-dos-Santos AJ, Matsumoto G, Snow BE, Bai D, Houston FP, et al. 2000. Regulation of T cell activation, anxiety, and male aggression by RGS2. *Proc. Natl. Acad. Sci. U.S.A.* 97:12272-7
69. Cho H, Harrison K, Kehrl JH. 2004. Regulators of G protein signaling: potential drug targets for controlling cardiovascular and immune function. *Curr. Drug Targets Immune Endocr. Metabol. Disord.* 4:107-18
70. Brinks HL, Eckhart AD. 2010. Regulation of GPCR signaling in hypertension. *Biochim. Biophys. Acta.* 1802:1268-75
71. Kass DA. 2005. Ventricular arterial stiffening. *Hypertension.* 46:185-93
72. Citro S, Malik S, Oestreich EA, Radeff-Huang J, Kelley GG, et al. 2007. Phospholipase C $\epsilon$  is a nexus for Rho and Rap-mediated G protein-coupled receptor-induced astrocyte proliferation. *Proc. Natl. Acad. Sci. U.S.A.* 104:15543-8
73. Zhang L, Malik S, Kelley GG, Kapiloff MS, Smrcka AV. 2011. Phospholipase C $\epsilon$  scaffolds to muscle-specific A Kinase Anchoring Protein (mAKAP $\beta$ ) and integrates multiple hypertrophic stimuli in cardiac myocytes. *J. Biol. Chem.* 286:23012-21
74. Heximer SP, Watson N, Linder ME, Blumer KJ, Hepler JR. 1997. RGS2/G0S8 is a selective inhibitor of G $\alpha$ q function. *Proc. Natl. Acad. Sci. U.S.A.* 94:14389-93
75. Hercule HC, Tank J, Plehm R, Wellner M, da Costa Goncalves AC, et al. 2007. Regulator of G protein signalling 2 ameliorates angiotensin II-induced hypertension in mice. *Exp. Physiol.* 92:1014-22
76. Romero DG, Plonczynski MW, Gomez-Sanchez EP, Yanes LL, Gomez-Sanchez CE. 2006. RGS2 is regulated by angiotensin II and functions as a negative feedback of aldosterone production in H295R human adrenocortical cells. *Endocrinology.* 147:3889-97
77. Heximer SP, Knutsen RH, Sun X, Kaltenbronn KM, Rhee M-H, et al. 2003. Hypertension and prolonged vasoconstrictor signaling in RGS2-deficient mice. *J. Clin. Invest.* 111:445-52

78. Gu S, Tirgari S, Heximer SP. 2008. The RGS2 gene product from a candidate hypertension allele shows decreased plasma membrane association and inhibition of Gq. *Mol. Pharmacol.* 73:1037-43
79. Yang J, Kamide K, Kokubo Y, Takiuchi S, Tanaka C, et al. 2005. Genetic variations of regulator of G-protein signaling 2 in hypertensive patients and in the general population. *J. Hypertens.* 23:1497-505
80. Mittmann C, Chung CH, Höppner G, Michalek C, Nose M, et al. 2002. Expression of ten RGS proteins in human myocardium: functional characterization of an upregulation of RGS4 in heart failure. *Cardiovasc. Res.* 55:778-86
81. Bondjers C, Kalén M, Hellström M, Scheidl SJ, Abramsson A, et al. 2003. Transcription profiling of platelet-derived growth factor-B-deficient mouse embryos identifies RGS5 as a novel marker for pericytes and vascular smooth muscle cells. *Am. J. Pathol.* 162:721-9
82. Seki N, Sugano S, Suzuki Y, Nakagawara A, Ohira M, et al. 1998. Isolation, tissue expression, and chromosomal assignment of human RGS5, a novel G-protein signaling regulator gene. *J. Hum. Genet.* 43:202-5
83. Zhou J, Moroi K, Nishiyama M, Usui H, Seki N, et al. 2001. Characterization of RGS5 in regulation of G protein-coupled receptor signaling. *Life Sci.* 68:1457-69
84. Cho H, Park C, Hwang I-Y, Han S-B, Schimel D, et al. 2008. Rgs5 targeting leads to chronic low blood pressure and a lean body habitus. *Mol. Cell. Biol.* 28:2590-7
85. Hamzah J, Jugold M, Kiessling F, Rigby P, Manzur M, et al. 2008. Vascular normalization in Rgs5-deficient tumours promotes immune destruction. *Nature.* 453:410-4
86. Posokhova E, Wydeven N, Allen KL, Wickman K, Martemyanov KA. 2010. RGS6/Gβ5 complex accelerates IKACH gating kinetics in atrial myocytes and modulates parasympathetic regulation of heart rate / novelty and significance. *Circ. Res.* 107:1350-4
87. Yang J, Huang J, Maity B, Gao Z, Lorca RA, et al. 2010. RGS6, a modulator of parasympathetic activation in heart. *Circ. Res.* 107:1345-9
88. Mirnics K MF, Stanwood GD, Lewis DA, and Levitt P. 2001. Disease-specific changes in regulator of G-protein signaling 4 (RGS4) expression in schizophrenia. *Mol. Psychiatry.* 6:293-301
89. Ingi T, Krumins AM, Chidiac P, Brothers GM, Chung S, et al. 1998. Dynamic regulation of RGS2 suggests a novel mechanism in G-protein signaling and neuronal plasticity. *J. Neurosci.* 18:7178-88
90. He W, Cowan CW, Wensel TG. 1998. RGS9, a GTPase accelerator for phototransduction. *Neuron.* 20:95-102
91. Rahman Z, Gold SJ, Potenza MN, Cowan CW, Ni YG, et al. 1999. Cloning and characterization of RGS9-2: a striatal-enriched alternatively spliced product of the RGS9 gene. *J. Neurosci.* 19:2016-26
92. Tekumalla PK, Calon F, Rahman Z, Birdi S, Rajput AH, et al. 2001. Elevated levels of ΔFosB and RGS9 in striatum in Parkinson's disease. *Biol. Psychiatry.* 50:813-6
93. Xie GX, Palmer PP. 2005. RGS proteins: new players in the field of opioid signaling and tolerance mechanisms. *Anesth. Analg.* 100:1034-42
94. Celver J, Sharma M, Kovoov A. 2010. RGS9-2 mediates specific inhibition of agonist-induced internalization of D2-dopamine receptors. *J. Neurochem.* 114:739-49
95. Roberts PJ, Der CJ. 2007. Targeting the Raf-MEK-ERK mitogen-activated protein kinase cascade for the treatment of cancer. *Oncogene.* 26:3291-310
96. Hurst JH, Hooks SB. 2009. Regulator of G-protein signaling (RGS) proteins in cancer biology. *Biochem. Pharmacol.* 78:1289-97
97. Daub H, Weiss FU, Wallasch C, Ullrich A. 1996. Role of transactivation of the EGF receptor in signalling by G-protein-coupled receptors. *Nature.* 379:557-60

98. Fischer OM, Hart S, Gschwind A, Ullrich A. 2003. EGFR signal transactivation in cancer cells. *Biochem. Soc. Trans.* 31:1203-8
99. Prenzel N, Zwick E, Daub H, Leserer M, Abraham R, et al. 1999. EGF receptor transactivation by G-protein-coupled receptors requires metalloproteinase cleavage of proHB-EGF. *Nature.* 402:884-8
100. Gu J, Wu X, Dong Q, Romeo MJ, Lin X, et al. 2006. A nonsynonymous single-nucleotide polymorphism in the PDZ-Rho guanine nucleotide exchange factor (Ser1416Gly) modulates the risk of lung cancer in Mexican Americans. *Cancer.* 106:2707-15
101. Berman DM, Wang Y, Liu Z, Dong Q, Burke L-A, et al. 2004. A functional polymorphism in RGS6 modulates the risk of bladder cancer. *Cancer Res.* 64:6820-6
102. Ishii M, Inanobe A, Fujita S, Makino Y, Hosoya Y, Kurachi Y. 2001. Ca<sup>2+</sup> elevation evoked by membrane depolarization regulates G protein cycle via RGS proteins in the heart. *Circ. Res.* 89:1045-50
103. Popov SG, Krishna UM, Falck JR, Wilkie TM. 2000. Ca<sup>2+</sup>/Calmodulin reverses phosphatidylinositol 3,4,5-trisphosphate-dependent inhibition of regulators of G protein-signaling GTPase-activating protein activity. *J. Biol. Chem.* 275:18962-8
104. Roman DL, Ota S, Neubig RR. 2009. Polyplexed flow cytometry protein interaction assay: a novel high-throughput screening paradigm for RGS protein inhibitors. *J. Biomol. Screen.* 14:610-9
105. Roman DL, Talbot JN, Roof RA, Sunahara RK, Traynor JR, Neubig RR. 2007. Identification of small-molecule inhibitors of RGS4 using a high-throughput flow cytometry protein interaction assay. *Mol. Pharmacol.* 71:169-75
106. Blazer LL, Zhang H, Casey EM, Husbands SM, Neubig RR. 2011. A nanomolar-potency small molecule inhibitor of regulator of G-protein signaling proteins. *Biochemistry.* 50:3181-92
107. Fitzgerald K, Tertyshnikova S, Moore L, Bjerke L, Burley B, et al. 2006. Chemical genetics reveals an RGS/G-protein role in the action of a compound. *PLoS Genet.* 2:e57.
108. Narayanan V, Sandiford SL, Wang Q, Keren-Raifman T, Levay K, Slepak VZ. 2007. Intramolecular interaction between the DEP Domain of RGS7 and the G $\beta$ 5 Subunit. *Biochemistry.* 46:6859-70
109. Sandiford SL, Slepak VZ. 2009. The G $\beta$ 5–RGS7 complex selectively inhibits muscarinic M3 receptor signaling via the interaction between the third intracellular loop of the receptor and the DEP domain of RGS7. *Biochemistry.* 48:2282-9
110. Varshavsky A. 1996. The N-end rule: functions, mysteries, uses. *Proc. Natl. Acad. Sci. U.S.A.* 93:12142-9
111. Sjögren B, Neubig RR. 2010. Thinking outside of the “RGS Box”: new approaches to therapeutic targeting of regulators of G protein signaling. *Mol. Pharmacol.* 78:550-7
112. Davydov IV, Varshavsky A. 2000. RGS4 Is arginylated and degraded by the N-end rule pathway in vitro. *J. Biol. Chem.* 275:22931-41
113. Hollinger S, Hepler JR. 2002. Cellular regulation of RGS proteins: modulators and integrators of G protein signaling. *Pharmacol. Rev.* 54:527-59
114. Snow BE, Antonio L, Suggs S, Gutstein HB, Siderovski DP. 1997. Molecular cloning and expression analysis of rat Rgs12 and Rgs14. *Biochem. Biophys. Res. Commun.* 233:770-7
115. Traver S, Bidot C, Spassky N, Baltauss T, De Tand MF, et al. 2000. RGS14 is a novel Rap effector that preferentially regulates the GTPase activity of galphao. *Biochem. J.* 350:19-29
116. Cho H, Kozasa T, Takekoshi K, De Gunzburg J, Kehrl JH. 2000. RGS14, a GTPase-activating protein for G $\alpha$ , attenuates G $\alpha$ - and G13 $\alpha$ -mediated signaling pathways. *Mol. Pharmacol.* 58:569-76

117. Shu F-j, Ramineni S, Amyot W, Hepler JR. 2007. Selective interactions between  $G\alpha 1$  and  $G\alpha 3$  and the GoLoco/GPR domain of RGS14 influence its dynamic subcellular localization. *Cell. Signal.* 19:163-76
118. Hollinger S, Taylor JB, Goldman EH, Hepler JR. 2001. RGS14 is a bifunctional regulator of Gai/o activity that exists in multiple populations in brain. *J. Neurochem.* 79:941-9
119. Hollinger S, Ramineni S, Hepler JR. 2003. Phosphorylation of RGS14 by Protein Kinase A potentiates its activity toward Gai. *Biochemistry.* 42:811-9
120. Willard FS, Willard MD, Kimple AJ, Soundararajan M, Oestreich EA, et al. 2009. Regulator of G-protein signaling 14 (RGS14) is a selective H-Ras effector. *PLoS One.* 4:e4884
121. Shu F-j, Ramineni S, Hepler JR. 2010. RGS14 is a multifunctional scaffold that integrates G protein and Ras/Raf MAPkinase signalling pathways. *Cell. Signal.* 22:366-76
122. Kiel C, Wohlgemuth S, Rousseau F, Schymkowitz J, Ferkinghoff-Borg J, et al. 2005. Recognizing and defining true Ras binding domains II: in silico prediction based on homology modelling and energy calculations. *J. Mol. Biol.* 348:759-75
123. Willard MD, Willard FS, Li X, Cappell SD, Snider WD, Siderovski DP. 2007. Selective role for RGS12 as a Ras/Raf/MEK scaffold in nerve growth factor-mediated differentiation. *EMBO J.* 26:2029-40
124. Lee SE, Simons SB, Heldt SA, Zhao M, Schroeder JP, et al. RGS14 is a natural suppressor of both synaptic plasticity in CA2 neurons and hippocampal-based learning and memory. *Proc. Natl. Acad. Sci. U.S.A.* 107:16994-8
125. Martin-McCaffrey L, Willard FS, Oliveira-dos-Santos AJ, Natale DR, Snow BE, et al. 2004. RGS14 is a mitotic spindle protein essential from the first division of the mammalian zygote. *Dev. Cell.* 7:763-9
126. Cho H, Kehrl JH. 2007. Localization of  $G\alpha$  proteins in the centrosomes and at the midbody: implication for their role in cell division. *J. Cell Biol.* 178:245-55
127. Martin-McCaffrey L, Willard FS, Pajak A, Dagnino L, Siderovski DP, D'Souza SJ. 2005. RGS14 is a microtubule-associated protein. *Cell Cycle.* 4:953-60
128. Simons SB, Escobedo Y, Yasuda R, Dudek SM. 2009. Regional differences in hippocampal calcium handling provide a cellular mechanism for limiting plasticity. *Proc. Natl. Acad. Sci. U.S.A.* 106:14080-4
129. Zhao M, Choi YS, Obrietan K, Dudek SM. 2007. Synaptic plasticity (and the lack thereof) in hippocampal CA2 neurons. *J. Neurosci.* 27:12025-32
130. Nakazawa K, Sun LD, Quirk MC, Rondi-Reig L, Wilson MA, Tonegawa S. 2003. Hippocampal CA3 NMDA receptors are crucial for memory acquisition of one-time experience. *Neuron.* 38:305-15
131. Neves G, Cooke SF, Bliss TV. 2008. Synaptic plasticity, memory and the hippocampus: a neural network approach to causality. *Nat. Rev. Neurosci.* 9:65-75
132. Rolls ET, Kesner RP. 2006. A computational theory of hippocampal function, and empirical tests of the theory. *Prog. Neurobiol.* 79:1-48
133. Pineda VV, Athos JI, Wang H, Celver J, Ippolito D, et al. 2004. Removal of  $G\alpha 1$  constraints on adenylyl cyclase in the hippocampus enhances LTP and impairs memory formation. *Neuron.* 41:153-63
134. Fu Z, Lee SH, Simonetta A, Hansen J, Sheng M, Pak DT. 2007. Differential roles of Rap1 and Rap2 small GTPases in neurite retraction and synapse elimination in hippocampal spiny neurons. *J. Neurochem.* 100:118-31
135. Ryu J, Futai K, Feliu M, Weinberg R, Sheng M. 2008. Constitutively active Rap2 transgenic mice display fewer dendritic spines, reduced extracellular signal-regulated



- kinase signaling, enhanced long-term depression, and impaired spatial learning and fear extinction. 28:8178-88
136. Zhu Y, Pak D, Qin Y, McCormack SG, Kim MJ, et al. 2005. Rap2-JNK removes synaptic AMPA receptors during depotentiation. *Neuron*. 46:905-16
  137. Kushner SA, Elgersma Y, Murphy GG, Jaarsma D, van Woerden GM, et al. 2005. Modulation of presynaptic plasticity and learning by the H-ras/extracellular signal-regulated kinase/synapsin I signaling pathway. *J. Neurosci*. 25:9721-34
  138. Kennedy MB, Beale HC, Carlisle HJ, Washburn LR. 2005. Integration of biochemical signalling in spines. *Nat. Rev. Neurosci*. 6:423-34
  139. Marty C, Ye RD. 2010. Heterotrimeric G protein signaling outside the realm of seven transmembrane domain receptors. *Mol. Pharmacol*. 78:12-8
  140. Conway AM, Rakhit S, Pyne S, Pyne NJ. 1999. Platelet-derived-growth-factor stimulation of the p42/p44 mitogen-activated protein kinase pathway in airway smooth muscle: role of pertussis-toxin-sensitive G-proteins, c-Src tyrosine kinases and phosphoinositide 3-kinase. *Biochem. J*. 337:171-7
  141. Alderton F, Rakhit S, Kong KC, Palmer T, Sambhi B, et al. 2001. Tethering of the platelet-derived growth factor beta receptor to G-protein-coupled receptors. A novel platform for integrative signaling by these receptor classes in mammalian cells. *J. Biol. Chem*. 276:28578-85
  142. Rodríguez-Muñoz M, de la Torre-Madrid E, Gaitán G, Sánchez-Blázquez P, Garzón J. 2007. RGS14 prevents morphine from internalizing Mu-opioid receptors in periaqueductal gray neurons. *Cell. Signal*. 19:2558-71
  143. Hepler JR, Cladman W, Ramineni S, Hollinger S, Chidiac P. 2005. Novel activity of RGS14 on G $\alpha$  and G $\beta\gamma$  nucleotide binding and hydrolysis distinct from its RGS domain and GDI activity. *Biochemistry*. 44:5495-502
  144. Oner SS, Maher EM, Breton B, Bouvier M, Blumer JB. 2010. Receptor-regulated interaction of Activator of G-protein Signaling-4 and G $\alpha$ i. *J. Biol. Chem*. 285:20588-94
  145. Hamm HE. 1998. The many faces of G protein signaling. *J. Biol. Chem*. 273:669-72
  146. Ross EM, Wilkie TM. 2000. GTPase-activating proteins for heterotrimeric G proteins: regulators of G protein signaling (RGS) and RGS-like proteins. *Annu. Rev. Biochem*. 69:795-827
  147. De Vries L, Zheng B, Fischer T, Elenko E, Farquhar MG. 2000. The regulator of G protein signaling family. *Annu. Rev. Pharmacol. Toxicol*. 40:235-71
  148. Schade MA, Reynolds NK, Dollins CM, Miller KG. 2005. Mutations that rescue the paralysis of *C. elegans* ric-8 (Synembryon) mutants activate the Gas pathway and define a third major branch of the synaptic signaling network. *Genetics*. 169:631-49
  149. Tall GG, Gilman AG, David PS. 2004. Purification and functional analysis of Ric-8A: a guanine nucleotide exchange factor for G-protein alpha subunits. *Methods Enzymol*. 390:377-88
  150. Krumins AM, Gilman AG. 2002. Assay of RGS protein activity in vitro using purified components. *Methods Enzymol*. 344:673-85
  151. Siderovski DP, Willard FS. 2005. The GAPs, GEFs, and GDIs of heterotrimeric G-protein alpha subunits. *Int. J. Biol. Sci*. 1:51-66
  152. Kimple RJ, Kimple ME, Betts L, Sondek J, Siderovski DP. 2002. Structural determinants for GoLoco-induced inhibition of nucleotide release by G $\alpha$  subunits. *Nature*. 416:878-81
  153. Willard FS, Zheng Z, Guo J, Digby GJ, Kimple AJ, et al. 2008. A Point mutation to G $\alpha$ i selectively blocks GoLoco motif binding. *J. Biol. Chem*. 283:36698-710
  154. Tõnissoo T, Kõks S, Meier R, Raud S, Plaas M, et al. 2006. Heterozygous mice with Ric-8 mutation exhibit impaired spatial memory and decreased anxiety. *Behav. Brain Res*. 167:42-8

155. Tõnissoo T, Meier R, Talts K, Plaas M, Karis A. 2003. Expression of ric-8 (synembryon) gene in the nervous system of developing and adult mouse. *Gene Expr. Patterns.* 3:591-4
156. An N, Blumer JB, Bernard ML, Lanier SM. 2008. The PDZ and band 4.1 containing protein Frmpd1 regulates the subcellular location of activator of G-protein signaling 3 and its interaction with G-proteins. *J. Biol. Chem.* 283:24718-28
157. Wang S-C, Lai H-L, Chiu Y-T, Ou R, Huang C-L, Chern, Y. 2007. Regulation of type V adenylylase cyclase by Ric8a, a guanine nucleotide exchange factor. *Biochem. J.* 406:383-8
158. Blumer JB, Chandler LJ, Lanier SM. 2002. Expression analysis and subcellular distribution of the two G-protein regulators AGS3 and LGN indicate distinct functionality. *J. Biol. Chem.* 277:15897-903
159. Pizzinat N, Takesono A, Lanier SM. 2001. Identification of a truncated form of the G-protein regulator AGS3 in heart that lacks the tetratricopeptide repeat domains. *J. Biol. Chem.* 276:16601-10
160. Wisner O, Qian X, Ehlers M, Ja WW, Roberts RW, et al. 2006. Modulation of basal and receptor-induced GIRK potassium channel activity and neuronal excitability by the mammalian PINS homolog LGN. *Neuron.* 50:561-73
161. Costa RM, Federov NB, Kogan JH, Murphy GG, Stern J, et al. 2002. Mechanism for the learning deficits in a mouse model of neurofibromatosis type 1. *Nature.* 415:526-30
162. Manabe T, Aiba A, Yamada A, Ichise T, Sakagami H, et al. 2000. Regulation of long-term potentiation by H-Ras through NMDA receptor phosphorylation. *J. Neurosci.* 20:2504-11
163. Sweatt JD. 2004. Mitogen-activated protein kinases in synaptic plasticity and memory. *Curr. Opin. Neurobiol.* 14:311-7
164. Wu G-Y, Deisseroth K, Tsien RW. 2001. Spaced stimuli stabilize MAPK pathway activation and its effects on dendritic morphology. *Nat. Neurosci.* 4:151-8
165. Hess HA, Röper J-C, Grill SW, Koelle MR. 2004. RGS-7 completes a receptor-independent heterotrimeric G protein cycle to asymmetrically regulate mitotic spindle positioning in *C. elegans*. *Cell.* 119:209-18
166. Lanier SM. 2004. AGS proteins, GPR motifs and the signals processed by heterotrimeric G proteins. *Biol. Cell.* 96:369-72
167. Oner SS, An N, Vural A, Breton B, Bouvier M, et al. 2010. Regulation of the AGS3-Gai signaling complex by a seven-transmembrane span receptor. *J. Biol. Chem.* 285:33949-58
168. Neitzel KL, Hepler JR. 2006. Cellular mechanisms that determine selective RGS protein regulation of G protein-coupled receptor signaling. *Semin. Cell Dev. Biol.* 17:383-9
169. Fenech C, Patrikainen L, Kerr DS, Grall S, Liu Z, et al. 2009. Ric-8A, a Ga protein guanine nucleotide exchange factor potentiates taste receptor signaling. *Front. Cell. Neurosci.* 3:doi: 10.3389/neuro.03.011.2009
170. Nishimura A, Okamoto M, Sugawara Y, Mizuno N, Yamauchi J, Itoh H. 2006. Ric-8A potentiates Gq-mediated signal transduction by acting downstream of G protein-coupled receptor in intact cells. *Genes Cells.* 11:487-98
171. Gibson SK, Gilman AG. 2006. G $\alpha$  and G $\beta$  subunits both define selectivity of G protein activation by  $\alpha$ 2-adrenergic receptors. *Proc. Natl. Acad. Sci. U.S.A.* 103:212-7
172. Duzic E, Coupry I, Downing S, Lanier SM. 1992. Factors determining the specificity of signal transduction by guanine nucleotide-binding protein-coupled receptors. I. Coupling of alpha 2-adrenergic receptor subtypes to distinct G-proteins. *J. Biol. Chem.* 267:9844-51
173. Gales C, Van Durm JJ, Schaak S, Pontier S, Percherancier Y, et al. 2006. Probing the activation-promoted structural rearrangements in preassembled receptor-G protein complexes. *Nat. Struct. Mol. Biol.* 13:778-86

174. Hein P, Rochais F, Hoffmann C, Dorsch S, Nikolaev VO, et al. 2006. Gs activation is time-limiting in initiating receptor-mediated signaling. *J. Biol. Chem.* 281:33345-51
175. Hughes TE, Zhang H, Logothetis DE, Berlot CH. 2001. Visualization of a functional Gαq-green fluorescent protein fusion in living cells. *J. Biol. Chem.* 276:4227-35
176. Hynes TR, Mervine SM, Yost EA, Sabo JL, Berlot CH. 2004. Live cell imaging of Gs and the β2-adrenergic receptor demonstrates that both αs and β1γ7 internalize upon stimulation and exhibit similar trafficking patterns that differ from that of the β2-adrenergic receptor. *J. Biol. Chem.* 279:44101-12
177. Mercier JF, Salahpour A, Angers S, Breit A, Bouvier M. 2002. Quantitative assessment of beta 1- and beta 2-adrenergic receptor homo- and heterodimerization by bioluminescence resonance energy transfer. *J. Biol. Chem.* 277:44925-31
178. Khafizov K. 2009. GoLoco motif proteins binding to Gαi1: insights from molecular simulations. *J. Mol. Model.* 15:1491-9
179. Natochin M, Gasimov KG, Artemyev NO. 2001. A GPR-protein interaction surface of Gαi: implications for the mechanism of GDP-release inhibition. *Biochemistry.* 41:258-65
180. Gabay M, Tall GG. 2011. Mammalian Ric-8A and Ric-8B are required for functional expression of heterotrimeric G-proteins. *FASEB J.* 25:804.5
181. Blumer JB, Cismowski MJ, Sato M, Lanier SM. 2005. AGS proteins: receptor-independent activators of G-protein signaling. *Trends Pharmacol. Sci.* 26:470-6
182. Heximer SP, Srinivasa SP, Bernstein LS, Bernard JL, Linder ME, et al. 1999. G protein selectivity is a determinant of RGS2 function. *J. Biol. Chem.* 274:34253-9
183. Lambert NA. 2008. Dissociation of heterotrimeric G proteins in cells. *Sci. Signal.* 1:re5
184. Yoshikawa K, Touhara K. 2009. Myr-Ric-8A enhances Gα15-mediated Ca<sup>2+</sup> response of vertebrate olfactory receptors. *Chem. Senses.* 34:15-23
185. Lee MJ, Dohlman HG. 2008. Coactivation of G protein signaling by cell-surface receptors and an intracellular exchange factor. *Curr. Biol.* 18:211-5
186. Vellano CP, Maher EM, Hepler JR, Blumer JB. 2011. G Protein-coupled receptors and Resistance to Inhibitors of Cholinesterase-8A (Ric-8A) both regulate the Regulator of G Protein Signaling 14 (RGS14)-Gαi1 complex in live cells. *J. Biol. Chem.* 286:38659-69
187. Casey PJ, Solski PA, Der CJ, Buss JE. 1989. p21ras is modified by a farnesyl isoprenoid. *Proc. Natl. Acad. Sci. U.S.A.* 86:8323-7
188. Deschenes RJ, Stimmel JB, Clarke S, Stock J, Broach JR. 1989. RAS2 protein of *Saccharomyces cerevisiae* is methyl-esterified at its carboxyl terminus. *J. Biol. Chem.* 264:11865-73
189. Schmidt WK, Tam A, Fujimura-Kamada K, Michaelis S. 1998. Endoplasmic reticulum membrane localization of Rce1p and Ste24p, yeast proteases involved in carboxyl-terminal CAAX protein processing and amino-terminal a-factor cleavage. *Proc. Natl. Acad. Sci. U.S.A.* 95:11175-80
190. Curtis J, Finkbeiner S. 1999. Sending signals from the synapse to the nucleus: possible roles for CaMK, Ras/ERK, and SAPK pathways in the regulation of synaptic plasticity and neuronal growth. *J. Neurosci. Res.* 58:88-95
191. Miller KG, Rand JB. 2000. A role for RIC-8 (Synembryn) and GOA-1 (Gα) in regulating a subset of centrosome movements during early embryogenesis in *Caenorhabditis elegans*. *Genetics.* 156:1649-60
192. Tavares A, Handy DE, Bogdanova NN, Rosene DL, Gavras H. 1996. Localization of α2A- and α2B-adrenergic receptor subtypes in brain. *Hypertension.* 27:449-55
193. Ochiishi T, Saitoh Y, Yukawa A, Saji M, Ren Y, et al. 1999. High level of adenosine A1 receptor-like immunoreactivity in the CA2/CA3a region of the adult rat hippocampus. *Neuroscience.* 93:955-67

194. Zhao M, Dudek SM. 2010. Vasopressin induces synaptic potentiation in hippocampal CA2 neurons. *Neuroscience Meeting Planner*. San Diego, CA, Society for Neuroscience. Program Number 550.7. Online.
195. Cao C, Huang X, Han Y, Wan Y, Birnbaumer L, et al. 2009. G $\alpha$ 1 and G $\alpha$ 3 are required for epidermal growth factor-mediated activation of the Akt-mTORC1 pathway. *Sci. Signal*. 2:ra17
196. Hollinger S, Hepler JR. 2003. Methods for measuring RGS protein phosphorylation by G protein-regulated kinases. *Methods Mol. Biol.* 237:205-19.
197. Snow BE, Hall RA, Krumins AM, Brothers GM, Bouchard D, et al. 1998. GTPase activating specificity of RGS12 and binding specificity of an alternatively spliced PDZ (PSD-95/Dlg/ZO-1) domain. *J. Biol. Chem.* 273:17749-55
198. Sambhi BS, Hains MD, Waters CM, Connell MC, Willard FS, et al. 2006. The effect of RGS12 on PDGF $\beta$  receptor signalling to p42/p44 mitogen activated protein kinase in mammalian cells. *Cell. Signal.* 18:971-81
199. Lee YS, Silva AJ. 2009. The molecular and cellular biology of enhanced cognition. *Nat. Rev. Neurosci.* 10:126-40
200. Bowers MS, Hopf FW, Chou JK, Guillory AM, Chang SJ, et al. 2008. Nucleus accumbens AGS3 expression drives ethanol seeking through G $\beta\gamma$ . *Proc. Natl. Acad. Sci. U. S. A.* 105:12533-8
201. Bowers MS, McFarland K, Lake RW, Peterson YK, Lapish CC, et al. 2004. Activator of G protein signaling 3: a gatekeeper of cocaine sensitization and drug seeking. *Neuron.* 42:269-81